2011

PLGA microparticle based vaccine carriers for an improved and efficacious tumor therapy

Yogita Krishnamachari
University of Iowa

PLGA MICROPARTICLE BASED VACCINE CARRIERS FOR AN IMPROVED AND EFFICACIOUS TUMOR THERAPY

By

Yogita Krishnamachari

An Abstract

Of a thesis submitted in partial fulfillment
of the requirements for the Doctor of
Philosophy degree in Pharmacy
in the Graduate College of
The University of Iowa

May 2011

Thesis Supervisor: Associate Professor Aliasger K. Salem

ABSTRACT

Cancer is a collection of diseases that is characterized by an uncontrolled proliferation of aberrant cells. The conventional treatment strategies including chemotherapy and radiotherapy prove detrimental to healthy cells and are unable to combat primary and secondary metastases. Hence immunotherapy is gaining momentum in cancer clinics and translational research labs as an alternative safer and more efficacious approach to tumor therapy. Vaccines based on antigen alone lack the ability to optimally activate the antigen presenting cells (APCs) including dendritic cells (DCs) to generate significantly greater antigen-specific T cell responses. A typical strategy to overcome this limitation has been the use of adjuvants in order to improve the immunogenicity of the vaccines. A newer class of adjuvants called toll like receptor (TLR) ligands recognize pathogen associated molecular patterns (PAMP) and thus elicit a Th-1 polarized response. The hypothesis of the current research is that co-delivery of antigen and adjuvant in a microparticulate carrier will elicit a strong cell-mediated immune response conferring anti-tumor immunity. Furthermore, we proposed that a combination of TLR ligands when co-delivered with an antigen will be able to mount a synergistic anti-tumor response in comparison to the delivery of antigen alone. There were three primary objectives of the study; 1) Fabrication, process design optimization and characterization of antigen and adjuvant co-loaded microparticles (MP), 2) Study the ability of the MP fabricated in step 1 in eliciting a potent immune response in a murine model by various routes of administration and 3) Study the effect of the various treatment as prophylactic and therapeutic cancer vaccines in a murine tumor model.

Objective 1 was achieved by optimizing various process parameters including PLGA type and concentration, surfactant concentration and modification of a previously reported double emulsification solvent evaporation technique. Process optimization lead to the development of the following 5 treatment groups, a) Empty PLGA MP, b) OVA PLGA MP, c) OVA + CpG PLGA MP, d) OVA + poly I: C PLGA

MP and e) OVA + CpG + poly I:C tri-component PLGA MP. The optimized microparticles exhibited a mean particle size of 1.5 µm with a smooth spherical surface and a desirable biphasic release pattern of the entrapped components. Results from step 2 indicated the ability of the co-delivery and the tri-component systems to generate several fold higher immunostimulatory response in comparison to the group treated with antigen alone. Of the two routes of administration tested, the intraperitonial (i.p) route gave the strongest response followed by intramuscular (i.m) route. A synergistic antibody response was observed upon vaccination with the tri-component model. Prophylactic vaccination studies showed that the co-delivery and tri-component system affording the strongest protection against aggressive tumor growth. The therapeutic studies also indicated enhanced tumor protection and 2-fold improvement in survival times when the mice vaccinated with the co-delivery and tri-component MP carriers in comparison to vaccination with microparticles loaded with antigen alone. The carriers also showed strong evidence for the generation of anti-tumor immunogenic memory.

In summary, the current study has laid an interesting premise for the use of immunotherapy using a combination of antigen and TLR adjuvants alone or in conjunction with chemotherapy as a treatment strategy for tumor therapy. This research is expected to lead to the utilization of PLGA delivery systems as novel carriers for cancer immunotherapy.

Abstract Approved: _____

Thesis Supervisor

_____

Title and Department

_____

Date

PLGA MICROPARTICLE BASED VACCINE CARRIERS FOR AN IMPROVED AND EFFICACIOUS TUMOR THERAPY

by

Yogita Krishnamachari

A thesis submitted in partial fulfillment
of the requirements for the Doctor of
Philosophy degree in Pharmacy
in the Graduate College of
The University of Iowa

May 2011

Thesis Supervisor: Associate Professor Aliasger K. Salem

Graduate College
The University of Iowa
Iowa City, Iowa

CERTIFICATE OF APPROVAL

_____

PH.D. THESIS

_____

This is to certify that the Ph.D. thesis of

Yogita Krishnamachari

has been approved by the Examining Committee
for the thesis requirement for the Doctor of Philosophy
degree in Pharmacy at the May 2011 graduation.

Thesis Committee: _____
Aliasger K. Salem, Thesis Supervisor

_____
Maureen Donovan

_____
Jennifer Fiegel

_____
Douglas Flanagan

_____
Dale E. Wurster

To my parents

ACKNOWLEDGMENTS

First and foremost, I wish to acknowledge the overwhelming support extended to me by my thesis advisor, Dr. Aliasger K Salem during the course of my graduate studies. Without his solid support I would not have been able to complete my dissertation as smoothly as I did. He was always readily accessible and provided all the logistic support towards execution and completion of this research project. With his profound knowledge in the subject he instilled tremendous confidence in me to keep the project moving and evolving.

I would also like to thank Dr. George Weiner for assistance in bringing this collaborative project together. His insights and suggestions were of tremendous value to this project and helped improve the design and implementation of the current work. I would like to thank my committee members Dr. Maureen Donovan, Dr. Jennifer Fiegel, Dr. Douglas Flanagan and Dr. Dale E. Wurster for their direction and advice towards the development and completion of my research. Their inputs and valuable suggestions during my thesis proposal defense and continued support thereafter added a new dimension of analysis and perspective to this project.

This research could not be undertaken without the help of all of the current and former members of the Salem Lab. Special thanks to Dr. Sean Geary and Dr. Caitlin Lemke for all their help with the project. Their expertise on immunology gave the current study a perspective in the right direction and helped strategize the experimental designs, research methodologies and analysis in the right direction. In addition to providing strong scientific support, they made the lab such a lively place with long relaxing stress buster chats, fun get-togethers and dinners. Former members Dr. Aiman Abbas, Dr. Jessica Graham, Dr. Janjira Intra and Megan Pearce aided in my early training in the lab and guided me in navigating through graduate school. Current lab members Dahai Jiang, NaJung Kim, Vijaya Joshi, Sheetal D'mello, and Kristan Sorenson have been a pleasure to work with, and have been helpful and encouraging with my research work. I have no

doubt that without these friendships formed with my colleagues, I would not have been able to work to the best of my abilities, and the ride surely would not have been as enjoyable.

I would like to extend a very special thanks to Dr. Jeff Reist and the entire team of the Pharm. D program for being instrumental in providing financial assistance during the first two years of my graduate studies. The financial support was an invaluable asset that helped ease a lot of monetary concerns and helped me continue my graduate studies smoothly. I would also like to extend my heartfelt gratitude to Dr. Keith Guillory for awarding me with a fellowship that helped me pursue my thesis with full focus and helped me put in increased time and efforts towards it.

I would also like to thank my family and friends for all of their love and support through the graduate school process. My parents have been the biggest support system all these years and without their love and encouragement I would not have seen this day in my life. Words are not enough to describe the precious moments I have spent with them all these years and all the love, happiness and support they have showered upon me. They have been the guiding light leading to my destination, helping me overcome every impediment that I have faced restoring my smile and confidence each time. My friends in the department, who made this journey a very pleasant one and for always being there in every moment of cheer and distress. A very special word of thanks to my friends Maya Bhavik and Vijaya who have been with me through this journey very closely and who made my stay in Iowa an extremely memorable one and giving me priceless moments of friendship that I will cherish through my life.

Last but by no means the least, I would like to thank University of Iowa and the Division of Pharmaceutics and translational therapeutics for giving me an excellent opportunity to fulfill my dreams and get a degree that I had always hoped to earn.

ABSTRACT

Cancer is a collection of diseases that is characterized by an uncontrolled proliferation of aberrant cells. The conventional treatment strategies including chemotherapy and radiotherapy prove detrimental to healthy cells and are unable to combat primary and secondary metastases. Hence immunotherapy is gaining momentum in cancer clinics and translational research labs as an alternative safer and more efficacious approach to tumor therapy. Vaccines based on antigen alone lack the ability to optimally activate the antigen presenting cells (APCs) including dendritic cells (DCs) to generate significantly greater antigen-specific T cell responses. A typical strategy to overcome this limitation has been the use of adjuvants in order to improve the immunogenicity of the vaccines. A newer class of adjuvants called toll like receptor (TLR) ligands recognize pathogen associated molecular patterns (PAMP) and thus elicit a Th-1 polarized response.

The hypothesis of the current research is that co-delivery of antigen and adjuvant in a microparticulate carrier will elicit a strong cell-mediated immune response conferring anti-tumor immunity. Furthermore, we proposed that a combination of TLR ligands when co-delivered with an antigen will be able to mount a synergistic anti-tumor response in comparison to the delivery of antigen alone. There were three primary objectives of the study; 1) Fabrication, process design optimization and characterization of antigen and adjuvant co-loaded microparticles (MP), 2) Study the ability of the MP fabricated in step 1 in eliciting a potent immune response in a murine model by various routes of administration and 3) Study the effect of the various treatment as prophylactic and therapeutic cancer vaccines in a murine tumor model.

Objective 1 was achieved by optimizing various process parameters including PLGA type and concentration, surfactant concentration and modification of a previously reported double emulsification solvent evaporation technique. Process optimization lead to the development of the following 5 treatment groups, a) Empty

PLGA MP, b) OVA PLGA MP, c) OVA + CpG PLGA MP, d) OVA + poly I: C PLGA MP and e) OVA + CpG + poly I:C tri-component PLGA MP. The optimized microparticles exhibited a mean particle size of 1.5 µm with a smooth spherical surface and a desirable biphasic release pattern of the entrapped components. Results from step 2 indicated the ability of the co-delivery and the tri-component systems to generate several fold higher immunostimulatory response in comparison to the group treated with antigen alone. Of the two routes of administration tested, the intraperitonial (i.p) route gave the strongest response followed by intramuscular (i.m) route. A synergistic antibody response was observed upon vaccination with the tri-component model. Prophylactic vaccination studies showed that the co-delivery and tri-component system affording the strongest protection against aggressive tumor growth. The therapeutic studies also indicated enhanced tumor protection and 2-fold improvement in survival times when the mice vaccinated with the co-delivery and tri-component MP carriers in comparison to vaccination with microparticles loaded with antigen alone. The carriers also showed strong evidence for the generation of anti-tumor immunogenic memory.

In summary, the current study has laid an interesting premise for the use of immunotherapy using a combination of antigen and TLR adjuvants alone or in conjunction with chemotherapy as a treatment strategy for tumor therapy. This research is expected to lead to the utilization of PLGA delivery systems as novel carriers for cancer immunotherapy.

TABLE OF CONTENTS

LIST OF TABLES

LIST OF FIGURES

LIST OF ABBREVIATIONS

APCs: Antigen presenting cells

BCA: Bicinchoninic acid

BMDCs: Bone marrow derived dendritic cells

CFA: Complete Freund's adjuvant

CpG: Cytosine-phosphate-guanine

CTLs: Cytotoxic T-lymphocytes

CTX: Cyclophosphamide

DCs: Dendritic cells

DOX: Doxorubicin HCl

dsRNA: Double stranded RNA

EE: Entrapment efficiency

ELISA: Enzyme linked immunosorbant assay

FACS: Fluorescence activated cell sorting

HBV: Hepatitis B vaccine

IFN-γ: Interferon-γ

IL: Interleukin

i.m: Intramuscular

i.p: Intraperitonial

mDCs: Myeloid dendritic cells

MHC: Major Histocompatability Complex

MP: Microparticles

MPLA: Monophosphoryl lipid A

NK: Natural killer cells

OVA: Ovalbumin

PAMP: Pathogen associated molecular patterns

PBS: Phosphate buffered saline

pDCs: Plasmacytoid dendritic cells

PLGA: Poly (lactide-co-glycolide)

Poly I:C: Polyinosinic-cytidylic acid

PRR: Pattern recognition receptors

s.c: Subcutaneous

ssDNA: Single stranded DNA

SEM: Scanning electron microscopy

TAAs: Tumor associated antigens

Th: T-helper cells

TLR: Toll-like receptor

TNF-α: Tumor necrosis factor-α

CHAPTER 1: INRODUCTION AND BACKGROUND

Cancer- Introduction and current treatment strategies

Cancer is a group of diseases that is characterized by uncontrolled proliferation and spread of aberrant cells. It is an insidious disease that originates from mutant DNA sequences that reroute crucial pathways that regulate tissue homeostasis, cell survival and cell death (1). The causes that trigger carcinogenesis are both external and internal. External include tobacco, chemicals, radiation, infectious organisms and internal that includes mutations, hormones and immune conditions. The development of most types of cancer requires several steps that occur over a prolonged period of time. One out of every eight deaths worldwide is due to cancer. According to the ACS Global Cancer Facts and Figures 2007, cancer causes more deaths than AIDS, tuberculosis and malaria combined. By the year 2050, the global burden is expected to grow to 27 million new cancer cases and 17.5 million cancer deaths (2).

Cancer staging is an important step in determining the choice of therapy and assessing the resulting prognosis (2). Staging describes the extent or spread of disease at the time of diagnosis. Stage is usually based on the size and location of primary tumor and whether or not metastasis has occurred. Stage is typically characterized as local if cancer cells are confined to the organ of origin, regional if there is aberrant cell growth in the neighboring areas and distant if they have spread from the primary site to distant organs (2).

The conventional treatment strategies for cancer include chemotherapy and radiation therapy. Radiation therapy is often combined with surgical intervention (3, 4). Although chemotherapy is usually the first line of treatment for most cancer types and enjoys a reasonable amount of success it suffers from several drawbacks. The most significant drawback is the inability to treat metastasis and tumor reoccurrence post initial treatment (5). A study by Brusamolino et al. showed that even in the most responsive

tumor in patients with Hodgkin's disease, the success rate of chemotherapy did not exceed 20% and virtually all patients showed signs of relapse (6). Secondly, chemotherapy being an intense treatment regimen is highly unsuitable for patients with underlying medical problems including heart diseases, renal failure and diabetes. Finally, even the most responsive tumors are susceptible to resistance after drug exposure making them unresponsive to chemotherapy. The resistance to chemotherapy is induced by the presence of multidrug resistance proteins called MRPs that are widely expressed in epithelial tumors. These proteins promote drug efflux and thus confer resistance to most anthracyclines, methotrexate, 6-mercaptopurine and campothecin derivatives; the drugs that are routinely used in cancer chemotherapy (7, 8). To combat drug resistance and toxicity issues, chemotherapy is often integrated with radiotherapy as a treatment alternative.

Radiotherapy refers to the use of radiation as a means for treating cancer. A beam of radiation is attenuated as energy is deposited along the radiation beam. High doses of radiation kill cells and prevent them from growing and dividing. However, this results in considerable irreversible damage to healthy cells (9). The biggest challenge in radiotherapy to date remains radiation dose optimization and precise control of radiation targeted to the region of cancerous cells. Although several computational models are being developed to overcome this challenge, clinical implementation still seems a distant dream due to the complexity in model formulation and the large patient size.

Owing to the critical challenges posed by chemotherapy and radiotherapy, the need for a more efficacious and less harmful cancer therapy still exists. Tumor vaccines and immunotherapy are attractive alternatives to conventional cancer treatments and have been increasingly investigated over the past two decades (5, 10, 11). The developing area of immunotherapy, in which the body's own immune system is activated to fight cancer, is particularly attractive (12). Immunotherapy targets tumor-associated antigens (TAAs)

and tumor-specific antigens (TSAs) that are specific to cancer cells thereby sparing healthy tissue and organs.

Immunotherapy as an approach to cancer treatment

Significant advances in cellular and molecular immunology have provided greater understanding of the interaction mechanisms between tumor and immune cells. This has lead to the development of strategies that can harness this understanding and translate these into novel therapies. The first report of successful immunotherapy for tumors was in 1881, when William Coley used bacterial toxins to obtain positive responses in sarcomas (11). The occurrence of cancers even in the presence of a functional immune system did lead to several doubts about the role of the immune system in combating cancer. Recent studies provide conclusive evidence to the development of immunotherapy in control of malignancy (13-19). An overview of the fundamentals of immunobiology is provided in the subsequent sections for a better understanding of the role of immunotherapy in cancer treatment and the specific aims of this research study.

The innate immune system comprises of cells and mechanisms that defend the host from any infection in a non-specific manner unlike adaptive immunity that confers lifelong protective immunity to re-infection from the same pathogen (20). Cells of the innate immune system are responsible for surveying the host for presence of any foreign material and exert an intrinsic anti-tumor effect. This occurs through induction of DNA damage by the generation of free radicals, cyclooxygenase-2 up-regulation and promotion of tissue angiogenesis and tissue remodeling (12, 21, 22). However, the innate immune response is not always sufficient to cure the disease. Therefore the utilization of the body's adaptive immunity is crucial in the development of immunotherapeutic vaccines. A critical component of the adaptive immune system is the antigen presenting cells (APCs) called dendritic cells (DCs). DCs play an important role in tumor antigen recognition, processing and subsequent stimulation of cytotoxic T-lymphocytes. These

cells reside in the bone marrow in an immature state with high phagocytic activity. Immature DCs capture antigen and subsequently migrate to the lymphoid organs and initiate an adaptive immune response by the B and T cells (23, 24). A DC lifecycle has been schematically shown in Figure I-1 describing the various stages starting from maturation until their apoptosis (24). Another type of immune cells that make up the body's immune system is the effector cells that include natural killer cells (NK), B and T-lymphocytes. Natural killer (NK) cells are a type of cytotoxic lymphocytes that kill tumor and virus-infected cells by perforating the cell membrane. B cells produce neutralizing antibodies that recognize foreign antigens by a complement activation pathway. The T-lymphocytes are responsible for orchestrating a cell-mediated immune response that plays a vital role in cancer immunotherapy and tumor elimination (25). The two types of T-lymphocytes include the CD4+ or helper T cells, and CD8+, also called cytotoxic T-lymphocytes or CTLs. CD4+ T cells are necessary to activate other immune cells, including B cells to produce antibody response and the CD8+ T cells. The CTLs directly target the antigen specific tumor cells and induce cell lysis by apoptosis that involves the role of several cytokines including interferon-γ (IFN-γ) (12).

The T-lymphocytes only respond to antigen that is bound to the Major Histocompatibility Complex (MHC) class I or II on an APC. Macrophages and DCs take up the antigen and present it on their surface as a marker. Presenting the antigen as a marker in this fashion directs effector T cells to recognize this marker in context of either MHC class I or class II and in turn activate CD4 and CD8 T-lymphocytes respectively (12). A T cell mediated immune response pathway has been shown in Figure I-2. A secondary pathway for tumor immunotherapy consists of the humoral immune system. The antibody response that is generated in response to an antigen is termed as humoral immunity. B cell activation results in production of antibodies that can bind to immunogenic cell surface proteins present on the surface of tumor cells and initiate complement mediated cell lysis. They may also induce apoptotic signals and/or increase

immunogenicity by facilitating an increased uptake and presentation of TAAs by the APCs.(12) Therefore enhancing B cell response *in-vivo* has the potential to generate a strong anti-tumor activity.

Mechanism of tumor recognition by immune system

Several theories have been proposed to explain the concept of immunosurveillance and the relation between immunobiology and cancer therapy. The initial hypothesis put forward by Ehrlich et al. stated that T cells constantly surveyed host tissues for nascently transformed cells and thus enabled recognition and apoptosis of primary tumor cells. Following this, Matzinger et al. put forth the "danger" model of immune activation. After considering several mechanisms for immunosurveillance, Dunn et al. finally expanded all the hypotheses to elucidate the role of innate and adaptive immunity in tumor immunotherapy (18). This model emphasizes the need of a second signal or co-stimulatory signal alongside the signal generated by the presence of tumor associated antigen. The secondary signal provides the stimulatory impetus for B and T cell activation that induces a cell-mediated cytotoxic immune response. The need to develop such a delivery system that can simultaneously provide the signal and co-signal formed the basis of this research study and our proposed hypothesis. Janeway et al. suggested that these co-signals could be triggered by activating the APCs via pattern recognition receptors (PRR) that bind to specific classes of foreign antigens (26). Such PRR specific ligands have been studied extensively in our current work and are described in greater detail in the subsequent sections.

Antigen and adjuvants for immunotherapy

Antigens

Tumor antigens are foreign proteins produced in tumor cells that triggers an immune response in the host (12). These are useful in identifying tumor cells and are

potential candidates for use in tumor immunotherapy as DCs have the ability to phagocytose these tumor-associated antigens (TAAs). Internalized antigen is processed into its constitutive peptides and is then loaded onto either MHC class I or II molecules. Typically intracellular antigens are presented in context of MHC class I and extracellular ones are presented in terms of MHC class II. The entire process of antigen uptake, degradation into peptide fragments and loading is called antigen presentation (27). However, peripheral DCs present antigens quite ineffectively. A co-signal from another source constituting a danger signal is thus required to induce DCs to enter a developmental program called maturation which transforms DCs into efficient APCs and T cell activators (28).

Adjuvants

Adjuvants are immunological substances when added to vaccines stimulate the immune system's response to the target antigen (29). The adjuvants serve to increase the efficiency of antigen uptake, intracellular transport and degradation and intracellular traffic of MHC class molecules. This cascade makes the DCs the most potent APCs and the only ones capable of activating T lymphocytes. These adjuvants function by either promoting a Th-1 or a Th-2 type of immune response. The next section gives a general understanding of these two subsets of T cell response and the need to induce a Th-1 biased response for tumor immunotherapy.

Th-1 and th-2 pathways in immune response

The antigen specific activation of effector T cells is aided by co-receptors on the T cell surface that distinguish between the two classes of MHC molecules. MHC class II specific T cells express the CD4 co-receptors which have specificity for MHC class II molecules. Furthermore, the CD4+ cells mediate either a Th-1 or a Th-2 subset of immune response based on the profile of cytokines produced (30). Although many factors

influence the "Th" differentiation, the most important factor is the cytokine environment. Studies by Hung et al. showed that interferon-γ (IFN-γ) and interleukin-12 (IL-12) are the main cytokines promoting Th-1 differentiation. Using the same *in-vitro* priming system, interleukin-4 (IL-4) was demonstrated to have the greatest influence in driving Th-2 differentiation (31, 32). Based on these findings, it can be concluded that the only means to induce a polarized Th-1 or Th-2 pathway is by use of appropriate adjuvants that can alter the cytokine environment. Stimulating macrophages and NK cells to secrete IFN-γ and IL-12 is an effective means to induce Th-1 pathway. Thus a Th-1 pathway can be induced by a stimulus that causes natural killer (NK) cells to cause IFN-γ production and IL-12 production by activated macrophages. In contrast, a Th-2 response is directed more at the secretion of specific antibodies and thus is relatively less important for tumor therapy. A Th-2 pathway can be induced by stimulating basophils and mast cells. The adjuvants that prime a Th-2 polarized response include alum and the adjuvants that provide the best stimuli to prime a Th-1 selective response are adjuvants called Toll-like receptor (TLR) ligands. These are described in detail the following sections (33-35).

Role of Th-1 cytokines in tumor resistance

As described above, early activation of type-1 innate effector cells such as DCs and NK cells which produce Th-1-inducing cytokines are essential for eliciting a Th-1-dependent tumor-specific CTL. The development of an efficient tumor-vaccine protocol that can elicit both type-1 innate and acquired immunity in tumor-bearing hosts would provide a novel strategy to induce complete cure of tumors.

Immune responses in tumor therapy require cytokine support from T-helper cells (CD4+). Several *in-vivo* studies have been used to demonstrate the role of cytokines in vaccine induced anti-tumor activity. Production of IFN-γ has been shown to be the most important cytokine in mitigating anti-tumor activity. IFN-γ plays an important role in the anti-proliferative activity of tumor cells. It also promotes both innate and adaptive

immune response. IL-12 is another important cytokine that promotes a cell-mediated adaptive immune response (33, 36). Deficiency of this cytokine increases susceptibility to chemically induced cancers. These studies showed the need to induce a Th-1 biased response for targeted tumor immunotherapy. The two pathways have been depicted in Figure I-3 (25).

TLR and the Toll pathway and role in Th-1 differentiation

The innate immune system has evolved to detect and defend the host from infections. The role of toll receptors in innate immunity was first described in Drosophila. "Drosophila Toll" is a transmembrane receptor that plays a role in host defense in fungal infections (29). Subsequently, a family of mammalian proteins structurally related to drosophila Toll was identified and collectively referred to as the Toll-like receptors (TLR). The TLR family consists of 10 members. Some of these are localized to the surface of the cells and the others reside in the endosomal compartments within the cells. These receptors identify pathogen associated molecular patterns (PAMP) and elicit a danger signal that alerts the immune system of a pathogen invasion (34, 36). Our study mainly focuses on TLR3 and TLR9 receptors that are located in the endosomal compartment and their associated ligands.

TLR3

Toll-like receptor 3 (TLR3) also known as CD283 (cluster of differentiation 283) is a protein that is encoded by the *TLR3* gene in humans and mice. TLR3 is a member of the Toll-like receptor family of pattern recognition receptors of the innate immune system. TLR3 plays a fundamental role in pathogen recognition and activation of innate immunity. This receptor is most abundantly expressed in placenta and pancreas, and is restricted to the dendritic subpopulation of immune cells. It recognizes double stranded RNA associated with viral infection, and induces the activation of nuclease factor; NF-κB

and the production of type I interferons. Double stranded RNA (dsRNA) is a viral product that is produced during the viral replication cycle. This forms an important intermediate in RNA synthesis. This is a ligand for TLR3. Binding to TLR3 by dsRNA induces of IFN- α and β which exert an anti-viral and immunostimulatory activity (37). It also promotes maturation of dendritic cells. Immunostimulatory activity of dsRNA is believed to be elicited by activation of dsRNA dependent protein kinase to induce a Th-1 response. Hence, ligands like natural or synthetic dsRNA motifs that bind specifically to TLR3 receptors play a potential role in tumor therapy (38).

TLR9

Toll-like receptor 9 is a protein that in humans is encoded by the *TLR9* gene. TLR9 recognizes unmethylated CpG sequences in DNA molecules. CpG sites are relatively rare (~1%) on vertebrate genomes in comparison to bacterial genomes or viral DNA. TLR9 is expressed by numerous cells of the immune system such as dendritic cells, B lymphocytes and natural killer (NK) cells. TLR9 is expressed intracellularly, within the endosomal compartments and functions to alert the immune system of viral and bacterial infections by binding to DNA rich in CpG motifs. TLR9 signals leads to activation of the cells initiating pro-inflammatory reactions that result in the production of cytokines such as type-I interferon and IL-12Bacterial DNA is a potent activator of immune cells. The critical involvement of TLR9 in recognition of bacterial DNA was demonstrated using TLR9 deficient mice (34, 39, 40). The immunostimulatory activity of bacterial DNA can be attributed to the presence of unmethylated CpG motif (Figure I-4). CpG activates DCs to produce a cytokine like IL-12 leading to development of Th-1 polarized immune responses (29).

Particulate vaccine carriers

The use of micro/nanoparticulate pharmaceutical carriers to enhance the efficacy of therapeutic agents is being increasingly investigated and many such carriers have been successfully developed to date (41-51). In tumor immunotherapy, the primary cargo of nanocarriers are peptides/proteins or DNA encoding tumor-associated antigens (TAAs). TAAs are proteins inappropriately or aberrantly expressed by tumor cells but not generally found in normal tissue. It is now widely accepted that most tumors express TAAs and it has been demonstrated through multiple animal tumor studies that the immune system can be triggered to recognize these TAAs as non-self and thereby affect a specific anti-tumor response. From an immunotherapeutic perspective, it would be desirable to develop novel carriers, carrying TAAs that can either actively or passively target DCs resulting in the generation of a strong tumor-specific cytotoxic CD8+ T lymphocyte (CTL) response (12, 36, 46). The targeting and consequent activation of DCs is of particular importance as DCs are initiators of immune responses. In order to stimulate a potent anti-tumor CTL activity, it is necessary to activate DCs to generate a pro-inflammatory (Th-1) response. Such a response involves the generation of IFN-γ producing T lymphocytes. Additionally, micro/nanocarriers can be designed to target the tumor itself resulting in a site-specific accumulation of the TAA and adjuvants and provide a controlled release for development of long-term antigenic memory. Micron sized or nanoscale carriers have the potential for addressing all the above mentioned goals due to their physico-chemical properties and ease of modification to improve tumor targetability. Such carrier systems offer unique advantages over the administration of the soluble form of the antigen. These include: 1) protection of the antigen and adjuvant from premature enzymatic and proteolytic degradation, 2) enhanced uptake of antigen and adjuvant into targeted tumor tissue either by the EPR effect or via active targeting with the use of ligands, and 3) enhance cellular uptake by DCs to trigger a strong immunostimulatory cascade. Furthermore, these nanoscale carriers offer the unique

advantage of multi-component loading which is of considerable significance particularly in immunotherapy where simultaneous delivery of antigens, immune-adjuvants and targeting ligands is optimal.

Additionally, due to their large surface area, these carriers can be surface functionalized with relative ease. The smaller size affords a large surface to volume ratio, thus increasing the efficiency of reaction kinetics and multiple surface derivatizations (52, 53). The fabrication of such multifunctional nanocarriers with controlled properties often requires the conjugation of proteins, peptides, polymers, cell-penetrating moieties, reporter groups and other functional and targeting ligands to the carrier surface. This modification is usually simple and in most cases proceeds via a non-covalent electrostatic interaction or by covalent conjugation of proteins and peptides onto the nanocarrier surface. Thus, the simplicity of design and use, coupled with multifunctionality makes nanoparticulates a versatile and attractive carrier system for tumor vaccines and immunotherapy. Examples of such carriers for vaccine therapy include liposomes, adenovirus based particles, particles prepared from biodegradable or natural polymers and inorganic particles (13, 16, 47, 54-61).

Although viruses are highly immunogenic they can be excessively immunogenic making them unsuitable for repetitive use or gene therapy. They also carry the risk of reversion to virulent form and potential contamination with replication competent virus. Another limitation with adenovirus (Ad) vaccines is the fact that adenoviruses are quite prevalent and most people have neutralizing antibodies against the most common serotypes, such as Ad5(62). Liposomes are another type of particulate vaccine carriers that can be formulated to be biodegradable and biocompatible. They are also used to effectively target APCs of spleen and liver macrophages. However, they do have a few limitations that include; suboptimal encapsulation of water soluble antigenic proteins, rapid clearance by the reticulo-endothelial system (RES), expensive to manufacture and

concerns of stability over storage (56). Cationic liposomes may also be associated with concerns of cellular toxicity (63).

PLGA based particulate vaccines are biodegradable and are an attractive delivery system for tumor vaccines. They possess several advantages that include; efficient passive DC targeting, high storage stability, ease of scale-up for pharmaceutical manufacture, prolonged pulsatile release and can deliver antigens that are presented by both MHC class I and MHC class II pathways (4, 27, 52). They do suffer from a few disadvantages that include production of an acidic microenvironment upon degradation. Such an acidic microenvironment can cause detrimental effects on the entrapped protein and antigens that include denaturation and aggregation. However such effects can be readily overcome by incorporation of neutralizing agents such as magnesium hydroxide and calcium carbonate. Another disadvantage associated with microparticle carriers is fabrication technique induced antigen/protein instability. The most commonly used fabrication techniques include homogenization and sonication. The heat and mechanical shear generated during this process can result in protein denaturation particularly for proteins with low thermal stability such as OVA. Low temperature fabrication conditions including use of an ice-bath and lower agitation speeds ensure protein stability during manufacture.

However, such process induced denaturation is not of significant concern in this work as we mainly focus on entrapment of OVA to function as an immunogen. Antigen stability only depends on the preservation of the small fragment of the epitope of recognition. The epitope is typically preserved even in a denatured protein thus reducing concerns of antigen instability caused during fabrication. However, enough care needs to be taken to maintain antigen in solution and prevent aggregation during the emulsification step of fabrication.

Choice of antigen and adjuvants

OVA as a protein antigen

Although almost any foreign structure can be recognized by antibody as an antigen, usually only proteins elicit a fully developed adaptive immune response (12). Proteins possess the ability to engage T cells which contributes to a strong antibody response and is responsible for immunological memory. Proteins engage T cells because the T cells recognize antigens as peptide fragments of proteins bound to MHC molecules and immunological memory is produced as a result of the initial immunization. This evokes the primary immune response termed as priming. Upon subsequent challenge with the same antigen, the immune system mounts a more potent response (12).

Ovalbumin (OVA) is a glycoprotein and the major constituent of egg white. It has a MW of 45 kDa and has an iso-electric point at pH 4.6 (64). It is a large and complex protein and hence has a more distant relationship to self proteins and is more likely to induce an immune response. It also contains a large fraction of peptides that are structurally dissimilar to self peptides that binds strongly to the MHC molecules. Another advantage of using OVA as a model antigen is that the immune response can be quantified thoroughly. Most detection techniques and immunoassays that have been developed to study an immune response have been modified to be OVA-specific making quantification easy and reliable.

CpG as a TLR9 adjuvant

CpG with sequence patterns like those found in bacterial DNA activates natural killer cells to secrete interferon-γ (IFN-γ) and generate a cell-mediated immune response (65). The specific sequence motif present in bacterial DNA that is responsible for triggering these immune responses is the unmethylated CpG dinucleotide flanked by two 5′ purines and two 3′ pyrimidines (Figure 4) (65). CpG is taken up by cells via adsorptive endocytosis and binds to the toll-like receptor 9 (TLR9). The immune response to TLR9

stimulations occurs in two phases: the first is activation of antigen-non specific innate immunity which in turn triggers an antigen-specific adaptive immunity involving the T lymphocytes.

TLR9 receptors are present within the endosomes in the intracellular compartment of B cells and plasmacytoid dendritic cells (pDCs). CpG triggers an immunostimulatory cascade inducing the maturation, differentiation and proliferation of multiple immune cells including B and T lymphocytes, macrophages, natural killer (NK) cells and macrophages that produce interleukin (IL)-1, 6, 12 and 18, interferon-γ (INF-γ) and tumor necrosis factor-α (TNF-α). Rapid induction of these immune responses and production of Th-1 related cytokines induces tumor cell death. The mechanism of tumor cell death following TLR9 activations by CpG follows three critical steps. First, purified B cells are activated when stimulated by CpG in the presence of antigen. Second, the increased expression of co-stimulatory molecules on B cells and other antigen presenting cells activate T cells. Finally it induces a Th-1 dominant cytokine environment in the secondary lymphoid organs leading to tumor cell death (4).

The distinguishing feature of CpG used as adjuvants is their unsurpassed induction of strong Th-1 responses. In a study by Cheng et al., a comparison between the efficacy of 19 different vaccine adjuvants was studied in a mouse model using mucin-1 (MUC1) peptide as a tumor antigen. CpG induced the most Th-1 biased immune response with the highest levels of IFN-γ secretion (29). Additionally, in comparison to the harsh local inflammatory effects of well characterized adjuvants like the complete Freund's adjuvant, CpG is relatively safe (66). In another phase I/II dose escalation study by Cooper et al (67)., healthy volunteers were randomized to receive three i.m. injections of alum-adsorbed hepatitis B vaccine (HBV) or CpG at different doses. HBV surface antigen-specific antibody responses were detected earlier and reached substantially higher titers in the CpG recipients. HBV vaccination with CpG also rapidly induced protective antibody titers even in HIV-infected subjects who had previously failed to

attain protective antibody levels following treatment with a standard regimen of HBV vaccination (67-69).

The strong Th-1 adjuvant effect of CpG makes it an ideal candidate to use with tumor antigens in cancer vaccines.

Poly I:C as TLR3 adjuvant

Polyinosinic cytidylic acid; poly I:C, is a synthetic analog of double stranded RNA (dsRNA), with one strand each of poly(inosinic acid) and one strand of poly(cytidylic acid) with an average molecular weight greater than 75 kDa.(38) This acts as a viral recognition motif for TLR3 mimicking a viral infection. Stimulation of TLR3 results in activation of signaling pathways and production of pro-inflammatory and anti-viral cytokines inducing an antigen specific Th-1 polarized immune response.(38)

The CD4+ T cell response with poly I:C as an adjuvant is multifunctional as shown by Steinman et al. (70). T cells produced multiple cytokines such as IFN-γ, TNF-α and IL-12 in high amounts. Poly I:C also increased the production and proliferation of CD4 T cells (71, 72). Although poly I:C is being more recently studied as an adjuvant to enhance immunogenicity of a vaccine, no systematic studies have been done to date on a tumor model. Additionally, there have been no studies showing the impact of delivering the adjuvant in a sustained manner in a particulate carrier. To address these gaps in tumor vaccine models and with the ultimate goal of developing a vaccine for tumor therapy, we used poly I:C as an adjuvant in our study.

The promising result from the aforementioned studies has prompted us to evaluate CpG, poly I:C and antigens in particulate carriers with the ultimate goal of being able to develop a prophylactic and therapeutic cancer vaccine.

PLGA as a particulate vaccine carrier

Poly(D,L-lactic-co-glycolic acid (PLGA) and polylactide (PLA) are biocompatible and biodegradable polymers that have FDA approval for human use. (Figure I-5) (66, 73). PLGA and PLA particles have shown great potential for protein, peptide and DNA delivery over the last two decades. These particles are fabricated using techniques such as emulsification/solvent evaporation. Several studies have shown that careful control over the formulation parameters such as surfactant concentration and stirring speed can be used to optimize loading levels and particle size. The main advantages of using PLGA/PLA particles from a cancer vaccine/immunotherapeutic perspective, is that they provide a non-toxic, protective vehicle for co-delivery of antigens and adjuvant that can be released over a sustained period of time. In addition, these particles are efficiently internalized by APCs as they possess comparable dimensions to the pathogens that the immune system has evolved to combat. Particulate antigens in the size range of 0.1 – 10 μm can induce CTL responses through MHC class I cross-presentation of antigen via the phagosome-cytosol pathway of antigen presentation (4). The mechanism of cross-presentation is unknown, but appears to be independent of the chemical nature of the particle. Nevertheless, it has been specifically demonstrated that PLGA and PLA particles are capable of promoting cross-presentation of antigen in APCs (27).

The use of biodegradable particles in tumor immunotherapy has primarily involved PLGA particles and they are therefore the primary focus here. PLGA particles were originally used for parenteral drug delivery due to: 1) their capacity to protect their cargo from degradation and 2) their ability to prolong the release of their cargo. Early animal studies by O'Hagan et al. (74) with PLGA vaccinations showed that a single subcutaneous injection of OVA entrapped in, rather than surface-attached to PLGA particles about 1.5 μm in size was a superior immunogen than soluble OVA. Specifically, the mice vaccinated with OVA-PLGA particles had enhanced levels of

OVA-specific IgG which remained high for 1 year. These results were repeated by Uchida et al. (75) using OVA entrapped in PLGA particles with a mean size of 14 μm. This group also showed that only one subcutaneous administration was necessary to generate a maximal OVA-specific antibody response and that the PLGA-OVA particles were more effective at inducing responses than complete Freund's adjuvant (CFA) combined with soluble OVA (52). Similar results were obtained by a different group (Igartua et al.) using bovine serum albumin as the immunogen entrapped in PLGA particles that were 1 μm in size (76). Thus it is evident that PLGA particles possess an intrinsic adjuvant effect which has been largely attributed to: 1) the ability of the particle to protect the immunogen from rapid degradation and clearance, 2) the release profile of the protein where sustained release of the immunogen occurs for lengthy periods (> 30 days) and 3) the efficiency with which the PLGA particles are taken up by DCs. In addition, it may be that empty PLGA particles themselves have modest, yet significant, adjuvant properties, as it was demonstrated that they are capable of up-regulating a co-stimulatory molecule (CD80) on *in-vitro* cultured bone marrow-derived murine DCs (52, 53).

Preclinical studies by Hamdy S. et al. showed that PLGA particles are efficiently taken up by murine DCs *in-vitro*. The same study went on to demonstrate that the TLR4 ligand, monophosphoryl lipid A (MPLA), was significantly better at inducing maturation of DCs *in-vitro* when provided in PLGA particles rather than in soluble form. In addition, whilst MPLA alone had little effect on cytokine production by DCs, the co-delivery of MPLA with PLGA resulted in the production of high levels of proinflammatory cytokines (IL-6, IL-12 and TNF-alpha) while IL-4 and IL-13 expression remained low (77). We have evaluated the immune potency of PLGA particles (~2.4 μm in diameter) co-loaded with tumor lysate proteins (from the B16 murine melanoma) and CpG in an *in-vivo* mouse tumor model (78). Additionally, PLGA is biodegradable and is degraded by non enzymatic hydrolysis of the ester backbone under the conditions of the body fluids.

The degradation leads to the formation of lactic and glycolic acid (monomeric components) and finally gives carbon dioxide and water. The structure of PLGA and degradation pathway is depicted in Figure I-6.

In summary, the goal of this research is to develop a particle based vaccine for prophylactic and therapeutic treatment for cancer. The hypothesis and specific aims of this study are described in detail in the next chapter.

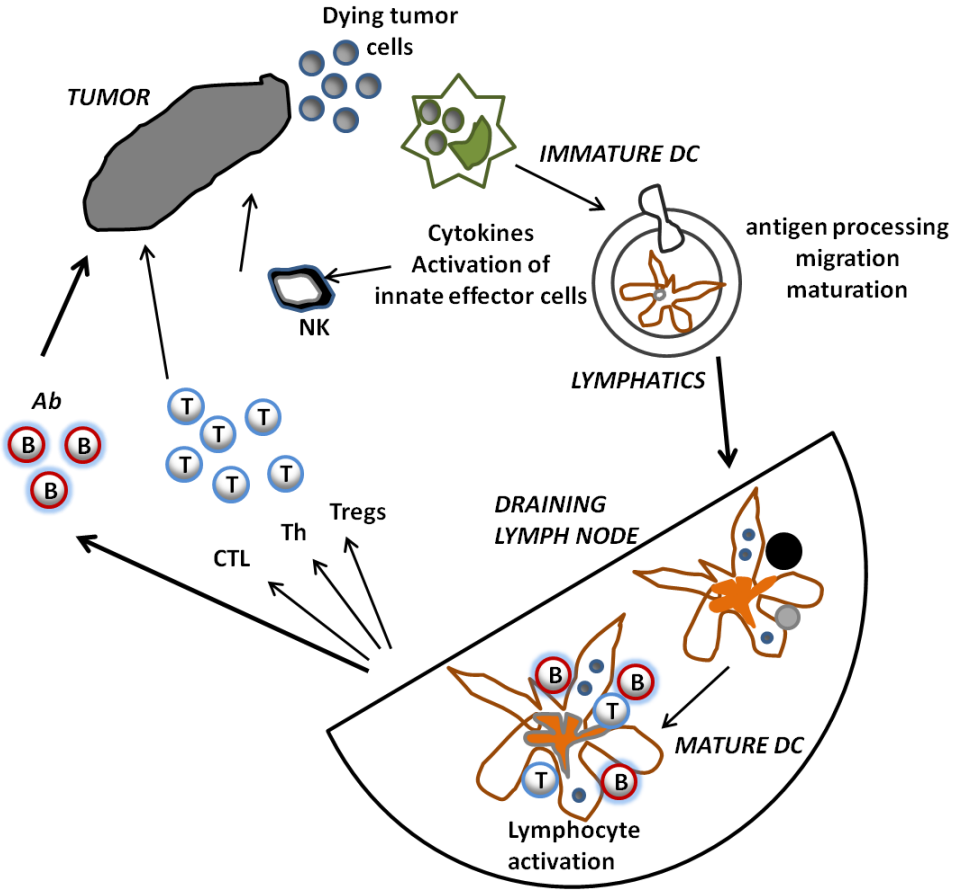

Figure I-1: Schematic of a dendritic cell (DC) lifecycle. (Adapted from 75). The life cycle of dendritic cells in the context of anti-tumor activity is shown here. Circulating precursor DCs enter tissues as immature DC where they can encounter dying tumor cells and their products. Upon tumor-cell recognition, DCs are activated and secrete cytokines. Cytokines secreted by DCs in turn activate effector cells of innate immunity such as macrophages and NK cells and migrate towards secondary lymphoid organs. These activated migratory DCs that enter lymphoid organs display MHC complexes, which recognize of non-self circulating antigen-specific T lymphocytes. Activated T cells help DCs for their terminal maturation, which allows lymphocyte expansion and differentiation leading to generation of effector cells and antibodies.

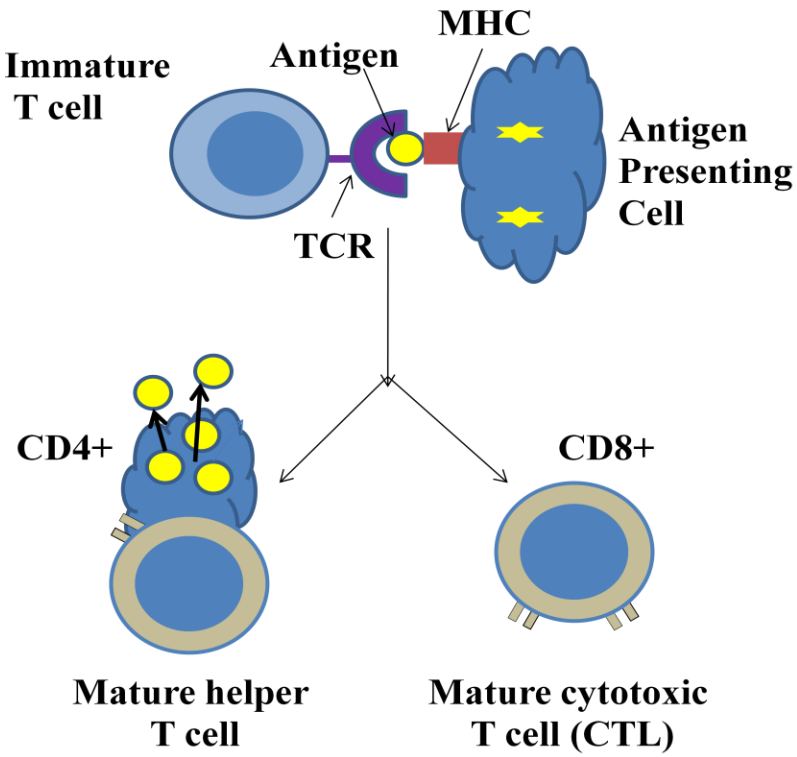

Figure I-2: Schematic of an immune response:
A T cell is activated when it encounters an APC, such as a dendritic cell or macrophage, which has encountered antigen and is expressing it on its surface in the context of an MHC molecule. Antigen presentation in context of MHC molecules to the T cell is necessary for it to mature into a specific T cell that is targeted against the antigen. Depending on the antigen presented (endogenous or exogenous), the T cell might mature into a CD4+ helper T cell, or a CD8+ cytotoxic T cell respectively.

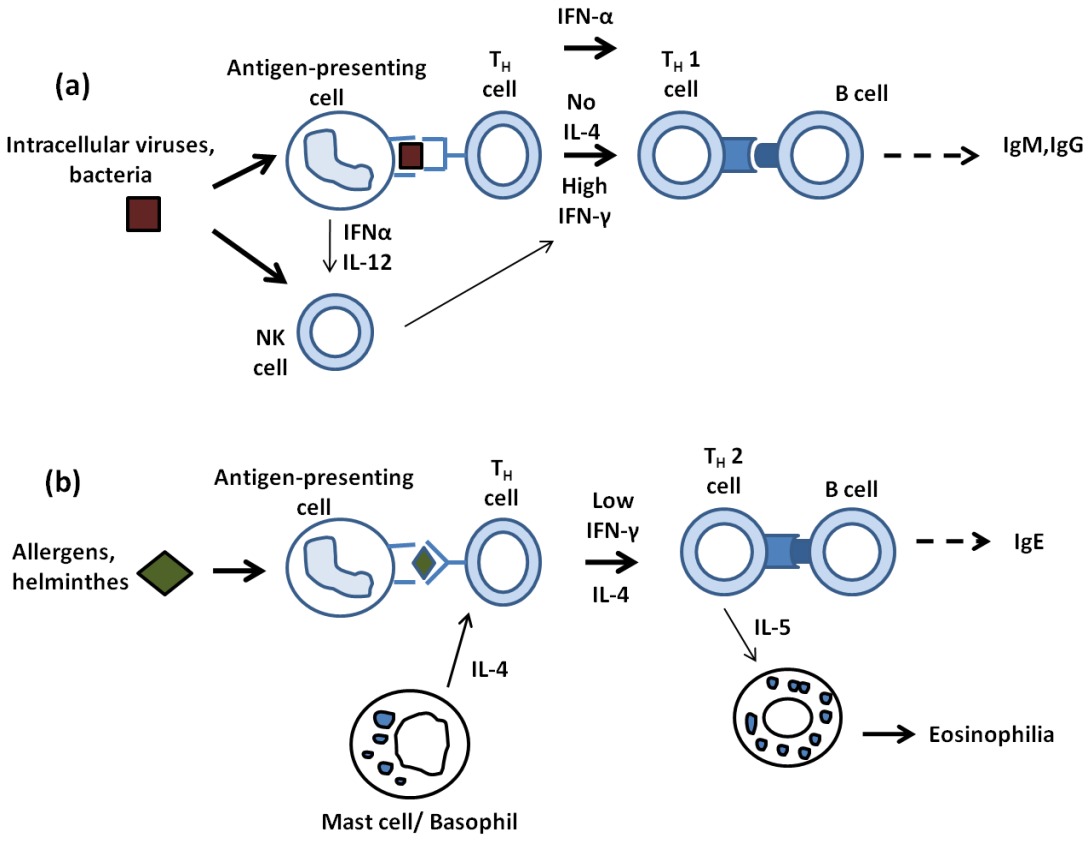

Figure I-3: The profile of CD4+ T cell response based on specific cytokine production that determines the phenotype (Th-1/Th-2) of subsequent immune response. (Adapted from 34).

5' TCCATGACGTTCCTGACGTT '3

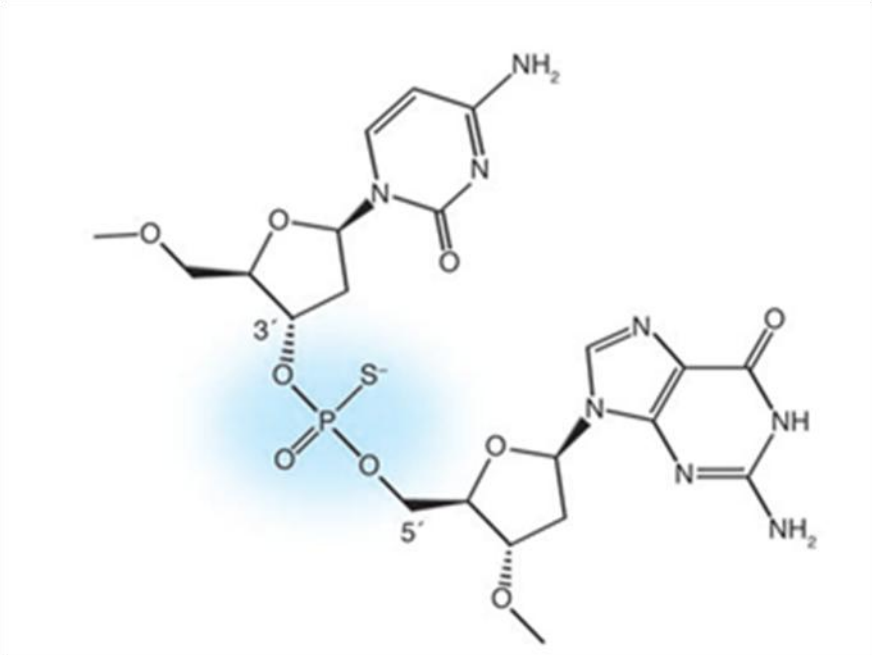

Figure I-4: Nucleotide sequence and phosphate backbone structure of CpG 1826. (Adapted from 65).

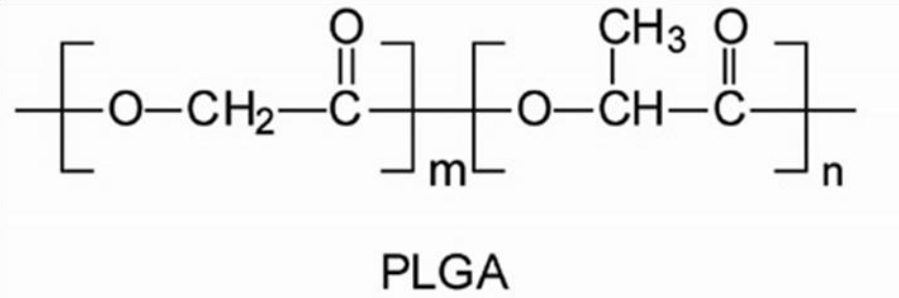

Figure I-5: Structure of poly-(D, L-lactide-co-glycolide) (PLGA).

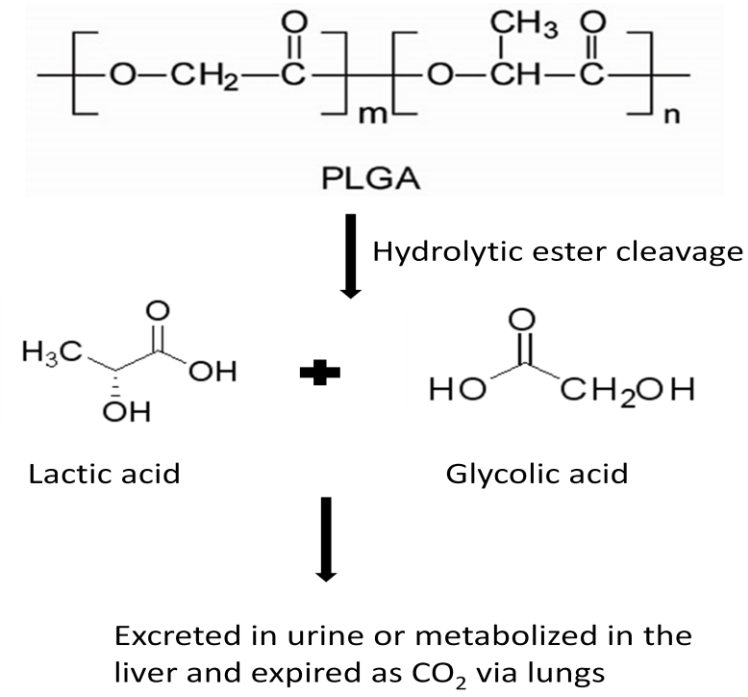

Figure I-6: Degradation Pathway of PLGA *in-vitro* and *in-vivo.*

CHAPTER II: HYPOTHESIS AND OBJECTIVES

Hypotheses

We have proposed two major hypotheses:

1. TLR3 and TLR9 adjuvants when co-delivered with an antigen in a particulate carrier will trigger stronger immunostimulatory anti-tumor activity in comparison to delivery of antigen alone either in solution or in particulate form.
2. A particulate delivery system capable of co-delivering both the TLR adjuvants along with the antigen will result in the combined detection of viral and bacterial associated molecular patterns. This will result in an enhanced antigen-specific stimulation of the immune system leading to an effective tumor immunotherapy.

Rationale for proposed hypotheses

1. When antigen is administered alone, it elicits strong Th-2 type immune responses. A significant shift in the isotype of antibody response can be achieved by co-administering the antigen and adjuvant (73). A recent study by our group showed that addition of CpG to a protein antigen showed a significant increase in production of IgG2a antibody, increasing the Th-1:Th-2 ratio over nine-fold (66). Additionally, studies by Mutwiri and colleagues have shown that delivery of CpG at the same site as antigen is essential for eliciting such a Th-1 polarized response. For example, co-administration of CpG and hepatitis B surface antigen (HBsAg) vaccine to the same site of the muscle significantly enhanced the antibody response. In contrast, when CpG was administered separately following the administration of the vaccine, it did not induce any significant improvement in immunostimulatory effects over the administration of vaccine alone (66). Although protein antigens and adjuvants including oligonucleotides, dsRNA are promising therapeutic tools in vaccine therapy, rapid cleavage by proteolytic enzymes and nucleases are impeding factors in

their effective activity. The half-life of CpG has been improved by synthesis of a nuclease resistant phosphothioate backbone (65). Although this synthetic molecule does show improvement in shelf-life there is still a need to improve stability. In a study by Malvy C. et al., the authors studied the intracellular degradation of oligonucleotides (ODN) and dsRNA. The percentage of intact ODN left at the end of 24 hours was less than 50% and dsRNA was about 60% (Figure II-1) (79, 80). This necessitates the need for delivery systems that can protect the antigen and adjuvants from pre-mature enzymatic degradation. Entrapment within the carrier system ensures localized delivery of adjuvant to the site of action affording protection from enzymatic degradation. Additionally, this serves as a controlled delivery vehicle to generate a long term immune response following a single administration, obviating the need for repeated delivery. The improved effects of a co-delivery approach can be attributed to a four component system: (1) TLR-adjuvant induced enhancement in APCs function, (2) TLR mediated activation of a cytokine cascade microenvironment that augments antigen specific immunity, (3) delivery of the antigen and adjuvant to the same APC and (4) the carrier system increasing protection of antigen and adjuvant against degradation and enhancing stability. This allows for the localization of a higher concentration of the antigen and adjuvant at the target site triggering a greater extent of cellular activation and immune response. The target immune response upon co-delivery of an antigen and adjuvant has been shown in Figure II-2 (4). Although there have been several papers describing the co-delivery of antigen and CpG in a PLGA particulate carrier, little attention has been given to optimize fabrication of such a system from a manufacturing, scale-up and cost-effectiveness standpoint. Therefore one of the primary objectives of this study was to optimize the microparticle fabrication process such that the loading of these expensive antigen and adjuvants is maximized. There has been no comprehensive study yet describing the

co-encapsulation of poly I:C along with a protein antigen in a particulate carrier as a delivery system for tumor immunotherapy applications.

It is well established that dsRNA and CpG are present during infection with large DNA viruses. Whereas it is well established that dsRNA is a significant PAMP produced during infection with large DNA viruses, recent evidence establishes unmethylated CpG DNA as a PAMP for large DNA viruses. Therefore, because CpG DNA and dsRNA are present during large DNA viral infection, Williams et al. predicted that dual recognition of these two PAMPs mimics viral infection, resulting in enhanced activation of the innate immune response (4, 81). Double-stranded RNA, which is recognized by TLR3 and CpG, which is recognized by TLR9 stimulate immune activities that are favorable for inhibiting tumor growth. DCs have shown distinct response pattern in terms of maturation and cytokine production to each of these individual TLR-adjuvants. Some of the earliest studies on TLR adjuvants showed that poly I:C, a TLR3 ligand, was found to be the most effective maturation stimulus for DCs. Additionally, activation of TLR3 is an essential component to generate a NK cell response to a viral infection. Furthermore, several studies have shown that CpG which is a TLR9 ligand has the most potential for enhancing a CD8+ cell mediated immune response which is critical for anti-tumor activity (71, 82). Recent studies by Gillanders et al. showed that naïve CD8 cells had detectable levels of TLR3 genes and hence treatment with a TLR3 ligand such as poly I:C could result in enhanced antigen-specific cytotoxic activity by a direct binding mechanism (83, 84). However, the cause of concern is that the distribution of these TLR receptors is highly species dependent. TLR3 receptors are more abundant in humans than in mice (85). Although TLR adjuvants individually may be ignored at certain low doses, Zhu et al. have proposed that the host may have evolved to recognize all these adjuvants when administered together as a combinatorial assault and possibly mount immune responses against these combinations in a synergistic manner (81).

However, such a hypothesis has not been explicitly explored so far. Hence, we propose that a combination of two or more TLR-adjuvants co-encapsulated with the antigen within the same microparticle carrier system could provide a synergistic immunostimulatory effect and the combination is likely to be capable of providing improved tumor clearance.

Specific aims

1. Fabrication of Ovalbumin (OVA)-loaded PLGA microparticles and characterization including particle size, entrapment efficiency (EE) and *in-vitro* drug release in phosphate buffered saline (PBS) pH 7.4.
2. Optimization of microparticulate fabrication process by studying the effect of key process variables and extrapolate the optimization results for fabrication of antigen adjuvant co-delivery carriers.
3. Study the ability of each of the antigen-adjuvant combination formulations to activate DCs to initiate an immune response.
4. Immunization studies in a mouse model and quantification of antigen-specific antibody response (humoral immune response) by ELISA
5. Prophylactic and therapeutic tumor challenge studies in a murine model for each of the antigen-adjuvant combination formulations.
6. Fabrication of a tri-component vaccine carrier with a single antigen and two adjuvants within the same microparticulate PLGA carrier and conduct studies under specific aims 3, 4 and 5 to study the ability of the system to induce synergistic immunostimulatory activity.

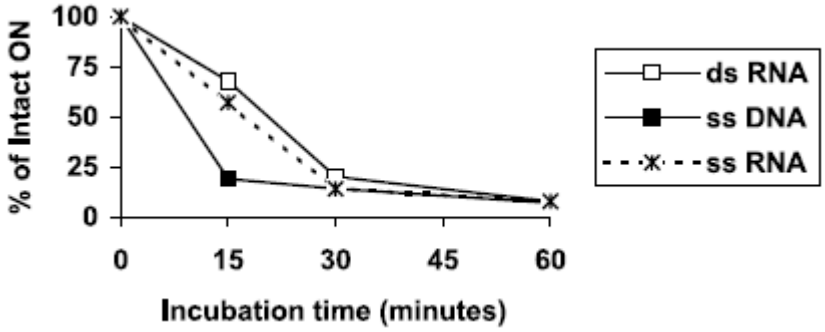

Figure II-1: Degradation kinetics of native single stranded oligonucleotide (ssODN) and double stranded RNA (ds RNA). Reproduced with permission from [77] Copyright©Elsevier B.V.

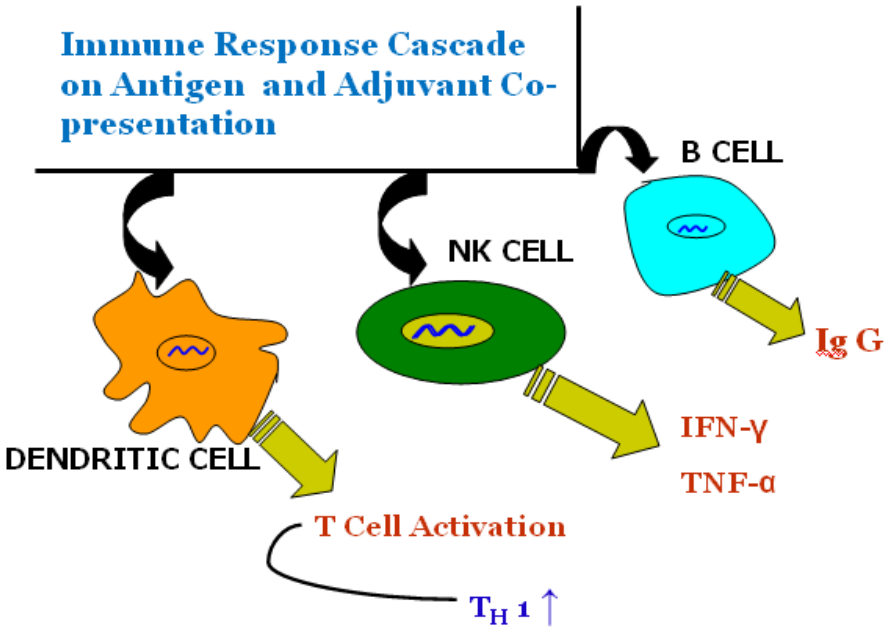

Figure II-2: Immunostimulatory cascade triggered upon co-presentation of an antigen and Toll-like receptor (TLR) ligand as an adjuvant.

CHAPTER III: DESIGN AND FABRICATION OF PLGA MICROPARTICLES AS A CARRIER FOR TUMOR ASSOCIATED ANTIGEN (TAA) AND ADJUVANTS FOR CANCER IMMUNOTHERAPY- EFFECT OF FORMULATION AND PROCESS VARIABLES

Introduction

Biocompatible microparticles have proved to very effective carriers for protein delivery (86). Poly (DL-lactide-co glycolide), commonly referred to as PLG or PLGA is a biocompatible polymer belonging to the class of hydroxyl esters. The hydrolysis of this material leads to the release of two acids that can be metabolized via the citric acid cycle (87, 88). The polymer has been hence used for many years for the production of biodegradable surgical sutures. Considering this material is well characterized and is approved by FDA for use in humans, this provides an obvious advantage for vaccine delivery. The biodegradability of PLGA microparticles as compared to non-biodegradable latex and polystyrene beads makes these a better carrier material for *in-vivo* applications. PLGA polymers can be converted into insoluble microparticles of a desired size range that can be loaded with therapeutic molecules. Several studies have shown that PLGA microparticles of appropriate size are efficiently taken up by mouse and human dendritic cells (DCs) and are slowly hydrolyzed so that prolonged antigen stimulation continues (89).

DCs have been reported to internalize a variety of particulate materials including apoptotic bodies, latex and polystyrene particles (90). As explained in the previous chapter, particulate antigens have been shown to be more efficient than soluble antigens for induction of cytotoxic T-lymphocyte (CTL) responses. PLGA itself has also been shown to augment the immune response thus serving as an adjuvant to the antigen that is encapsulated within this system. The adjuvant effects of PLGA microparticles were

studied by measuring the levels of DC activation markers. The up-regulation effects were at least comparable if not greater than that elicited by known adjuvants such as alum and complete Freund's adjuvant (89, 91, 92). The mild adjuvant properties of PLGA can be attributed to the hydrophobicity of the polymer and recognition of these anionic polymers by scavenger receptors on cell surface. Hydrophobicity of PLGA is a direct function of the lactide to glycolide ratio in the co-polymer. Higher lactide ratios render a higher degree of hydrophobicity and confer adjuvant properties to the polymer. Additionally, the adjuvant effect of PLGA is devoid of any injection site inflammatory shock effects associated with other conventional adjuvants. PLGA microparticle carrier also allows DCs to cross-present the antigen (93). As described in the previous chapter, exogenous antigens are typically presented by MHC class II pathway while endogenous antigens are presented in context of MHC class I. Rapid cross-presentation by pDCs might be important for early priming of memory $CD8^+$ T cell responses, whereas priming by both mDCs and pDCs at later time points could enhance both recall and new responses to an antigen. Cross-presentation is the display of peptides derived from exogenous antigens on MHC class I molecules (12). Macrophages and DCs have been shown to be competent for cross-presentation. Cross presentation of soluble OVA can occur, but it is extremely inefficient as it requires constant incubation with protein antigen. Remarkably, the prolonged antigen presentation via PLGA microparticles due to its sustained release properties has shown to increase the cross-presentation efficiency several-fold (91). This can be further improved by incorporation of TLR adjuvants within these PLGA microparticles (94).

Having justified the need for such a polymeric carrier for antigen delivery and its advantages in detail in the current and previous chapters, the primary focus of this chapter is on the design of these PLGA based carrier systems for antigen and/or adjuvant co-delivery. PLGA types, lactide to glycolide stoichiometric ratios, molecular mass and process parameters including fabrication method and formulation variables are the factors

that influence the efficient and successful use of these systems as carriers for tumor immunotherapy.

Peptide/protein antigens, adjuvants etc. frequently exhibit hydrophilic characteristics and attempts to load them in hydrophobic substrates has been a challenging task. Although enough methods on a single emulsion (o/w) design has been successfully and robustly developed for hydrophobic drugs in PLGA systems, the entrapment of proteins has often met with poor efficiency (87). In order to minimize drug loss, a double emulsion (w/o/w) technique was developed by Ogawa et al. (95, 96) which has now been routinely adapted for antigen entrapment within microparticles (Figure III-1). This method allows the drug to be initially solubilized in an internal aqueous phase. However, this method still presents significant difficulties and requires fine tuning the process according to our specific needs.

Along with higher drug loading, another important criterion that governed the choice of PLGA type for microparticle fabrication was the residence time of these microparticles within the APCs. Mature DCs and macrophages typically display a life-span of 20-25 days upon microparticle uptake and continued antigen presentation. Hence it is critical to ensure complete release of the entrapped component within this time span to provide controlled and continued immune stimulatory effect. Antigen and adjuvant release from these microparticles is a combination of diffusion controlled release at the early stages up to day 5. Following this, the polymer shows molecular weight decrease due to hydrolysis and the release is a function of diffusion and extent of polymer degradation and molecular weight loss. PLGA 50:50, with a lactide to glycolide ratio of 1:1, shows the fastest degradation rate with a typical degradation time of up to 4 weeks. Such a degradation profile was in conjunction with our specific aims making this polymer the first choice in our study design.

Several studies have shown higher protein entrapment in a high molecular weight grade PLGA 75:25 owing to the higher hydrophobicity of this polymer type. The

hydrophobic domains in an antigen or a protein interact with the hydrophobic region in the polymer during the fabrication process resulting in higher retention of the antigen in the polymeric phase improving the overall EE of the process. The higher hydrophobicity can impede drug release due to slower degradation phase. However, the presence of macrophage enzymes, esterases within the cells have been shown to accelerate the process *in-vivo* at least 1.5- 2 fold faster. As a compromise between process efficiency, EE and release, PLGA 75:25, MW 30 kDa formed our second polymer of choice if PLGA 50:50 did not result in accomplishment of the specific aims of microparticle fabrication process as described below (97).

Currently, our main goal was to obtain a final formulation that contains the appropriate dose of the active antigen; OVA alone or in combination with adjuvants; CpG or poly I:C or both. The optimization to ensure high loading of the components in a reproducible manner is of paramount importance as both the adjuvants are expensive and scarcely available. The other important delivery vehicle characteristics that influence the type and strength of immune response generated are the size of the carrier and route of delivery. The ideal carrier must release the entrapped antigen and adjuvant within the life-cycle of the antigen presenting cells (APCs). Therefore, we followed a five point optimization target approach as follows:

1. Achieve entrapment efficiencies of the individual encapsulated components to be at least 50 % as an effective compromise between particle size and loading efficiency. The target was to achieve efficient loading efficiency without compromising with the phagocytic ability of the APC in taking up larger particle.
2. Fabricate microparticles within a size range of 1-2 µm. This was based on studies conducted by several groups who studied the relationship between particle size and efficiency of phagocytosis.[88] This study was an *in-vitro* cell uptake model conducted using polystyrene beads. The high degree of

hydrophobicity of polystyrene can result in untoward aggregation effects in media this invalidating the size effects in certain cases. Hence a preliminary study done in our lab using differential sized microparticles prepared from PLGA 50:50, MW 30 kDa was used a deciding tool for the optimum size.

3. Achieve complete release of the entrapped antigen and adjuvant components within 25-30 days which is the average life-span of the macrophages and DCs (98).
4. A microparticulate carrier that will generate a burst release of its cargo to trigger a potent and immediate antigen-specific immune response, followed by a continual release to generate antigen-specific memory T cells.
5. The optimized formulation can be readily extrapolated to any therapeutic model antigen/protein with minor modifications.

There are several factors that can influence the efficiency of encapsulation, particle size and *in-vitro* release kinetics, which can be suitably modified to increase the efficiency of the process. A detailed description of formulation and process variables is described in the experimental methods section. The information generated by such a study can help shape future vaccine design strategies and give further insight into the factors affecting the formulation efficiency of particulate carriers.

The optimization was designed to be a two part process. Considering, the relative costs of antigen OVA and the two adjuvants poly I:C and CpG, the first set of optimization was done for microparticles loaded only with OVA. The fabrication conditions can be readily extrapolated to the other two components, given the similarity in their hydrophilic properties. The next step in the design was to optimize loading of two and three components in the system by further alteration of the design conditions for the single component system. Such an approach will help build a robust formulation protocol for single, dual and tri-component PLGA particulate carriers.

Materials and methods

Materials

PLGA (50:50 Inherent viscosity 0.2 dL/g) and PLGA (75:25 Inherent viscosity 0.41 dL/g) was purchased from Lactel Absorbable Polymers (Cupertino, CA). Poly (vinyl alcohol) (PVA 87-89 % hydrolyzed MW 30- 67,000 Da) was purchased from Sigma-Aldrich (St. Louis, MO). Ovalbumin (OVA) from chicken egg white, grade VII purified and poly I:C sodium salt was purchased from Sigma-Aldrich. (St. Louis, MO). CpG-1826 was purchased from Coley Pharmaceuticals (Dusseldorf, Germany). All other chemicals and solvents including dichloromethane (DCM) and acetonitrile used were of analytical grade. The analytical instrument; Hitachi-4000 SEM was a part of the Central Microscopy Research Facility (CMRF) at University of Iowa, Iowa City, IA.

Methods

I. OVA-loaded PLGA MP: Homogenization method

The internal aqueous phase consisted of 5.5- 6 mg of OVA solubilized in 1% aqueous solution of PVA as a surfactant. This was emulsified into an oil phase containing 200 mg PLGA(50:50, Inherent viscosity 0.2 dL/g) dissolved in DCM using a micro-tip probe sonicator set at level 3 (Sonic Dismembrator Model 100, Fisher Scientific, Pittsburgh, PA). This primary w/o emulsion was then poured into 50 mL of external aqueous phase containing PVA as a surfactant and rapidly homogenized using a high speed homogenizer at 9500 rpm for 30 seconds to form the secondary w/o/w emulsion. Stirring was then continued using a magnetic stirrer until complete evaporation of DCM. The particles were collected by centrifugation at 7000 x g for 10 minutes, washed three times with DI water and lyophilized overnight (Labconco Freezone 4.5, Labconco Kansas City, MO).

II. OVA + CpG and OVA + poly I:C co-loaded PLGA MP: Homogenization method

The internal aqueous phase consisted of OVA (5.5 – 6 mg) and poly I:C or CpG (3 mg each) solubilized in 1% aqueous solution of PVA as a surfactant. The internal aqueous phase volume was kept the same as the single component OVA system, This was emulsified into an oil phase containing 200 mg PLGA (50:50 Inherent viscosity 0.2 dL/g or PLGA (75:25 Inherent viscosity 0.41 dL/g) dissolved in DCM using a micro tip probe sonicator set at level 3 (Sonic Dismembrator Model 100, Fisher Scientific, Pittsburgh, PA). This primary w/o emulsion was then poured into 50 mL of external aqueous phase containing PVA as a surfactant and rapidly homogenized using a high speed homogenizer at 9500 rpm for 30 seconds to form the secondary w/o/w emulsion. Stirring was then continued using a magnetic stirrer until complete evaporation of DCM. The particles were collected by centrifugation at 7000 x g for 10 minutes, washed three times with DI water and lyophilized overnight (Labconco Freezone 4.5, Labconco Kansas City, MO).

III. Characterization of microparticles

III.1 Particle Size

A suspension of the lyophilized microparticles in DI water at a conc. of 0.1-0.2 mg/mL was used to analyze the particle size using Zetasizer Nano ZS (Malvern, Southborough, MA). Microparticle morphology was assessed by scanning electron microscopy (SEM, Hitachi S-4000, Japan). In order to place more than one sample on the same stub, the samples were first places on a semi-conductor silicon wafer chips (Central Microscopy Research Facility, UIowa, IA). Briefly, air-dried microparticles were placed on adhesive carbon tabs mounted on SEM specimen stubs. The specimen stubs were coated with approximately 5 nm of gold by ion beam evaporation before examination in the SEM operated at 5 kV accelerating voltage.

III.2 Entrapment Efficiency (EE)

The supernatant collected during centrifugation was used to analyze the free (un-entrapped) TLR ligand and OVA. The EE was then calculated as follows:

EE (%) = [(Initial amount of OVA/CpG/poly I:C – Free OVA or CpG or poly I:C / Initial amount of OVA or CpG or poly I:C)]\\] *100 *(III-1)*

Alternatively, the EE of OVA/TLR ligand in the microparticles was calculated by directly measuring the amount of the actives in the particles. For analysis of poly I:C/CpG, 5-10 mg of lyophilized PLGA microparticles was dissolved in 200 µL DCM and the precipitated poly I:C/CpG was extracted by adding 10-fold excess phosphate buffered saline (PBS). The extraction procedure was repeated 2-3 times until no further active component could be detected in the aqueous extract. Poly I:C/CpG content was analyzed by HPLC and fluorescent spectroscopy as described in the analytical methods section. For analysis of OVA, 5-10 mg of particles was digested overnight using 0.3N NaOH. The digested solution was then neutralized and OVA content was analyzed using bicinchoninic acid assay (BCA) as described in the next section. The standard OVA solution was also treated the same way for EE calculations to account for any hydrolysis of OVA caused by 0.3N NaOH.

Mass balance up to 95% was achieved between the two approaches. Hence for all further analysis, the first method was pursued as it was a more rapid approach to estimate drug entrapment.

IV. Analytical methods

IV.1 Ovalbumin (OVA)

Free OVA in supernatant or OVA loaded in microparticles was analyzed using micro-BCA assay. This colorimetric approach is based on the principle of reduction of Cu^{+2} to Cu^{+1} in the presence of OVA. The Cu^{+1} then reacts with bicinchoninic acid in an alkaline medium to form a purple colored complex that is analyzed colorimetrically at

562 nm. The BCS working solution was prepared by combining 50 parts of BCA stock solution with one part of 4% $CuSO_4*5H_2O$ just before the protein assay. The samples (100 µL) were pipeted into microplate wells (Microwell-96-well plates, Nunc, Germany) and were mixed with 200 µl of BCA working solution. This microtiter plate was incubated at 37 °C for 60 minutes, cooled for 15minutes to room temperature and the intensity of color development was then measured at 562 nm with a Microplate Reader (SpectramaxPlus, CA). The standard solution of OVA in a concentration range of 10-1000 µg/mL) was prepared by serial dilutions of the OVA stock solution in PBS. Following the BCA assay, the standard curve was generated from the linear relationship between intensity of the purple complex and the concentration of OVA. All the measurements were done in triplicate.

IV.2 Poly I:C

High performance liquid chromatography; HPLC (Waters 2690 coupled with Empower Software (Waters, Boston MA) was used for the analytical assay of poly I:C. The column was a LiChrospher Merck C18 Column (Sigma Aldrich, St.Louis, MO) 5 µm packing (150mm × 3.9 mm I.D.). The mobile phase was a mixture of acetonitrile: 50 mM phosphate buffer pH 6.5 at a ratio of 20: 80 (v/v) and the flow rate was 1 mL/min. Poly I:C was detected at 260 nm with a retention time of 1.9 minutes. Forty µL of drug solution was injected for both standards and samples. The concentration of poly I:C was quantified by the peak area method from the associated calibration curve. The standard solution of poly I:C in a concentration range of 5- 100 µg/mL) was prepared by serial dilutions of the poly I:C stock solution in PBS. Following the HPLC assay of standard solution of poly I:C, the standard curve was generated from the linear relationship between peak area and the concentration of poly I:C. All the measurements were done in triplicate.

IV.3 CpG

CpG was analyzed by fluorescence spectroscopy by the use of Oligogreen, a fluorescent probe for the quantitative estimation of oligonucleotides. The excitation and emission wavelengths were set at 480 and 520 nm respectively and relative fluorescence intensity was used to calculate CpG concentration. The standard solution of CpG in a concentration range of 0.1 – 2 µg/mL was prepared by serial dilutions of a CpG stock solution in PBS. The Oligogree^{TM} detection reagent was prepared by a 200-fold dilution in either 1X Tris-EDTA (TE) buffer or PBS. The samples (100 µl) were pipeted into microplate wells (Microwell-plates, Nunc, Germany) and were mixed with 100 µl of detection reagent. This microtiter plate was incubated for 5 minutes at room temperature in dark. The fluorescence intensity was then measured with a Microplate Reader (SpectramaxPlus 384, Molecular Devices Inc., Sunnyvale, CA). Following the fluorescence assay of standard solutions of CpG, the standard curve of was generated from the linear relationship between relative fluorescence intensity and the concentration of CpG. All the measurements were done in triplicate.

V. Effect of formulation variables on characteristics of OVA-loaded PLGA MP: Design optimization

V.1 Effect of polymer concentration

Concentration of PLGA (50:50 inherent viscosity 0.2 dL/g) at 1.67, 3.3 and 6.67 % w/v was used to fabricate the microparticles. The total volume of the internal organic phase was kept constant at 5 mL while the amount of polymer was varied to achieve the desired concentration. In all the cases, the ratio of the internal aqueous phase to organic phase was kept constant at 1:10.

V.2 Effect of emulsifier concentration

External aqueous phase emulsifier (PVA) concentration at 1 %, 3 % and 5 % w/v was used to fabricate the microparticles. The polymer (PLGA 50:50 inherent viscosity 0.2 dL/g) concentration was kept constant at 3.33 % w/v in all the formulations.

V.3 Effect of volume of internal aqueous phase

Internal aqueous phase volume used was 200, 300 and 600 µL, keeping the internal organic phase volume constant and polymer concentration was maintained at 3.34% and surfactant concentration was maintained at 1% w/v in all the formulations.

VI. Statistical analysis

Group data are reported as mean ± standard deviation. Differences between groups are analyzed by one way analysis of variance with a Tukey post-test analysis. Levels of significance were accepted at the $p < 0.05$ level. Statistical analyses were performed using Prism 5.0 software (Graphpad Software Inc., San Diego, CA).

Results

Part A. OVA-loaded PLGA MP: Design optimization

I. Analytical method robustness

I.1 Standard curve of Ovalbumin assayed by BCA assay

A standard curve with definite concentration range was studied in order to evaluate a suitable concentration range for analysis of OVA entrapped with the microparticles and that released from microparticles. Understanding the need to develop a sensitive colorimetric assay to enable the analysis of very small amount of OVA that is released from PLGA microparticles over the first few days, few assay parameters including sample volume and detection reagent amounts were varied to obtain the most sensitive and robust method. The plot of absorbance as a function of concentration is displayed in Figure III-2. As shown in Figure III-2, the color intensity increased linearly with respect to OVA concentration of 23-400 µg/mL with an r^2 value of 0.99.

I.2 Standard Curve of Poly I:C assayed by HPLC

A standard curve with definite concentration range was studied in order to evaluate a suitable HPLC analytical method for measuring the concentration of poly I:C (Figure III-3). As shown in Figure III-3, the peak area value increased linearly with respect to the poly I:C concentration of 5-100 µg/mL with an r^2 value of 0.9999. The results indicated that the HPLC method developed for the detection and quantification of poly I:C is a suitable, reliable and robust method. Additionally, the assay did not show any interference in the presence of OVA (data not shown) indicating the suitability of the method for analysis of poly I:C in a two component PLGA system.

I.3 Standard Curve of CpG assayed by Oligogreen quantification for ssDNA

The most commonly used technique for measuring oligonucleotides and ssDNA concentration is the determination of absorbance at 260 nm (A260). The major

disadvantage of the absorbance method is the interference caused by the presence of contaminants that lower the assay sensitivity. Hence we chose an alternative technique that involved the use of Quant-iT™ OliGreen® ssDNA reagent, an ultra-sensitive fluorescent nucleic acid stain for quantifying oligonucleotides and single-stranded DNA (ssDNA) in solution. As shown in Figure III-4, the relative fluorescence intensity increased linearly with respect to CpG concentration of 0.1-2 µg/mL with an r^2 value of 0.99. The results indicated that this method developed for the detection and quantification of CpG is a suitable, reliable and robust method. This method too did not show any interference from OVA or PLGA.

II. Effect of formulation variables on characteristics of OVA-loaded PLGA MP: Step I Optimization

II.1 Effect of polymer concentration

Figures III-5A and III-5B show the effect of polymer concentration on the particle size and EE of OVA-loaded PLGA microparticles. It can be seen that increasing the polymer concentration from 1.67 to 6.6 % w/v increased the particle size from 1.5 µm to 4 µm. The increase in particle size can be attributed to the increased amount of polymer present within the emulsion droplet. Additionally, since the homogenization speed was kept constant for all the three formulations, an increased amount of polymer increased the polymer solution viscosity. This could have lowered the efficiency of droplet size reduction causing an increase in particle size. Similarly, the increased polymer concentration resulted in an increase in EE from 37 to 61%. The increase in polymer solution viscosity along with the increase in polymer amount available to encapsulate the OVA resulted in an increased mass transfer resistance to the entrapped antigen reducing its loss via diffusion to the external phase thereby increasing the entrapment efficiency.

Particle size is an important parameter affecting the uptake of the particulate antigen following phagocytosis by DCs. A study by Reece et al. published in

immunology and cell biology, showed that polystyrene beads less than 2.5 μm in size showed the maximum efficiency of uptake by DCs and B-cells.(92) Although PLGA is slightly more hydrophilic than polystyrene and that might affect its uptake, the uptake is still expected to remain an inverse function of the particle size of the beads.(90) Taking our target particle size and antigen loading into consideration, for all the following experiments the polymer concentration was kept constant at 3.33 % w/v.

II.2 Effect of emulsifier concentration

Figures III-6A and III-6B show the effect of surfactant (PVA) concentration on the particle size and EE of OVA-loaded PLGA microparticles. Increasing the surfactant concentration from 1 to 5 % w/v decreased the particle size from 3 to 1 μm. At a surfactant concentration of 1 and 2 % w/v, there was a small difference in the particle size. However, at a concentration of 5 % w/v, the particle size reduced sharply to 900 nm. The decrease in particle size can be attributed to the formation of smaller emulsion droplet due to a higher concentration of the surfactant at the oil/water interface in the primary and secondary emulsion. The effect of surfactant concentration on EE followed an inverse pattern. As expected from the results of the particle size, EE at a surfactant concentration of 1 and 2% w/v displayed no significant difference with an average entrapment efficiency of 42 %. However, at a surfactant concentration of 5 % w/v the EE reduced to 30 %. Smaller particles formed at higher surfactant concentration resulted in a higher surface area that resulted in an increased diffusion and loss of OVA to the external phase during microparticle fabrication.

Following this process parameter optimization, the PVA concentration was fixed at 1% w/v in the internal and external aqueous phase.

II.3 Effect of internal aqueous phase volume on EE and morphology of OVA-loaded PLGA MP

Figure III-7 shows the effect of internal aqueous phase volume on OVA loading efficiency in PLGA microparticles. When a larger internal phase volume of 600 µL was used, a lower loading efficiency was seen (35 %). On the other hand, the usage of a smaller volume (200 µL) as internal aqueous phase produced a significantly higher loading efficiency (62 %). This result seemed reasonable. Loading efficiency is likely to depend on the internal aqueous phase volume employed. The larger the internal aqueous phase volume at similar polymer concentrations, the thinner was the PLGA layer (DCM phase). Because this polymer layer acts as a barrier through which the internal OVA is diffused to the external phase, the thinner oil phase is expected to give rise to higher diffusion rate. Thereby the probability of OVA leakage from the internal aqueous to the external aqueous phase will increase. The smaller internal aqueous phase volume was found to be advantageous for obtaining high loading efficiency.

Additionally, the smaller internal volume of internal aqueous phase surrounded by a denser organic phase reduces the loss of entrapped components. This results in formation of microparticles with reduced surface porosity as observed in Figure III-8. The reduced surface porosity may be advantageous in controlling the burst release of the entrapped antigen thus affording a more continuous and sustained release of the entrapped component. A more detailed SEM cross-sectional analysis would be needed to accurately describe the porous structure of the microparticles.

The next objective was to optimize the loading of antigen and an adjuvant within the same microparticle system thereby forming a dual component particulate carrier. Summarizing all the optimization design from step I, the key formulation variables influencing loading and particle size were polymer concentration and the volume of the internal aqueous phase. Expecting the loading to be affected by a competitive retention within the polymer layer and diffusion towards the external phase, we realized it was

prudent to increase the polymer concentration to accommodate an efficient dual component loading within the same microparticle. Since no prior data for entrapping poly I:C within a particulate carrier was available, this optimization design served as a good starting point to fabricate this dual component system co-entrapping OVA and poly I:C.

Part B. Characterization of OVA + CpG and OVA + poly I:C co-loaded PLGA MP: Design optimization

A double emulsion solvent evaporation technique (w/o/w) as described in the methods section was used to entrap the antigen and adjuvant components simultaneously within the microparticles. PLGA (50:50 inherent viscosity 0.2 dL/g) was used at a concentration of 6.67% w/v and the internal aqueous phase volume for solubilizing OVA and poly I:C/CpG was 200 µL and the internal aqueous to organic phase ratio was maintained at 1:10 similar to all the formulations that were studied. Figure III-9 shows the decrease in entrapment efficiency of OVA when entrapped alongside poly I:C/CpG in comparison to being loaded as a single component in the PLGA carrier. Upon co-loading, EE significantly reduced by 17% with average loading being 50%. The particle size of both the formulations however still remained reasonable with an average diameter of 4.5 µm. Despite the reduction in EE, the loading of OVA still met our target objective of being able to achieve at least a 50% loading of the active component. However, the loading of poly I:C and CpG in the dual component vehicles was 12 and 4 % respectively (Figure III-9). CpG is a small 20-base pair oligonucleotide with an average MW of 6-7 kDa. ODNs typically have very high affinity for water and the smaller size facilitates the diffusion even further leading to its poor loading in the dual component system. Poly I:C although is lightly larger in molecular size to that of OVA, is more hydrophilic being a synthetic nucleic acid. Additionally, the iso-electric point of OVA is around 4.8 and pH of the internal aqueous phase is around 5.5. The decreased solubility of OVA in the external phase at this pH along with interaction of the hydrophobic domains of the

protein with PLGA improves OVA retention in the organic phase thus retaining a high percent of OVA within the microparticles.(99)

The entrapment efficiencies of poly I:C and CpG were significantly below the target loading and given the scarce and expensive nature of these adjuvants, CpG in particular, it was imperative to strategize formulation approaches to improve the efficiency of the process.

VI. Effect of formulation variables on characteristics of OVA + CpG and OVA + poly I:C co-loaded PLGA MP (Co-loading design optimization)

VI.1 Effect of polymer viscosity and type

PLGA with a lactide to glycolide co-polymer ratio of 50:50 and 75: 25 (Lactel Absorbable Polymers, Cupertino, CA) with a low and high grade of inherent viscosity respectively were used. The low viscosity grade had an inherent viscosity of 0.2 dL/g (MW ~ 8000 Da) and the high viscosity grade had an inherent viscosity of 0.41 dL/g (MW ~ 25- 30000 Da). The polymer concentration is both cases were maintained at 6.67 % w/v and the internal aqueous phase volume was kept at 200 µL as optimized in Part A.

VI.2 Effect of fabrication technique

As a variation in fabrication technique and in an attempt to decrease the particle size whilst improving the EE, a double sonication method was employed to fabricate the microparticles. The method has been described in detail below.

OVA + CpG and OVA + poly I:C co-loaded PLGA MP: Sonication method

The internal aqueous phase consisted of OVA (5.5 – 6 mg) and/or poly I:C and CpG (3 mg each) solubilized in 1% w/v aqueous solution of PVA as a surfactant. The internal aqueous phase volume was kept the same as that for the homogenization technique optimized at 200 µL. This was emulsified into an oil phase (2 mL) containing 6.67 % w/v (PLGA 75:25 inherent viscosity 0.41 dL/g) dissolved in DCM using a micro

tip probe sonicator set at level 3 (Sonic Dismembrator Model 100, Fisher Scientific, Pittsburgh, PA). This primary w/o emulsion was then immediately sonicated into 6 mL of 1% PVA aqueous phase containing PVA for 30 seconds at the same setting as above to generate the secondary emulsion. To protect the antigen and adjuvant from the heat generated during this double sonication process, the entire process was carried out in an ice-bath. The secondary emulsion was then dropped slowly into a beaker containing 50 mL of 1% PVA and stirring was continued using magnetic stirrer until complete evaporation of DCM. The particles were collected by centrifugation at 7000 x g for 5 minutes, washed three times with DI water and lyophilized overnight (Labconco Freezone 4.5, Labconco Kansas City, MO).

VI.3 Differential centrifugation for reducing polydispersity of microparticles

OVA-loaded PLGA microparticles were used as a representative sample to determine polydispersity and standard deviation of microparticles prepared by homogenization and sonication techniques. Particle size was analyzed on the Nicomp 380 ZLS (Particle sizing systems, FL) particle size analyzer. The intensity weight function was used to determine mean particle size and standard deviation. The representative distributions have been shown in Figure III-19. As seen in Figure III-19A and III-19B, when all the particle were collected at 7000 rpm, the particle exhibited large standard deviations of 1.2 and 2.5 µm when fabricated by the sonication and homogenization method respectively. Microparticles were first centrifuged at 1000 rpm to remove and particles larger than 5 µm and this step was again repeated at 2000 rpm. Finally the particles were spun at 5000 rpm to collect particles in the desired size range of 1.5 to 2 µm. The supernatant recovered after this spin was discarded to remove any finer sized particles. These particles separated by this technique showed a mean particle size of 700-800 µm and a standard deviation of 300 µm (Figure III-19C). Since these steps resulted

in considerable loss of microparticle yield, for the final fabrication process, the spinning step at 2000 rpm was omitted to collect a higher fraction of particles.

VI.4 Effect of fabrication technique on release profiles of OVA, poly I:C and CpG

Cumulative release of OVA, poly I:C and CpG from the dual component microparticles prepared by either the sonication or the homogenization method were compared. 50 mg of PLGA microparticles co-entrapping OVA and poly I:C/CpG was suspended in 3 mL phosphate buffered saline (PBS, pH 7.4). The samples were shaken in a water bath at 37 °C at 100 rpm. 200 µL of sample was withdrawn at pre-determined time intervals. The sample was centrifuged using a microcentrifuge (Eppendorf) at 7000 rpm for 5 minutes and the supernatant was used for release analysis. The microparticle sediment was redispersed in 200 µL volume of the same release medium and replenished back to the release sample container. Released OVA, poly I:C and CpG samples were assayed using micro BCA, HPLC and by fluorescence spectroscopy respectively as described in the previous sections. All measurements were performed in triplicate.

VI.5 Effect of the addition of salt (sodium chloride, NaCl) in the external aqueous phase to improve the EE of CpG

The presence of OVA either alone or co-entrapped with poly I:C or CpG can exert a strong osmotic pressure gradient. This results in rapid influx of water from the external aqueous phase into the internal phase to dilute it resulting in loss of entrapped components. In order to reduce the osmotic flux, 1- 2 % w/v of sodium chloride was added to the external aqueous phase to improve the EE of the process.

VII. Effect of formulation variables on characteristics of OVA + CpG and OVA + poly I:C co-loaded PLGA MP: Step II optimization-

VII.1 Effect of polymer viscosity on entrapment efficiency

Figure III-10 shows the entrapment efficiencies of the individual components in microparticles fabricated with the low molecular weight PLGA grade and Figure III-11 shows a direct comparison depicting the effect of polymer type and molecular weight/inherent viscosity. It can be seen that the increase in polymer weight significantly improved the EE of poly I:C resulting in a two-fold increase from 12 to 24%. Similarly, the EE of CpG also improved from a poor 4 to 10% with the increase in PLGA molecular weight. It is possible that increase in viscosity on increasing the molecular weight might have decreased the diffusion rate of the two hydrophilic adjuvants into the external aqueous phase thus increasing their loading. However, the increase in viscosity has a significant impact on the particle size of the microparticles. The size of the microparticles increased from 3.5 µm to 4-4.5 µm. The loading efficiency of OVA also improved from 50- 70% by use of a higher MW more hydrophobic grade PLGA.

Although the improvement in entrapment efficiency was a positive outcome of both these modified variables including MW and co-polymer ratio, the increase in particle size was a concern since the uptake of the large particles will be significantly impaired with the possibility of the larger particles forming a depot upon subcutaneous (s.c) or intramuscular (i.m) administration instead of being readily up-taken by the DCs in the draining lymphoid tissue at the site of administration.

To circumvent this problem, a modified fabrication technique was employed to achieve a dual target of improved EE and reduced particle size.

VII.2 Effect of fabrication method on particle size and entrapment efficiency

Figure III-12 gives a direct comparison of the impact of homogenization and sonication on the entrapment efficiency of OVA and poly I:C/CpG. The EE of poly I:C

improved from 24 % to a significantly higher loading at 46% achieving our target loading of the adjuvant. CpG also showed a 2.5 fold improvement in EE from 10 to 24%. Considering, the small size of the adjuvant and loading attempts by several groups for this molecule, this loading efficiency was a significant success in design optimization for an antigen-adjuvant co-loaded system. As seen in the SEM images in Figure III-13 there was a significant reduction in particle size as well as poly-dispersity of the particles. The mean size of the microparticles decreased from an average size of 4.5 ± 1 to 1.5 µm ± 0.5 µm.

The purpose of using of an ultrasonicator probe for the formation of the secondary emulsion is the efficient breakdown of the oil phase into small droplets that are well dispersed in the external phase. The small volume of the external phase (6 mL) maintained during the second emulsification step as opposed to homogenization into a 50 mL volume reduces the size of the sink into which OVA and poly I:C/CpG can diffuse into. The finely dispersed secondary emulsion when added slowly into a large external phase volume, results in a faster solidification of the microparticles. This is due to instant diffusion of DCM into the large external phase and rapid evaporation at the oil-water interface facilitated by the larger surface area.

VII.3 Effect of fabrication method on release profiles of OVA, poly I:C and CpG

Figures III-14, III-15 and III-16 give a direct comparison of the impact of homogenization and sonication on the release profiles of OVA and poly I:C/CpG co-loaded microparticles. Formulation parameters are important determinants for the release behavior of the microparticles. Release of encapsulated hydrophilic molecules from PLGA microparticles generally shows a biphasic profile. An initial rapid release due to the burst effect is usually followed by a sustained release because of the gradual degradation of polymer. All the three components showed an initial burst release followed by a more controlled release. CpG shows the fastest release exhibiting nearly 50

% release at the end of 5 days when the microparticles were prepared by the sonication method (Figure III-16). In contrast, OVA and poly I:C showed about 30 and 40 % release respectively (Figure III-14 and III-15). Furthermore, the microparticles prepared by the sonication technique showed an enhanced burst effect and overall higher cumulative release of all three components in comparison to the homogenization method. This can be attributed to the formation of smaller particles by the sonication method. The higher surface area associated with the smaller particles resulted in a higher release rate.

VII.4. Effect of the addition of salt (sodium chloride, NaCl) to external aqueous phase to improve EE of CpG

The result of the effects of salt addition on the entrapment efficiency of CpG is shown in Figure III-17. The addition of salt to the outer water phase to counter the high osmolarity of the internal phase significantly improved the entrapment efficiency of CpG from 24 % to 44% (Figure III-17). Furthermore, microparticles prepared with salt in the external phase presented free-flowing microparticles because of the dense and smooth surface (Figure III-18). This surface morphology was particularly favorable as it improved dispersibility and syringibility of the microparticles when reconstituted in the injection medium.

Discussion (I)

The goal of these experiments was to develop an effective delivery system that carried an antigen and adjuvant for co-delivery into an antigen presenting cell (APC). The design optimization was measured through *in-vitro* functionality parameters including particle size, entrapment efficiency (EE) and *in-vitro* release profiles. PLGA microparticles have been studied for sustained antigen delivery and immune response enhancement for more than a decade by several groups (64, 66, 73, 100-106). Early developments of such vaccines were basically technology-driven, stemming from the

biocompatibility of these polymers coupled with the ability to tailor their properties based on the bioerosion rates of these polymers. More recently, other features have become equally or even more appealing, such as the adjuvancy of such microparticles. When used as a material for microparticles, the PLGA hydrophobicity will also affect interactions of the microparticles with phagocytosing cells like macrophages and DCs, these interactions are of crucial importance for use of these systems in vaccine formulations (97).

There have been several groups that have worked on optimizing loading of a protein/peptide in a systematic manner. However, in most cases these studies have been for the development of a single shot vaccine for long term antigen delivery or development of bioadhesive microparticles for oral/mucosal delivery. For example, Eratalay et al. developed a particulate system containing OVA as a model antigen for subcutaneous delivery (107). The particle size of this system was in the range of 4 μm which is a reasonable size for uptake by DCs. However, the maximum loading of OVA that was achieved was only 15%. A subsequent study by Uchida et al. in a more comprehensive manner enhanced the OVA entrapment to 60 % (108). However, the enhancement in EE came at the expense of producing a microparticle with a diameter of 15-18 μm.

The loss of protein during the microparticle preparation process is attributed to two major factors. One is due to the mechanical breakage of the nascent microparticles during formation and the other is the diffusion resulting from the concentration gradient. The mechanical breakage is difficult to avoid during fabrication of microparticles. On the other hand, the protein diffusion rate can be adjusted by changing the preparation and formulation parameters, such as the protein solubility, polymer concentration, inner water volume of W/O emulsion, emulsification method addition of excipients, osmotic pressure and polymer solidification rate (87, 109). All these parameters affect the degree of protein loss directly or indirectly and thus the entrapment efficiency.

Based on the results of the various studies published, we decided to study the effect of the most important process variables identified to attain our target of achieving high loading/entrapment efficiency with a reduced particle size suitable for uptake by the target immune cells. Polymer concentration has been widely studied to be one of the most critical parameters affecting drug loading, particle size of the carrier and *in-vitro* release profile. Given our end objective of loading two and/or three components within the same carrier, effect of polymer concentration formed a primary parameter in this study. Another important reason to achieve an increased amount of antigen loading per mg of PLGA particles is to improve antigen stability. The uttermost important criterion for delivery systems is the capacity to deliver the entrapped material in a bioactive form, i.e., a fully immunogenic form for eliciting an antigen specific immune response. Antigen instability is, however, one of the major obstacles in the development of microparticle based vaccines. Instability arises through the various stages of processing, storage and application. Naturally, the extent of chemical and physical instability affects the immunogenicity of entrapped and released antigen. Antigen stability may be hampered at various stressful stages, such as the generation of the aqueous/organic interface (w/o emulsion) in the fabrication process or in the final freeze-drying stage. Issues of antigen instability may be resolved through solid-state microencapsulation or physicochemical stabilization of the antigen itself, as well as through improving encapsulation conditions and the fabrication process (110). Our studies showed an improved loading efficiency of OVA with an increase in polymer concentration. These results also gave us a starting point for the amount of polymer needed to co-entrap two components simultaneously requiring the formation of a more viscous polymeric phase to hold both the components.

While polymer concentration functions as an important parameter affecting loading, surfactant concentration functions as the most important parameter affecting the particle size of the microparticulate carrier. The results of our studies showed a compromise in EE at the cost of obtaining smaller particles with an increased PVA

concentration. Internal aqueous phase volume is one of the least studied parameters influencing microparticle characteristics, but is often times the most critical parameter that influences loading and particle morphology. With moderately hydrophilic drugs, modification of this parameter becomes relatively difficult, given the solubility of the compounds. In case of our work, the high solubility of all the components worked to our advantage enabling the use of a minimal volume of the aqueous phase. The small internal phase volume ensured formation of a dense polymeric layer around the aqueous droplet hindering the diffusional loss of the entrapped components. The smallest aqueous phase volume gave high loading efficiency for the particles with a smooth surface morphology.

Since the broader objective of this research project was to fabricate a co-delivery vehicle targeting the immune cells, the next step involved further optimization of the parameters from step 1 as described in section II. Although CpG has been in use as an adjuvant for more than a decade now, it is only recently that efforts have been directed towards developing a particulate carrier for CpG to prevent rapid degradation in the biological environment. A few groups have evaluated the fabrication of co-delivery vehicle incorporating CpG with various tumor antigens (94, 111). High and efficient loading of CpG sequences into microparticles is currently impaired by its high hydrophilicity and negative charge. However, none of these groups have carried out a systematic study of parameters influencing and improving CpG loading and release. In a study conducted by Heit and colleagues, the group worked on developing a vaccine delivery carrier co-encapsulating OVA and CpG (58). Although a good loading efficiency with OVA peptide was achieved, the loading of CpG was very poor with about 1 µg of CpG being loaded per mg of PLGA microparticles. The poor loading increases the microparticulate mass to be injected for the required dose making administration inconvenient. In another study by Roman and co-workers, the authors developed a similar carrier co-entrapping OVA and CpG. The authors managed to successfully attain a high payload of CpG with a loading efficiency of over 50%. This was achieved by using a

novel state of the art fabrication technique called total recirculation one machine system (TROMS^{TM}) (112). However, this technology is expensive and not readily available making routine fabrication difficult. Similarly, like several other groups, loading efficiency in this case was improved using chitosan to complex CpG to retard its diffusion (111). However, chitosan is known to complex pDNA-like molecules with high affinity impeding their release upon DC uptake. A few studies in our lab have also shown detrimental efforts to CpG and antigen functionality upon complexation with chitosan (Figure III-20). In this particular study, the effect of immune response strength was measured using the CTL assay as described here. A ^{51}Cr release assay was used to measure prostate specific antigen (PSA)-specific lysis of target cells. In a 24 well plate, 10^7 cells/well were seeded for each immunization group. Following a 5 day co-culture at 37 ^{o}C, the effector splenocytes were harvested and separated from dead cells using a Ficoll separation. Target PSA cells were labeled with 100 μCi of $Na_2{}^{51}CrO_4$ for 1 hr, washed twice, and resuspended at 5 x 10^4 cells/ml. The effector cells were diluted serially down a 96 well round bottom plate, and 100 μl targets added to each well, giving effector: target (E:T) ratios from 100:1 to 3.125:1. After a 4 hr incubation at 37 ^{o}C, the plate was centrifuged at 1000 rpm for 10 minutes, and 100 μl of the supernatant was taken from each well and counted in the COBRA II gamma counter (Packard Instrument Company, IL). The specific lysis was calculated using the formula:

(sample lysis-spontaneous lysis)/(maximum lysis-spontaneous lysis) *100 (III-2)

It can be seen from Figure III-18 that chitosan delivered solely with AdPSA depressed the CTL response, compared to AdPSA alone.

With this study as a reference and given the cost and lack of large number of resources for CpG, a comprehensive study to improve its loading formed an important part of our study. In a final attempt to improve the entrapment efficiency of CpG further, the effect of the presence of additives like NaCl in the external phase was examined. While the w/o/w is an attractive option to facilitate the introduction of hydrophilic

components, the presence of multiple components increases the osmotic pressure of the internal phase. Under the influence of an osmotic gradient, the organic phase of w/o/w emulsion allowing the passage of water into the internal emulsion phase. An important prerequisite for the entrapment of a hydrophilic drug is the dispersion of the aqueous phase into small droplets. The organic (middle) phase separates the internal water droplets from the external aqueous phase, thus acting as a diffusional barrier and reducing the migration of the protein and the adjuvants into the outer phase. Nevertheless, an exchange between the two aqueous phases (external and internal) does occur as a consequence of the solubility of OVA, poly I:C and CpG in particular. The influx of water into the internal aqueous phase increases the volume of w_1 phase and the thickness of the oil layer around the internal droplets decreases reducing the diffusional resistance barrier thickness. If the osmotic pressure difference across the organic phase, O, is extreme, then the passage of water is so rapid that an almost immediate rupture of the O phase with expulsion of the internal droplets occurs. Alternatively, diluting the internal phase to reduce the osmotic pressure is not an acceptable approach because the encapsulation efficiency decreases markedly with increasing volume of the internal aqueous phase (Figure III-7) (113, 114).

The next step was to fabricate microparticles co-entrapping poly I:C and the antigen OVA. The earliest study describing the adjuvant properties of poly I:C was studied by Talmadge et al.(37). Their study showed that the systemic administration of soluble poly I:C significantly reduced tumor burden. However, optimal immunotherapy was schedule dependent requiring 3-5 injections of a high dose (1 mg/kg) of poly I:C per week for a minimum of 4 weeks. In an another study by Steinman and co-workers, multiple injections of soluble poly I:C served as an adjuvant to allow a DC-targeted protein to induce protective CD4 T cell responses at a mucosal surface (70). The CD4 T cell response with poly I:C as an adjuvant was multifunctional, i.e., the T cells produced high amounts of multiple cytokines such as IFN- γ, TNF- α, and IL-12. A

microparticulate formulation providing a controlled release of the adjuvant over prolonged periods of time will circumvent problems associated with repeated administration and thus improve patient compliance in a clinical setting. Additionally, in a prophylactic setting a single shot vaccine is the most desirable form of vaccination.

Although poly I:C has been used as an adjuvant to enhance immunogenicity to a vaccine protein in mice models, the ability to develop a co-delivery carrier of poly I:C and antigen has not been explored before. The first step prior to fabrication of a microparticulate system was to develop an analytical method for poly I:C quantification to determine loading and evaluate release profiles. The analytical method developed based on a reverse-phase; RP-HPLC proved to be a robust technique with minimal intra-day and inter-day variability. The final optimized formulation also exhibited high loading efficiency (10 µg of poly I:C/mg PLGA particles) with an entrapment efficiency of 50 % in a co-delivery system (Figure III-18) and 70% in a single component vehicle.

VIII. Design and fabrication of a tri-component vehicle co-entrapping CpG, poly I:C and antigen OVA

Part A: Introduction and fabrication challenges

We hypothesize that a combinatorial vehicle incorporating poly I:C and CpG can result in a synergized immunostimulatory response. This response generated would be a direct response to the recognition of viral and bacterial pathogen associated molecular patterns (PAMP) respectively. Such an approach might prove more effective than either treatment modality with each of the adjuvants alone in combination with the antigen (dual component carriers). Additionally, a few studies have shown that although these specific adjuvants do increase the number of multifunctional effector T cells in the absence of an infection (prophylactic vaccine model), they often fail to function in the presence of an active infection (81). We hypothesize that the simultaneous activation of TLR ligands by these adjuvants might result in an improved activation of the effector T

cells and thus overcome this defect. Lanzavecchia and co-workers recently proposed the possibility of using this synergistic TLR stimulation in real life, to mimic pathogens that contain several TLR agonists that trigger TLRs in different cellular compartments (115). Continuing this hypothesis, Bagchi et al. further showed that TLRs 2, 5, 7, and 9 can co-operate with TLRs 3 and 4 to enhance proinflammatory cytokines to have applications in tumor therapy (116). This synergistic activation has been shown to enhance cytokine activity *in-vitro*. However, till date no research group has explored the possibility of fabricating a microparticulate system that can co-deliver the TLR agonists along with the antigen and study the synergistic activity of these ligands in an *in-vitro* and *in-vivo* setting. Furthermore, no group thus far has explored the activity of such a tri-component delivery system in a prophylactic and therapeutic tumor model.

Although the hypothesis seemed promising, developing such a tri-component delivery system posed several challenges. OVA, CpG and poly I:C are all hydrophilic components and thus provide an increased resistance to entrapment within a hydrophobic carrier like PLGA. A preliminary attempt to load all the three components using the optimized formulation approach proved to be challenging. The EE of poly I:C was reduced from 50% in the dual component carrier to 35% when present in the tri-component carrier. The loading of CpG was less than 2 %. The presence of three components increases the theoretical loading and limits the drug carrying capacity of the polymer. An increase in polymer concentration to improve the carrying capacity of the microparticles did not improve the loading efficiency of CpG. A closer examination of the physico-chemical properties of the individual components better explained the poor loading efficiency associated with CpG in particular. Poly I:C and CpG carry an overall negative charge owing to a phosphate back bone. We hypothesize that a similarity in charge perhaps resulted in a mutually strong repulsive forces being exerted and a complete expulsion of the low molecular weight CpG. The increase in PLGA concentration disproportionately to reduce the extent of CpG expulsion into the external

phase was not the most desirable approach as this would retard the release rate of the entrapped components. An increased PLGA concentration would impede the antigen burst release and the overall release rate. Additionally, despite the marginal increase in the loading of CpG, the requirement of the carrier to provide 40-50 % loading of this component still remained unattained.

In an attempt to overcome the difficulty associated with fabricating such a tri-component system, a novel design approach was attempted which is described in detail under Part B of this section.

Part B: Design of a tri-component vaccine carrier- Introduction to a novel fabrication approach

Since a simultaneous encapsulation of both the adjuvants seemed to be a challenging task, we proposed a particulate carrier that can co-entrap poly I: C and the antigen OVA and associating the third component CpG with the surface of the microparticle. CpG and not poly I:C was chosen as the component that could be surface adsorbed taking into consideration a few studies that were used as a precedent for this approach. Singh et al. utilized charged microparticles to adsorb CpG on the surface of PLGA microparticles and co-deliver CpG adsorbed on cationic microparticles (117). In Singh et al.'s study, they examined the ability of adsorbed CpG to elicit antibody response to anthrax associated antigen upon intraperitonial immunization in mice (Figure III-21). The groups in the study were soluble antigen mixed with soluble CpG, antigen adsorbed to PLGA with no adjuvant, CpG adsorbed to PLGA with soluble antigen, and PLGA with antigen adsorbed mixed with PLGA with CpG adsorbed. A significant adjuvant effect on antibody (Figure III-21) and CTL responses were observed with the group where CpG was surface adsorbed onto PLGA microparticles administered along with soluble antigen. However, in this case the empty cationic microparticles were fabricated utilizing a cationic surfactant -cetyltrimethylammonium bromide (CTAB).

Conventional methods for fabrication of cationic or positively charged PLGA microparticles include emulsion-solvent evaporation techniques utilizing either didodecyldimethylammonium bromide (DMAB) or cetyltrimethyl ammonium bromide (CTAB) as the surfactant during the emulsification step of fabrication. However, the low LD_{50} values of 408 and 280 mg/kg for cetrimide and DMAB respectively often restricts their use. In contrast polyvinyl alcohol (PVA) exhibits a LD_{50} of 20 gm/kg and hence is often considered as the safest stabilizer for microparticle fabrication. The particles fabricated using cationic surfactants also exhibited significant aggregation resulting in poor dispersibility.

Hence an alternate approach to design of cationic microparticles using polyethyleneimine (PEI) was pursued. The method is described schematically in Figure III-22 and is explained in detail in the following paragraph.

B1: Fabrication of cationic PLGA microparticles eco-entrapping OVA and poly I:C

The polymer of choice was PLGA 85:15 inherent viscosity 0.52 dL/g with an acid (-COOH) end group for further modifications. The inherent viscosity was similar to the PLGA grades used for the fabrication of the dual component systems. The similarity in MW ensures a similarity in release kinetics of the entrapped components. Additionally, the lactide-glycolide ratio was also comparable to the PLGA 75:25 grade used for the fabrication of the dual component systems. Poly I:C and OVA were co-loaded within this carrier system using the same method as described in the earlier section VII.2. The particles were analyzed for size and entrapment efficiency. Following lyophilization, the particles were modified using EDC-NHS for conjugation of a cationic polymer on the surface. Briefly, 100 mg of the particles were suspended in 3 mL MES buffer (pH 5.5). 20-fold molar excess of EDC (1-Ethyl-3-[3-dimethylaminopropyl] carbodiimide HCl and sulfo-NHS (N-hydroxysuccinimide) over PLGA was used for modification. The calculated amounts of EDC and NHS were dissolved in 1 mL MES buffer each and was

slowly added to the particles under constant stirring. Stirring was continued for 1 hour. The particles were then centrifuged and washed twice with PBS to remove any unreacted EDC-NHS. The particles were then suspended in 3 mL of autoclaved PBS. A 15-fold molar excess of cationic polymer, PEI was used for surface conjugation thus rendering an overall positive charge to the OVA and poly I:C co-loaded PLGA particles. The cationic polymer was suspended in 2 mL PBS. The particles were then added drop wise into the PEI solution under constant stirring and the reaction was allowed to proceed at room temperature for 3 hours. The particles were then collected by centrifugation, washed and lyophilized overnight. The particles were then analyzed for OVA and poly I:C content to account for any loss during the chemical conjugation steps. PEI conjugation was confirmed by a change in zeta potential from a slightly negative charge to a distinct positive charge. Fluorescamine (4-phenylspirofuran-2(3H), 10-phthalan]-3, 30-dione) is used for colorimetric quantification of primary amines and is used to quantify the amount of PEI conjugated to the microparticles. PEI-conjugated microparticles were hydrolyzed in 0.1N NaOH overnight and the PEI content is measured using spectrofluorometric analysis (SpectramaxPlus 384 Microplate reader, Molecular Devices, Sunnyvale, CA). Fluorescamine reacts with primary amines in PEI to form pyrrolinones, which are excited at 390nm and have an emission peak at 475–490 nm. The amount of PEI in microparticles was estimated using standard curves of PEI.

B2: Conjugation of CpG to the surface of cationic PLGA microparticles

Briefly, CpG was incubated with the PLGA microparticles modified above at a concentration of 10 µg CpG/mg particles at 4 °C for 6 h. The resulting particles were centrifuged at 7000 rpm for 5 min on a microcentrifuge and washed twice with the loading buffer to obtain the tri-component microparticles. The supernatant was collected and analyzed by fluorescence spectroscopy (SpectramaxPlus Plus384 Microplate reader, Molecular Devices, Sunnyvale, CA) for CpG content using the Oligogreen ssDNA assay

reagent. CpG loading on the cationic microparticles was calculated by subtracting the pDNA content in the supernatant from the initial concentration of CpG added.

Results and discussion (II)

The chemical conjugation pathway for fabricating cationic PLGA-PEI microparticles using EDC and sulfo-NHS is shown in Figure III-23. 1-Ethyl-3-[3-dimethylaminopropyl]carbodiimide hydrochloride (EDC or EDAC) is a zero-length cross-linking agent used to couple carboxyl groups to primary amines. This cross-linker has been used in diverse applications such as forming amide bonds in peptide synthesis, attaching haptens to carrier proteins to form immunogens, labeling nucleic acids through 5' phosphate groups and creating amine-reactive NHS-esters of biomolecules. EDC reacts with a carboxyl to form an amine-reactive *O*-acylisourea intermediate. If this intermediate does not encounter an amine, it will hydrolyze and regenerate the carboxyl group. In the presence of *N*-hydroxysulfosuccinimide (Sulfo-NHS), EDC can be used to convert carboxyl groups to amine-reactive Sulfo-NHS esters. This is accomplished by mixing the EDC with a carboxyl containing molecule and adding Sulfo-NHS.

The characteristics of the microparticles including particle size and zeta potential prior to and post PEI conjugation is given in Table III-3. Microparticles that were covalently conjugated with PEI on the surface showed a 1.5-fold increase in their average size in comparison with the original PLGA microparticles used for conjugation. PLGA microparticles co-entrapped with OVA and poly I:C display a net negative surface charge of -40 mV due to the presence of surface carboxylic groups associated with the polymer. After the introduction of PEI, the surface charge of the microparticles became positive with net values ranging from +25 to +30 mV. The positive charge can be attributed to the presence of abundant amino groups on the surface (Table III-2).

The loading and the entrapment efficiencies of the PLGA microparticles co-entrapping OVA and poly I:C prior to and after conjugation with PEI is given in Table

III-4. It can be seen that the chemical conjugation process resulted in a 10-12% reduction in the loading efficiency of OVA and poly I:C. The reduction in EE was in sync with the burst release that is associated with OVA and poly I:C when exposed to an aqueous medium. CpG loading on the microparticles was an efficient process exhibiting an adsorption efficiency of nearly 50%. It can be further observed that upon CpG adsorption on the surface the particles revert back to being negatively charged owing to the phosphate back-bone on CpG that renders an overall negative charge to the particles (Table III-3).

Thus we have for the first time successfully designed a polymeric carrier system that can co-deliver multicomponents (antigen and the two adjuvants) within the same carrier system with a synergistic anti-tumor effect. In this novel approach, OVA and poly I:C is entrapped inside the PLGA microparticle matrix and CpG is adsorbed on the surface of the PLGA microparticle. The next chapter focuses on the application of the dual and tri-component particulate carriers in a prophylactic and therapeutic tumor model.

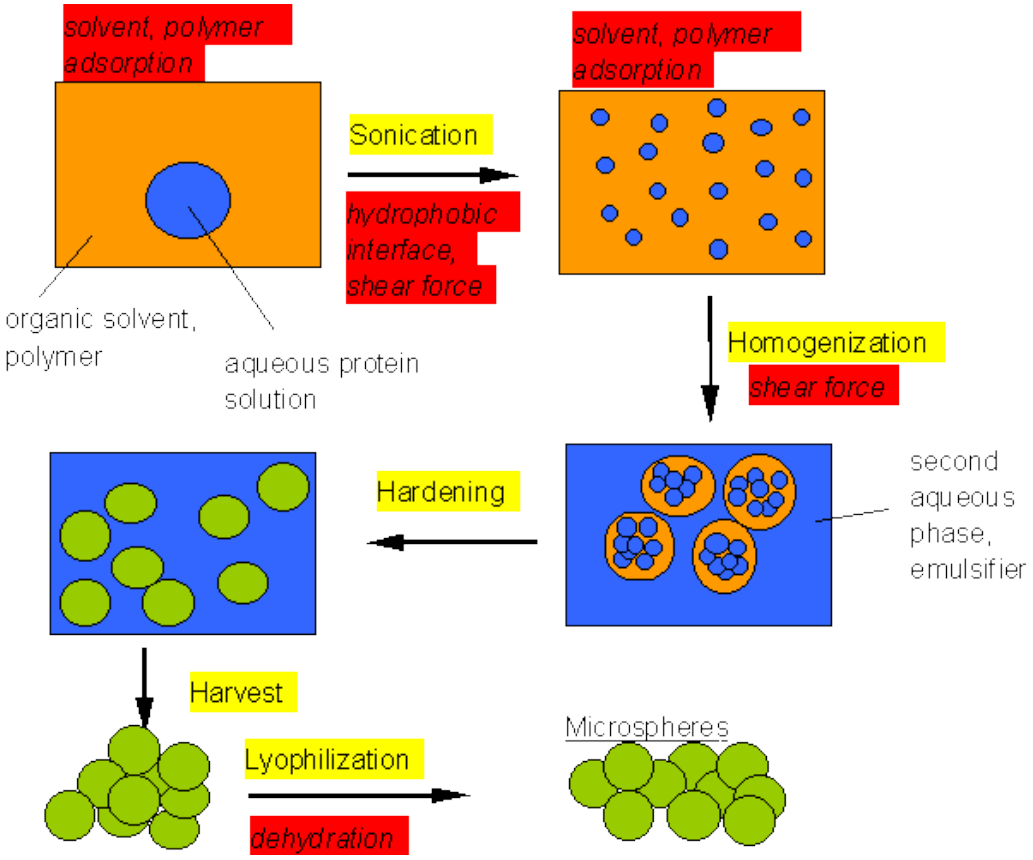

Figure III-1: Microparticle fabrication technique using double emulsion solvent evaporation process.

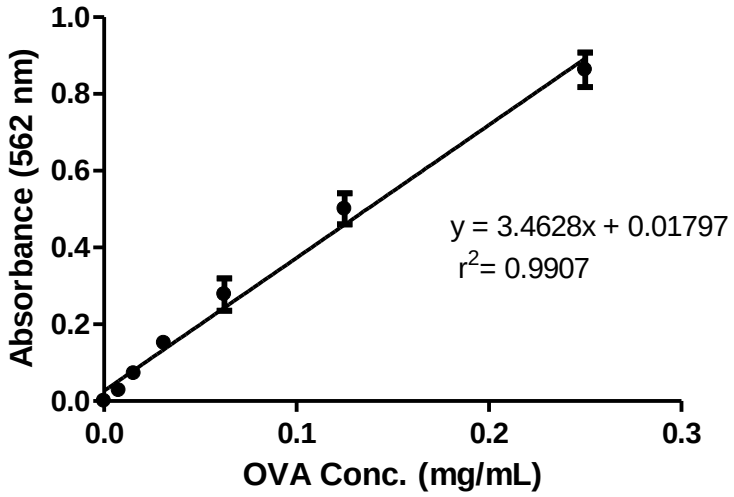

Figure III-2: Standard Curve of Ovalbumin (OVA) analyzed using micro-BCA assay. Data is represented as the mean ± standard deviation (*n* = 3).

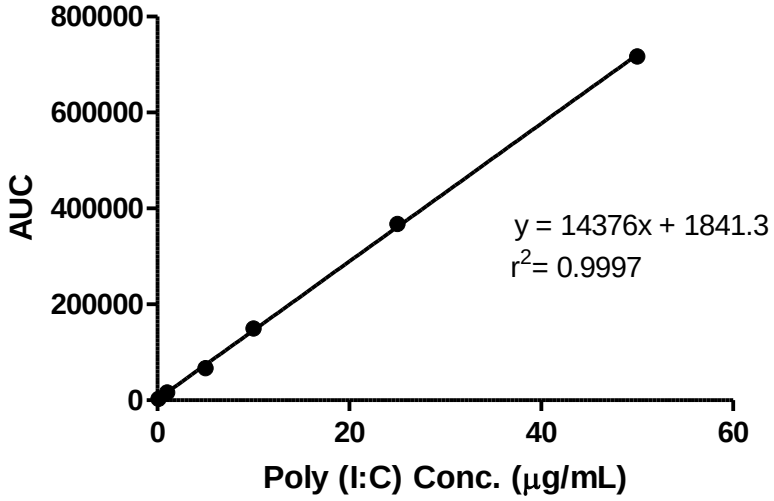

Figure III-3: Standard Curve of poly I:C analyzed using HPLC. Data is represented as the mean ± standard deviation (*n* = 3).

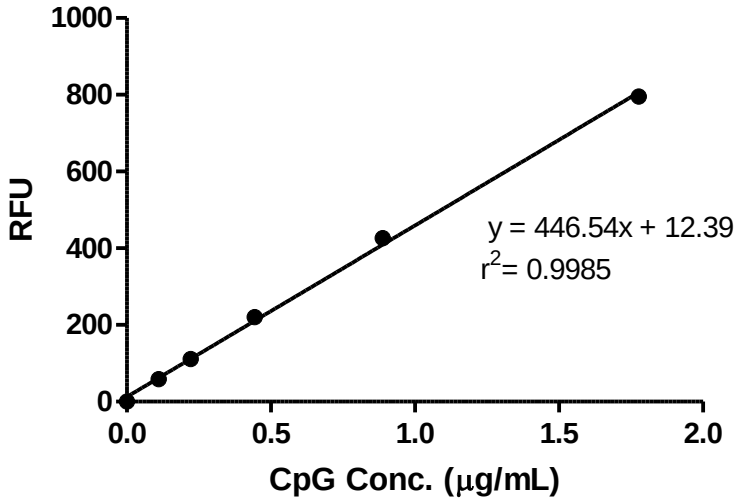

Figure III-4: Standard curve of CpG analyzed by Oligogreen Quanti ssDNA fluorescence assay. Data is represented as the mean ± standard deviation (n = 3).

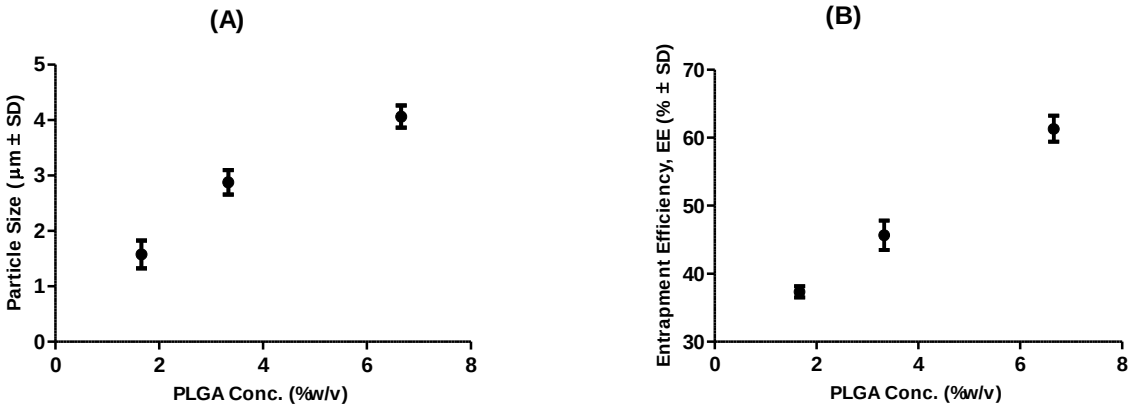

Figure III-5: Effect of PLGA 50:50 (MW 7000 Da) conc. on particle size (A) and entrapment efficiency (B) of OVA-loaded PLGA microparticles. Data is represented as the mean ± standard deviation (n = 3).

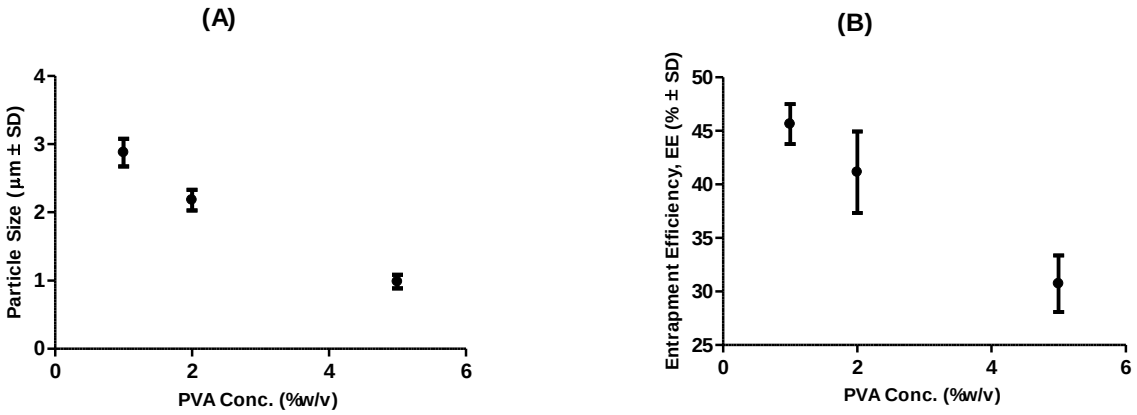

Figure III-6: Effect of emulsifier (PVA) conc. on particle size (A) and entrapment efficiency (B) of OVA-loaded PLGA 50:50 (MW 7000 Da) microparticles. Data is represented as the mean ± standard deviation (n = 3).

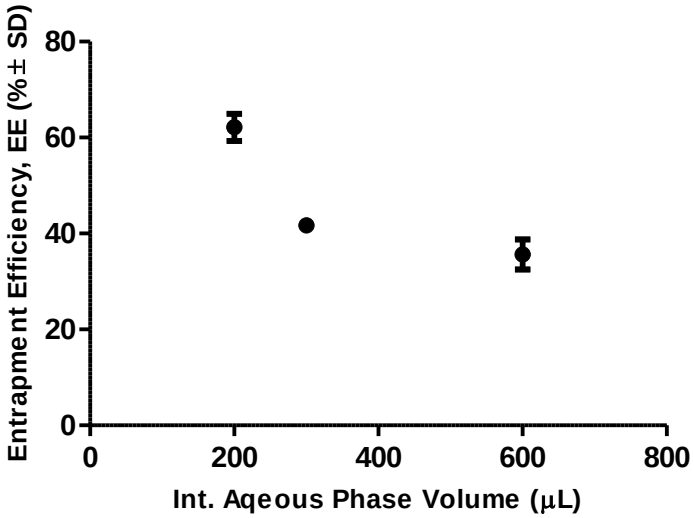

Figure III-7: Effect of internal aqueous phase volume on the entrapment efficiency of OVA in OVA-loaded PLGA 50:50 (MW 7000 Da) microparticles. Data is represented as the mean ± standard deviation (n = 3).

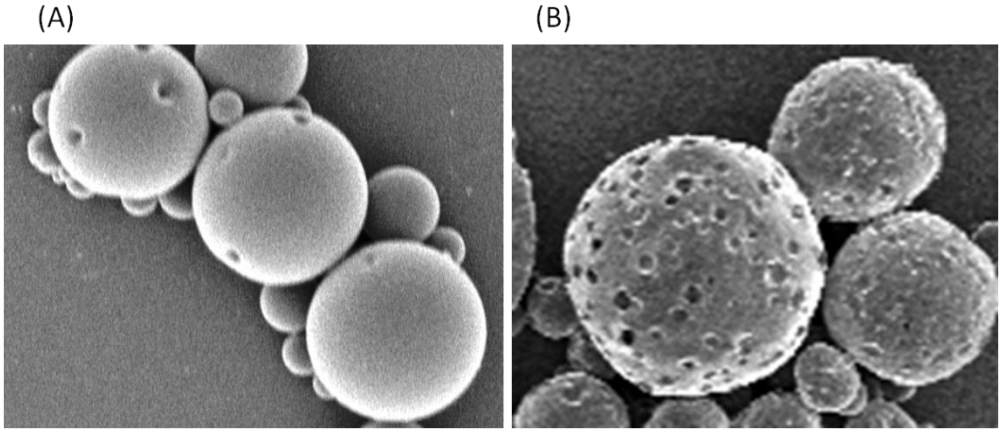

Figure III-8: Effect of internal aqueous phase volume; 200 µL (A) and 600 µL (B) on the porosity of OVA and poly I:C co-loaded PLGA 50:50 (MW 7000 Da) microparticles.

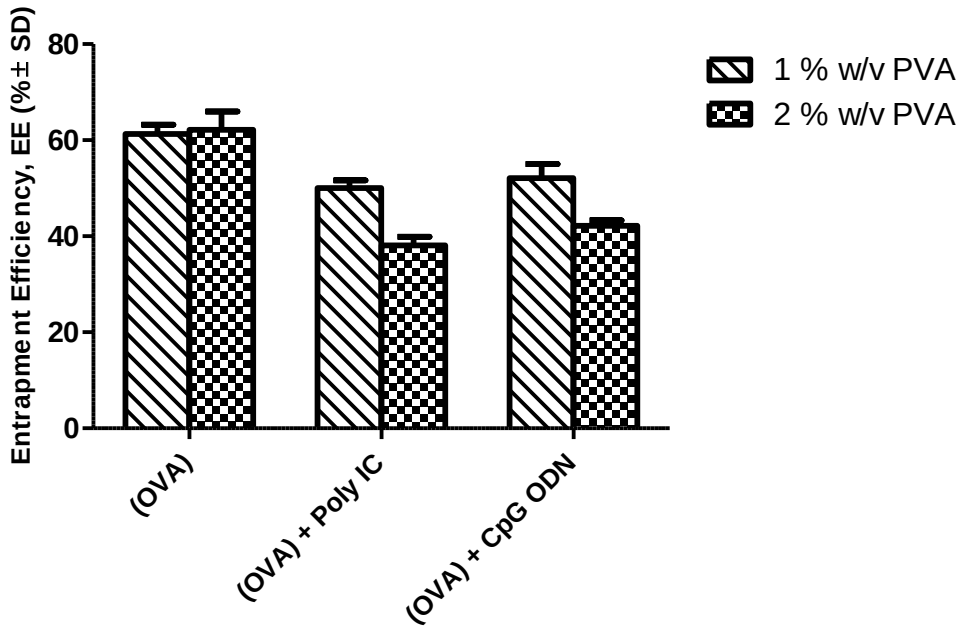

Figure III-9: Effect of co-entrapment of a second component on the entrapment efficiency of OVA in the co-delivery PLGA 50:50 (MW 7000 Da) microparticles. Data is represented as the mean ± standard deviation (n = 3).

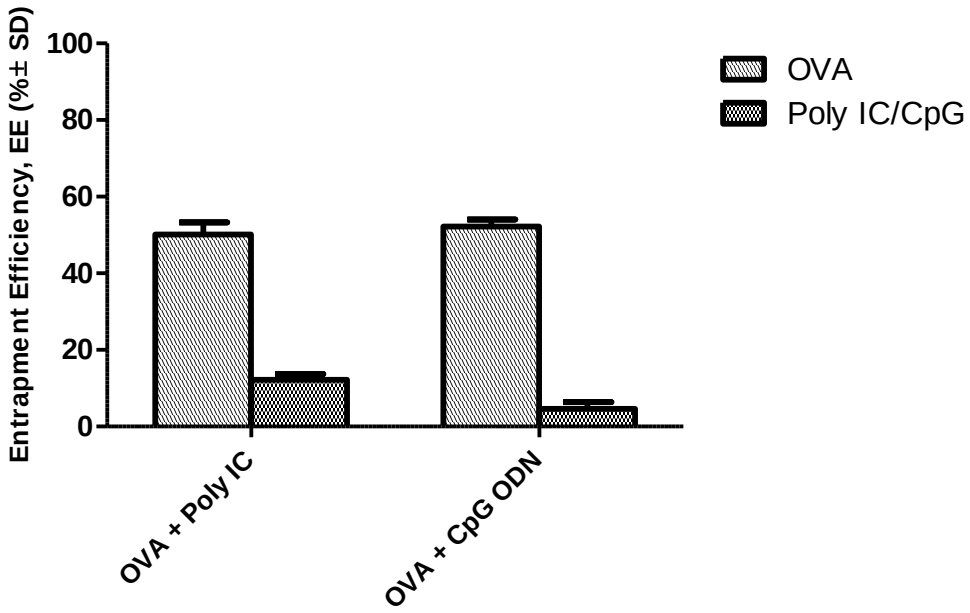

Figure III-10: Entrapment efficiency of OVA, poly I:C and CpG in OVA + poly I:C/CpG co-loaded PLGA 50:50 (MW 7000 Da) microparticles. Data is represented as mean ± standard deviation (*n = 3*).

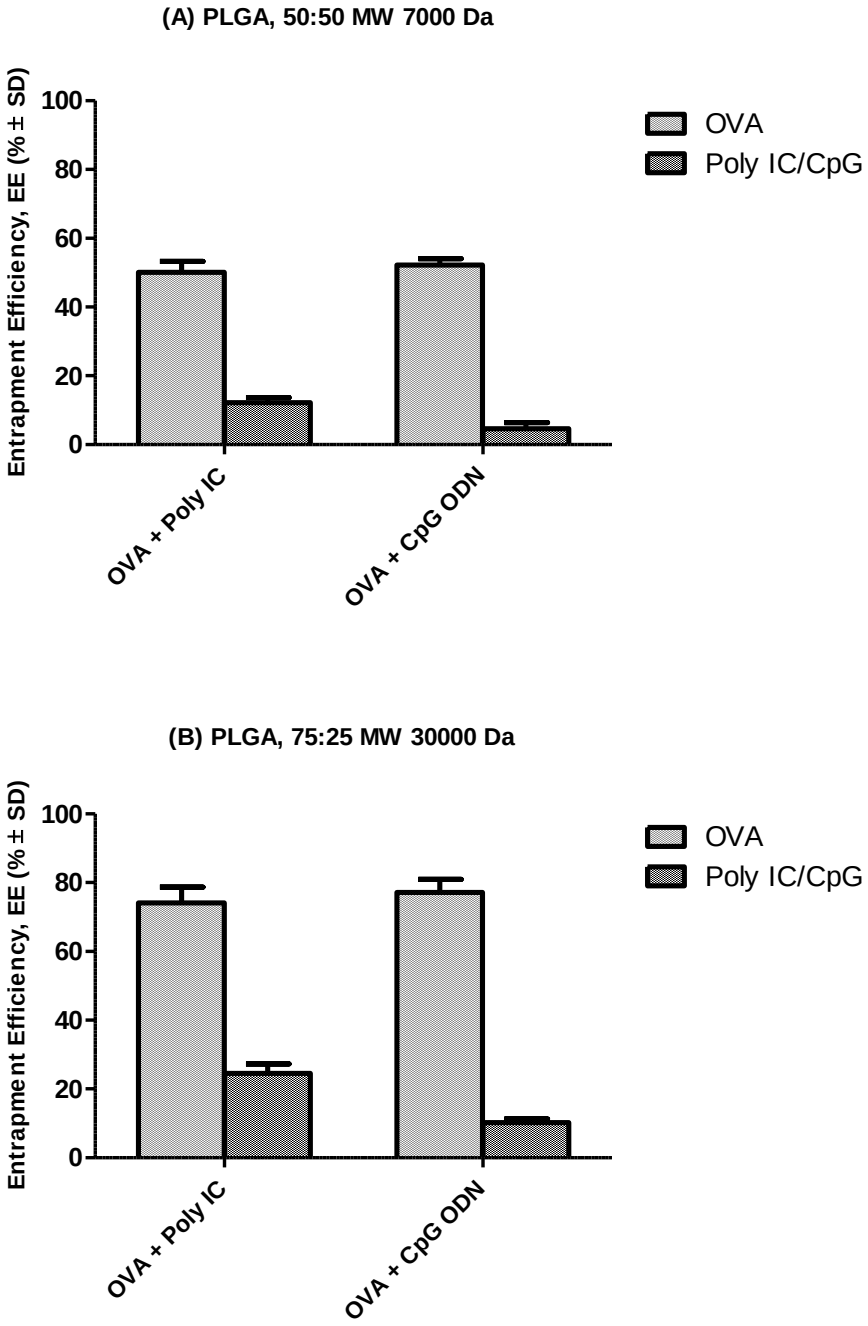

Figure III-11: Effect of type and molecular weight of PLGA on entrapment efficiencies of OVA and poly I:C/CpG in the co-delivery (A) low molecular weight PLGA 50:50 MW 7000 Da) and (B) PLGA 75:25 MW 30000 Da microparticles. Data is represented as mean ± standard deviation. (*n = 3*).

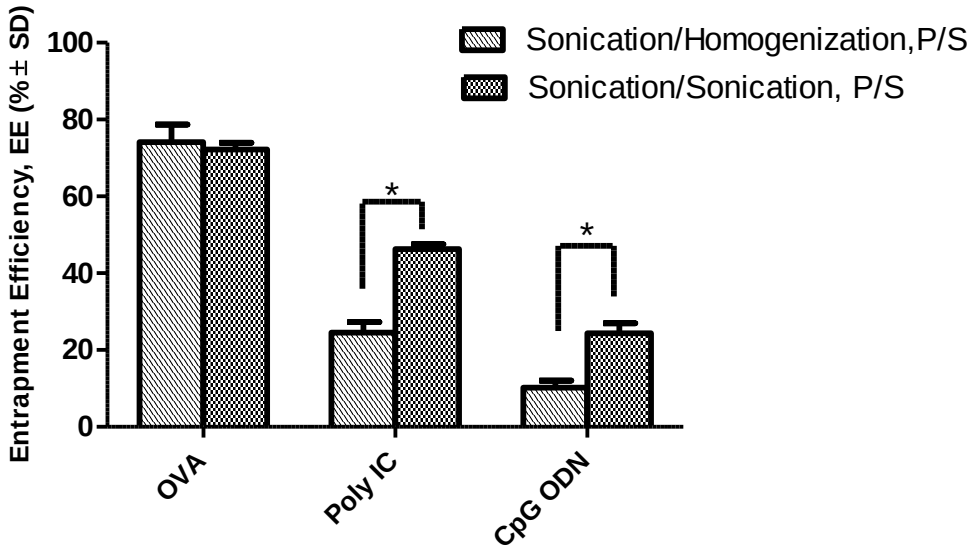

Figure III-12: Effect of method of microparticle fabrication on entrapment efficiencies of OVA and poly I:C/CpG in PLGA 75:25 (MW 30000 Da) co-delivery carriers. Data is represented as mean ± standard deviation. (*n = 3*).

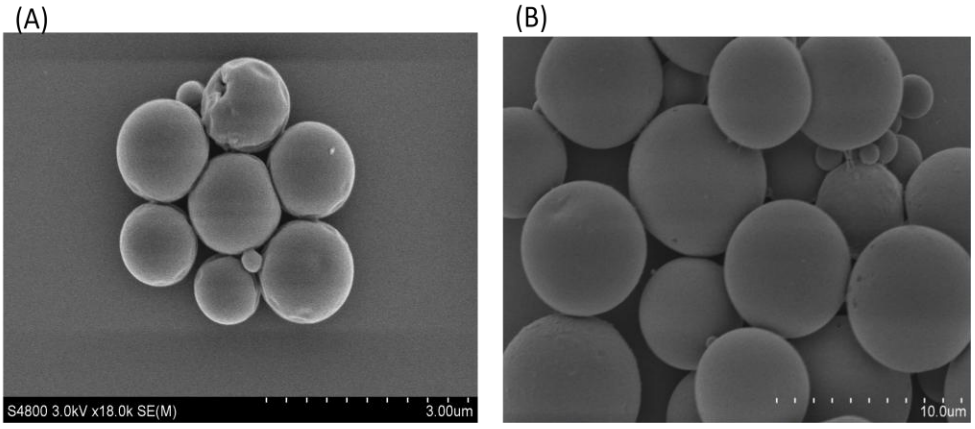

Figure III-13: Effect of method of microparticle fabrication, double sonication (A) and sonication/homogenization (B) on the particle size of OVA + poly I:C co-loaded PLGA 75:25 (MW 30000 Da) microparticles.

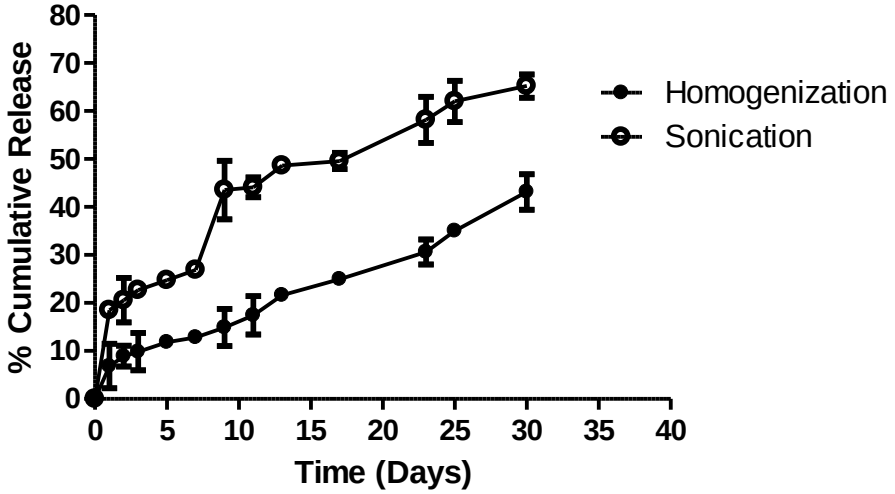

Figure III-14: Effect of method of fabrication on the *in-vitro* release profile of **OVA** from OVA + poly I:C co-loaded PLGA75:25 (MW 30000 Da) microparticles in PBS, pH 7.4. Data is represented as mean ± standard deviation (*n = 3*).

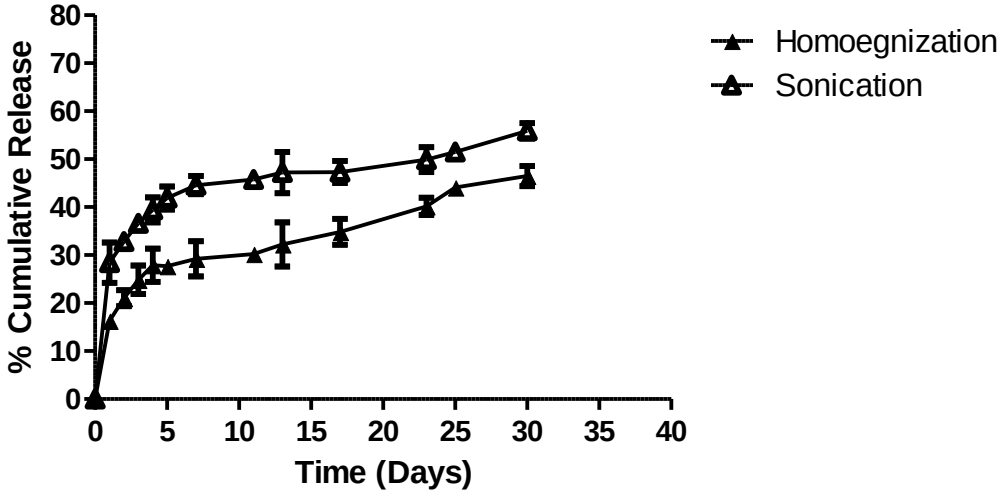

Figure III-15: Effect of method of fabrication on the in-vitro release profile of **poly I:C** from OVA + poly I:C co-loaded PLGA 75:25 (MW 30000 Da) microparticles in PBS, pH 7.4. Data is represented as mean ± standard deviation (*n = 3*).

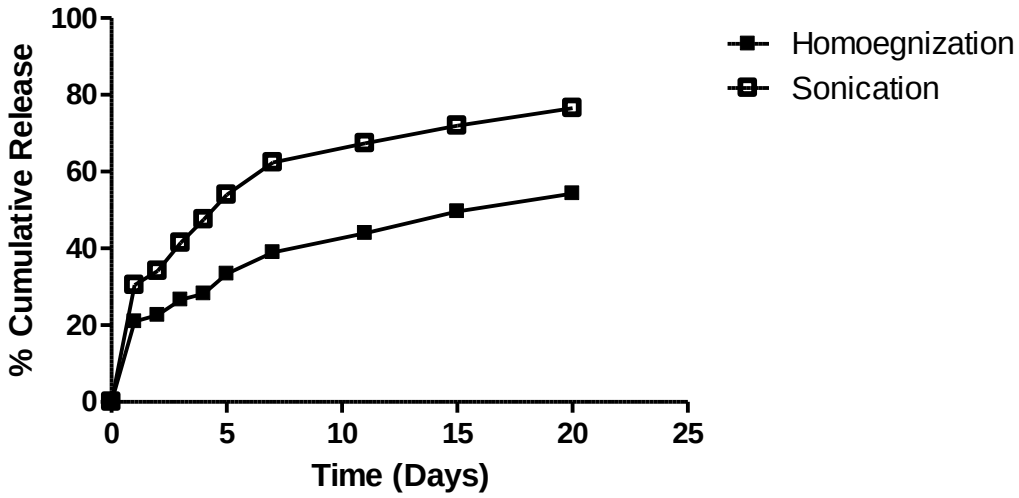

Figure III-16: Effect of method of fabrication on the *in-vitro* release profile of **CpG** from OVA + CpG co-loaded PLGA 75:25 (MW 30000 Da) microparticles in PBS, pH 7.4. Data is represented as mean ± standard deviation (*n = 3*).

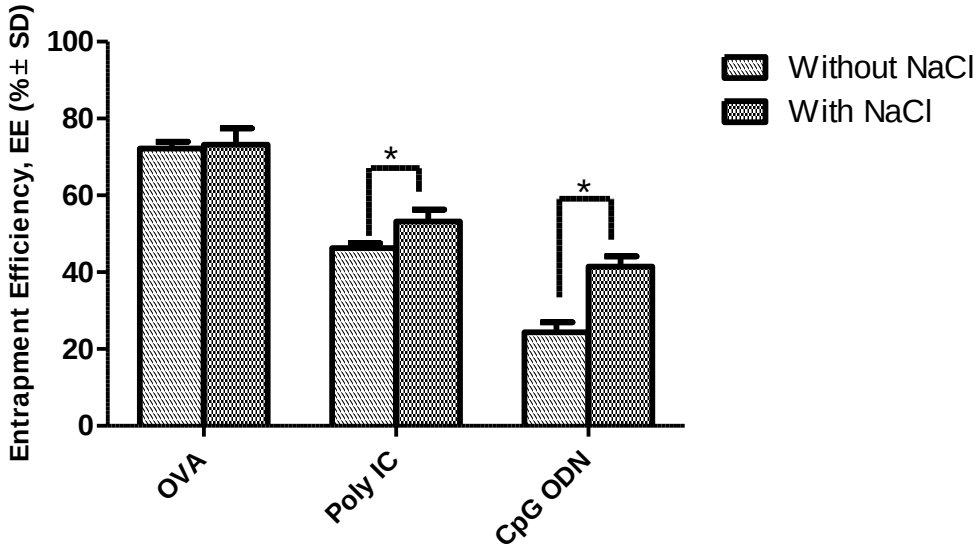

Figure III-17: Effect of the addition of NaCl on entrapment efficiency of OVA + poly I:C/CpG PLGA 75:25 (MW 30000 Da) microparticles made by double sonication method. Data is represented as mean ± standard deviation (*n = 3*).

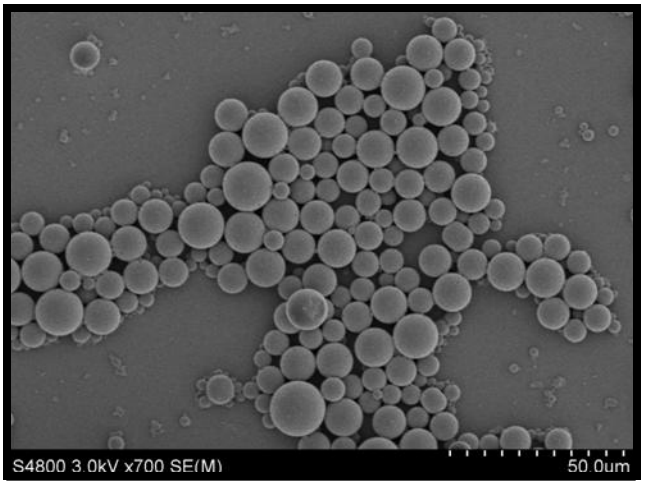

Figure III-18: SEM image of OVA + CpG co-loaded PLGA 75:25 (MW 30000 Da) microparticles made by double sonication technique in the presence of NaCl in the external aqueous phase prior to any differential centrifugation for size based separation. Mean size of the MP was 2 ± 1.2 µm.

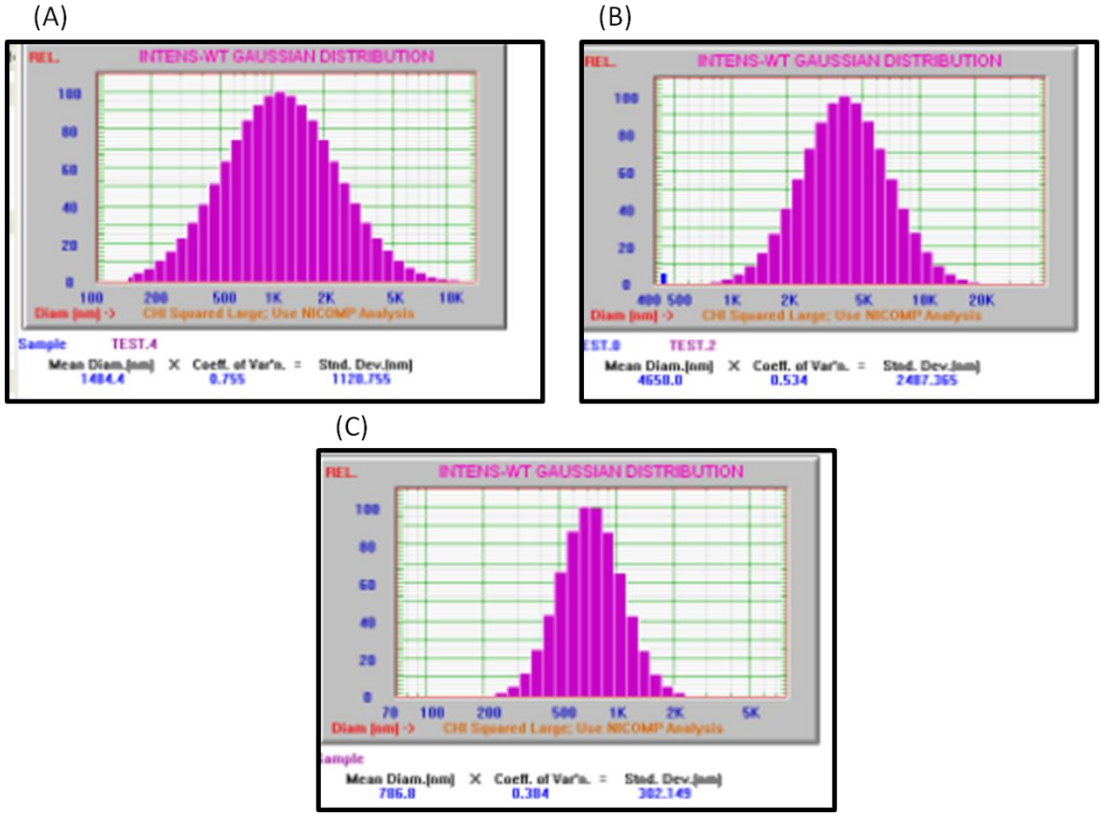

Figure III-20: Mean intensity-weighted particle size and standard deviation of OVA-loaded PLGA 75:25 (MW 30000Da) microparticle particles prepared by (A) homogenization and (B) sonication collected by single step centrifugation at 7000 rpm, (C) represents OVA-loaded PLGA 75:25 (MW 30000 Da) microparticles collected by multi-step differential centrifugation method and prepared by double sonication technique.

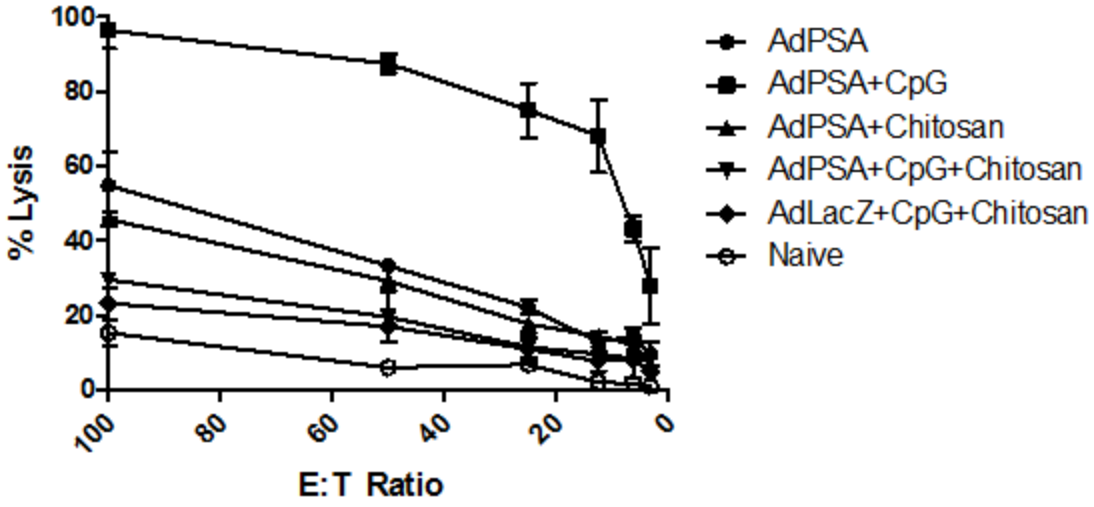

Figure III-20: Cytotoxic T cell activity (CTL) data showing chitosan hindering the activity of adenovirus + CpG vaccine. Data is represented as mean ± standard deviation (*n = 3*). (Unpublished date by our group).

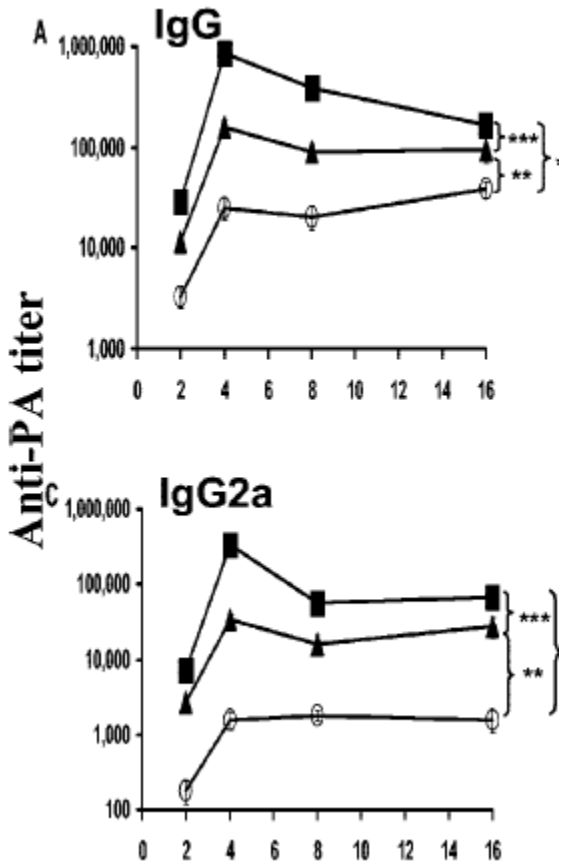

Figure III-21: IgG and IgG2a anti-PA antibody titers in anthrax vaccine adsorbed (AVA) vaccinated mice. Male A/J mice were immunized intraperitoneally with 200 µg of AVA (○) with and without 20 µg of free (▲) or PLG-adsorbed CpG (■). CpG adsorbed on the surface of cationic PLGA microparticles shows the maximum immunostimulatory effect. Reproduced with permission from (94). Copyright©Elsevier B.V.

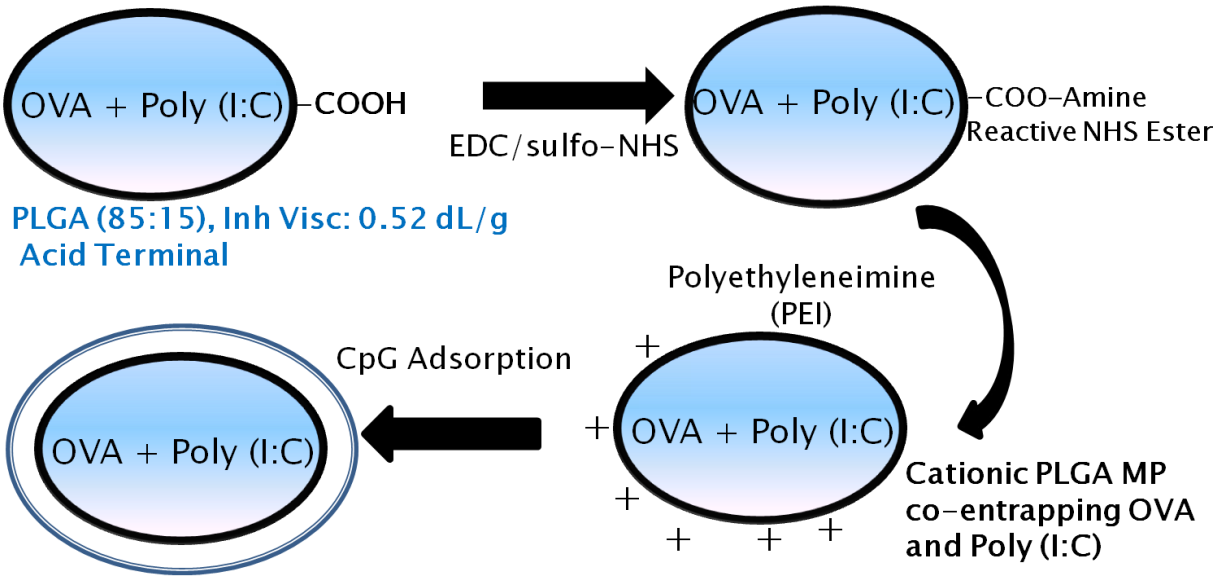

Figure III-22: Scheme for fabrication of OVA + poly I:C and CpG co-loaded tri-component PLGA 85:15 (MW 40000 Da) microparticles.

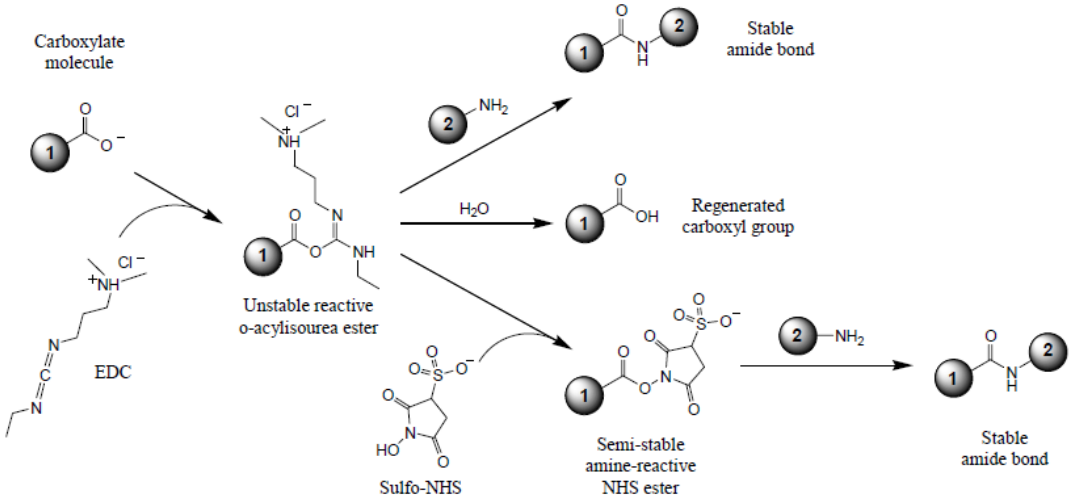

Figure III-23: Scheme for chemical conjugation of polyethylenimine (2) to OVA + poly I:C co-loaded PLGA 85:15 (MW 40000 Da) microparticles with a carboxylic acid end group (1).

Table III-1: Optimized PLGA 75:25 (MW 30000 Da) Microparticulate (MP) formulations developed for tumor immunotherapy

Formulation Group	Contents
I	Empty
II	OVA
III	OVA + poly I:C
IV	OVA + CpG
V	OVA + poly I:C + CpG*

* Denotes the microparticles were fabricated using PLGA 85:15 (MW 40000 Da) with a carboxylic acid terminal

Table III-2: Particle size of the various optimized PLGA75:25 (MW 30000 Da) microparticulate (MP) formulations developed for tumor immunotherapy in a murine model

Formulation (MP)	Particle Size (μm ± SD)
Empty	1.5 ± 0.4
OVA	1.3 ± 0.5
OVA + poly I:C	1.6 ± 0.7
OVA + CpG	1.4 ± 0.3
OVA + poly I:C + CpG*	2.2 ± 0.5

* Denotes the microparticles were fabricated using PLGA 85:15 (MW 40000 Da) with a carboxylic acid terminal

Table III-3: Effect of PEI conjugation and CpG adsorption on the zeta potential of tri-component PLGA 85:15 (MW 40000 Da) MP

Zeta Potential (mV ± SD)		
Unmodified	**After PEI Conjugation**	**After CpG Adsorption**
-40.1 ± 3.4	+27.3 ± 4.1	-12.2 ± 4.6

Table III-4: Effect of PEI conjugation on entrapment efficiency of OVA and polyI:C during tri-component PLGA 85:15 (MW 40000 Da) MP fabrication

Entrapped Component	**Average Loading (µg/mg PLGA MP)**	
	Before PEI Conjugation	**After PEI Conjugation**
OVA	20.18	16.8
Poly I:C	7.1	6.0

CHAPTER IV: PROPHYLACTIC AND THERAPEUTIC ANTI-TUMOR EFFECTS IN A T CELL LYMPHOMA MODEL WITH PLGA BASED VACCINES CO-DELIVERING AN ANTIGEN AND TLR ADJUVANT

Introduction

The current response rate to cancer vaccine formulations is approximately 3.0%. The most important issue that still needs to be addressed to improve the success rate of vaccine formulations is to improve the qualitative and quantitative T cell responses (118). The second issue is the lack of immune strategies that can activate a robust and lasting immune response against cancer antigens. Typically in cancer immunotherapy, most antigens used are weakly immunogenic as they are either self or host realized. Thus the eventual success of cancer immunotherapy is dependent on the development of carriers that can co-deliver the antigen and adjuvant to the specialized antigen presenting cells (APCs). Upon vehicle uptake, the entrapped adjuvant is available to interact with the TLR receptors that are crucial to initiate cell-mediated immunostimulatory cascades.

Among the various carrier systems including liposomes, viral vectors and virosomes, micro/nanoparticles made of PLGA are of special interest and most widely studied carriers for both small and large molecules (119, 120). In addition to their biodegradable nature and safe toxicity profile they afford great formulation flexibility in order to accommodate both the antigen and immunomodulator molecules like adjuvants. Another advantage to these systems is the ability of the antigen to present and process the antigen by two independent pathways (MHC class I and II) with the final outcome of simultaneous activation of CD4 and CD8 T cell immune responses (91, 97). TLR3 ligand like poly I:C and TLR9 ligand such as CpG have the ability to provide the co-stimulatory signal that elicit the aforementioned type of immune responses.

The long-term objective of this research and the main focus of this chapter is the development of vaccines that can co-deliver OVA along with either poly I:C or CpG or both and study the effectiveness of these systems in a prophylactic and therapeutic tumor model. This research draws its proof of concept from a previous study done by our group in which we showed that co-delivery of OVA as a model antigen and CpG dramatically induces an enhanced interferon; IFN-γ secretion (66). This activation was superior to what was observed in mice immunized with antigen alone. However, a comprehensive study including dendritic cell (DC) cell activation, immune response quantification and tumor protection in a prophylactic and therapeutic setting has not been studied so far. Hence the broad objective of this research is to develop PLGA vaccine carriers that could significantly stimulate anti-tumor immunity

While the previous chapter focused extensively on the fabrication of these co-delivery and tri-component carriers, the main focus of this chapter is on the ability of these carriers to induce DC activation and maturation, induction of antigen-specific B and T cell responses and ability to induce anti-tumor immunity. The effects of intraperitonial (i.p) vs. intramuscular (i.m.) routes of administration in eliciting an antigen-specific antibody immune response have also been evaluated from a prophylactic vaccination standpoint. In addition to this, the efficacy of the various vaccination groups has also been evaluated in a therapeutic tumor model.

Materials and methods

Materials

PLGA (75:25, Inherent viscosity, 0.41 dL/g) were purchased from Lactel Absorbable Polymers (Cupertino, CA). Poly (vinyl alcohol) (PVA, 87 – 89 % hydrolyzed, MW 30-67,000 Da) was purchased from Sigma-Aldrich (St. Louis, MO). Ovalbumin from chicken egg white, grade VII purified and poly I:C sodium salt were purchased from Sigma-Aldrich. (St. Louis, MO). CpG-1826 was purchased from Coley Pharmaceuticals

(Dusseldorf, Germany). All other chemicals and solvents including dichloromethane (DCM), acetonitrile used were of analytical grade. All the instruments including Hitachi-4000 SEM, Bio-Rad Radiance 2100MP, Zeiss Confocal 710 confocal microscopes and FACSCAN-2 flow cytometer were used at the Central Microscopy Research Facility (CMRF), UIowa, Iowa City, IA.

Methods

I. Fabrication of PLGA based vaccination carriers

Empty PLGA MP (group 1), OVA-loaded PLGA MP (group 2), OVA + CpG co-loaded PLGA MP (group 3), OVA + poly I:C co-loaded PLGA MP (Group 4) were all prepared by double emulsion solvent evaporation technique as described in detail in chapter III using a double sonication method to form both the primary and secondary emulsions. Briefly, the antigen either alone (5.5 – 6mg) or in combination with one of the adjuvants ;CpG/poly I:C (3 mg each) was added to 200 µL of 1% PVA and emulsified into 2 mL DCM containing 6.67 % w/v PLGA 75:25 (MW 30 kDa) using an ultraprobe sonicator at 10 watts for 30 seconds on an ice-bath. This primary emulsion was then rapidly poured into 4 mL 1% PVA and further sonicated at 10 watts power for 30 seconds. This secondary emulsion was then diluted into 50 mL 1% PVA containing NaCl and allowed to stir using a magnetic stir-bar until complete evaporation of DCM. The formed microparticles were collected at 5000 rpm, washed three times with deionized water and lyophilized overnight.

The tri-component PLGA MP carrying OVA along with CpG and poly I:C was prepared by a modified approach as explicitly explained in section VIII of chapter III.

All the microparticle formulations were characterized for particle size, loading efficiency of the individual components and *in-vitro* release kinetics as described in chapter III.

II. Fluorescent labeling of OVA

A solution of OVA at 2 mg/mL was prepared in 50 mM PBS (pH 7.4). N-hydroxysuccinimide (NHS)-Rhodamine (Pierce Scientific, Rockford, IL) with excitation and emission wavelengths at 550 and 575 nm was used as the labeling agent for OVA. Briefly, the protein solution was slowly added to the 1mg vial of the labeling reagent. The mixture was pipeted up and down 10 times until the dye completely dissolved and this mixture was incubated for 60 minutes in dark at room temperature. The mixture was then dialyzed in a 200-fold excess volume PBS using a SnakeSkin dialysis tubing (Pierce Scientific, Rockford, IL) with a molecular weight cut-off (MWCO) of 2000 Da for 8 hours. This was done to remove any un-conjugated or free labeling dye. The labeled protein was then lyophilized overnight to obtain rhodamine-labeled OVA.

III. Fluorescent labeling of CpG

ULYSIS Nucleic acid labeling kit for labeling CpG was purchased from Molecular Probes (Invitrogen Detection Technologies, Carlsbad, CA). The fluorescent dye used was Ulysis 1653-Alexa-Fluor 568 with excitation and emission wavelengths at 576 and 600 nm respectively. Stock solution of this dye was prepared in dimethylformamide (DMF). A 50-fold molar excess of the labeling dye over CpG was used for efficient conjugation as per manufacturer's protocol. 2 mg of CpG was precipitated by adding $1/10^{th}$ volume of 3M sodium acetate (pH 5.2) and 2-fold excess ethanol. The mixture was frozen for 30 minutes and then centrifuged for 15 minutes at 12000 rpm to collect the precipitated CpG. 50-fold molar excess of the labeling dye solution in 1X Tris-EDTA (TE) buffer was added to the precipitated CpG and the reaction mixture was incubated for 80 minutes in dark at room temperature. The reaction was then stopped by plunging the reaction mixture tube in ice. The unreacted or free labeling dye was then separated in a manner similar to OVA as described in section II

using a SnakeSkin dialysis tubing with a MWCO of 2000 Da. CpG was then stored as a solution in TE buffer at 4 °C until further use.

IV. *In-vitro* generation of bone marrow-derived dendritic cells (BMDCs) and assessment of microparticle uptake by confocal microscopy

A naïve mouse was sacrificed and its skin surrounding legs was removed using scissors and forceps. The leg was then removed by cutting with scissors high up in the hip/pelvic region. The leg was then placed in a petri dish to remove skin and muscle. The legs were placed in 70% ethanol for 2 -3 minutes. The sterilized legs were then transferred to a fresh petri dish containing PBS to remove as much muscle and fat as possible. An incision was made on the bone at the extremities of the joints using scissors and then, using a 30-1/2 gauge needle, the bone marrow was flushed into a petri dish containing 5 mL growth media. The cells were then collected in a 15 mL tube and centrifuged 10 minutes at 1200 rpm (240 x g) and resuspended in 10 mL of growth media and then counted using bacteriological grade dishes, the cells were then plated at $2x\ 10^6$ cells per dish in 10 mL of growth media containing 20 ng/mL of GM-CSF and incubated at 37°C in 5% CO_2 condition. After 3 days, 10 mL of media containing 20 ng/mL GM-CSF was added followed by the same procedure on day 6 and 8. The cells were ready to be used for experiments between days 8 and 10.

Cultured BMDCs ($1x10^5$) were then seeded on a cover-glass (24 x 24 mm) and grown for 24 hours. Then, cells were incubated with either rhodamine-conjugated CpG-loaded PLGA MP or rhodamine-conjugated OVA-loaded PLGA MP overnight at 37 °C. The cells were then washed 3 times with cold PBS. The lysosome was then labeled with LysoTracker Green-DND-26 (Molecular Probes, Rockford, IL) with excitation and emission wavelengths of 504 and 511 nm respectively. The final concentration of this labeling dye was 50 nM in cell-culture media. The incubation was carried out for 45 minutes at 37 °C. The cells were then washed three times with cold PBS and fixed with 4

% formaldehyde solution for 30 minutes at room temperature and mounted using DAPI-containing Vectashield mounting medium for nucleus staining (Vector Laboratories, UK). Then the slides were covered with coverslips followed by 4 °C storage in dark before they were visualized under multiphoton/confocal microscope (Bio-Rad Radiance 2100MP and Zeiss Confocal 710, CMRF, UIowa). Orthogonal sections from stacked images were taken to confirm the presence of particles within the cell and not localized to the cell surface.

V. Particle size and morphology by SEM

A droplet of a dilute solution of each of the MP vaccine carriers was placed on a silicon wafer chips (CMRF, UIowa, IL) and allowed to air dry at room temperature. The silicon wafer chips allow multiple sample examination simultaneously and being semi-conductors prevent electrical charge build up. The silicon wafers were then placed on adhesive carbon tabs mounted on SEM specimen stubs. The specimen stubs were then sputter coated with approximately 5 nm of gold by ion beam evaporation before examination in the SEM operated at 5 kV accelerating voltage.

VI. Dendritic cell (DC) activation and up-regulation assessment by fluorescence activated cell sorting (FACS)

BMDCs were isolated and cultured as described in the previous section. The cells (1×10^5) were incubated for 48 hours with 100 μg microparticles containing OVA alone (2 μg) or OVA and poly I:C (2 and 1 μg of each respectively) or OVA and CpG (2 and 1 μg of each respectively) or tri-component MP (2, 1 and 1 μg of OVA, poly I:C and CpG respectively) or empty microparticles. In addition, the cells were also treated with soluble poly I:C or CpG to serve as positive controls. In order to identify and enumerate the DC activation markers like CD80 and CD86 (details about the markers has been explained in the results section), we chose to use flow cytometry to characterize these cell subsets. In

a flow cytometry setup, laser light is focused on a narrow stream of the cell suspension which passes cells through the detector one at a time. The detectors that measure light scattering convert the light to electrical pulses. An analog to digital converter allows the events to be plotted on a graphical scale, for viewing information about the chemical and physical structure of the cell. Based on the forward and side scatter of the light from the cells, the cell volume and shape can be determined. Fluorescence Activated Cell Sorting (FACS) is a specialized type of flow cytometry that allows cells to be labeled with fluorochromes, and then from a mixed population, be separated into subpopulations based on the fluorescence and light scattering characteristics of the cell. In our studies, for example, the use of florescent-labeled antibodies to the co-stimulatory CD80 and CD86 molecules can allow us to identify and enumerate the extent of DC activation upon MP uptake by these specialized antigen presenting cells. (Figure IV-1).

VII. Animal Care and Handling

Before beginning any animal experiments, animal training and education courses were carried out through the University of Iowa's Animal Care and Use committee adapted from National Institutes of Health (NIH) guidelines for animal care and use. Instruction including proper handling and restraint of mice, which minimizes stress on the animal and prevent aggression or defensive responses to handling. For all cases involving anesthesia, a Ketamine/Xylazine mixture was injected i.p. to deliver 87.5 mg/kg Ketamine and 2.5 mg/kg Xylazine in a 100 µL injection. This provides full anesthesia within a few minutes for approximately 20-30 minutes, with animals returning to full consciousness and mobility within 2 hours. At the end of the studies, or to harvest spleens, mice were euthanized using CO_2 and death confirmed by cervical location. Throughout the course of all experiments, mice were monitored every alternate day to monitor for sickness and excessive tumor growth. During tumor challenge studies, mice were euthanized if at any point they appeared ill from tumor burden, or the tumor grew

larger than 25 mm in any direction. Great care was taken to optimize formulations prior to immunization to minimize the number of animals necessary for each experiment while retaining significance

VIII. Tumor cell lines and animals

C57Bl/6 (6-8 weeks old) mice were purchased from the National Cancer Institute (Bethesda, MD) and were maintained in air-filtered cages before use.

EG.7-OVA were used to measure *in-vivo* tumor growth in the prophylactic and therapeutic tumor models. EG7 is an OVA-expressing thymoma cell line often used as a tumor model. Many studies have been successfully performed where OVA has been used as a model antigen system to prophylactically protect against EG7 tumor challenge in mice. Examples include vaccination of mice subcutaneously (3000 cells/mouse) with Th-1-polarised dendritic cells (DC1) that were pulsed with OVA.(121) This treatment resulted in doubling the survival times of mice challenged with EG7 cells compared to naïve tumor-challenged mice. The number of studies using EG.7 cells as a therapeutic model have been few and far in between and our study aims to explore the potential to use the same model to derive conclusions about the potential use of immunotherapeutic treatment strategies in such models too.

The cells were maintained in RPMI-1640 supplemented with 10% fetal bovine serum (FBS), 1% sodium pyruvate and 0.05 mg/ml gentamycin in a humidified 5% CO_2-containing atmosphere.

IX. Prophylactic immunization

The following six groups were used to study the efficacy of microparticle (MP) based vaccines for prophylactic tumor immunotherapy.

1. OVA-loaded PLGA MP
2. OVA + CpG co-loaded PLGA MP

3. OVA + poly I:C co-loaded PLGA MP
4. OVA + poly I:C + CpG co-loaded PLGA MP
5. OVA + poly I:C + CpG non-particulate (soluble)
6. Naïve untreated mice served as a control

The dose of OVA was kept constant at about 100 µg per mouse and the adjuvant dose of CpG and poly I:C was kept at 50 µg per mouse. In case of the tri-component system, the dose of OVA was kept constant at 100 µg and the dose of poly I:C and CpG was 40 µg each respectively in the tri-component system. All the lyophilized MP formulations were reconstituted in sterile PBS; pH 7.4 prior to administration in mice. The number of mice per group was 3. Two routes of vaccination; intraperitonial (i.p) and intramuscular (i.m) were employed to study the impact of the route of vaccination on immune response. The former is a route that generates a systemic immune response. This was a preferred method owing to the success of this approach in a previous study by our group. The intramuscular route (i.m) stimulates a local immune response. The first day of vaccination was considered as time point 0 (prime dose) and the mice were boosted with the same formulations at the same dose again on day 14. Serum samples were collected on day 14 prior to the booster dose and day 28 to measure antigen-specific antibody responses. Mice were bled on day 21 to collect blood and isolate the peripheral blood lymphocytes to enumerate the antigen specific- T cell lymphocytes by tetramer staining.

X. Analysis of antigen-specific antibody response by ELISA

Serum from mice at predetermined time points following immunization was obtained by sub-mandibular bleeding. Microtiter ELISA plates (Immulon, Thermo Fisher Scientific, Rockford, IL) were coated with a 5 µg/mL ovalbumin (OVA, Grade VII purified, Sigma Aldrich, St. Loius, MO) and incubated overnight at 4° C. The wells were then blocked with 2% milk for 2hours. The cells were then washed thoroughly three times with PBS containing 0.05% tween 80. Serial dilutions of serum were added and

incubated overnight. The plates were again washed three times with PBS containing 0.05% tween 80. Following this, anti-mouse heavy chain-specific goat IgG1, or IgG2a (Southern Biotechnology Associates, Birmingham, AL) primary antibodies at 1:1000 dilution were added and incubated for 4 hours. The last step was the addition of alkaline phosphatase conjugated secondary antibody (mouse IgG1 and IgG2a) and the samples were incubated for an additional two hours and washed thoroughly with PBS-Tween. Finally, the colorimetric substrate p-nitrophenylphosphate (PNP tablets (Sigma-Aldrich, St.Loius, MO) reconstituted in TRIS buffer, pH 8.0) was added and the plates were incubated in dark for 30 minutes for color development. The negative control was pretreatment (naïve) mouse serum. Plates were evaluated spectrophotometrically using a microplate reader (SpectramaxPlus 384, Molecular Devices, Sunnyvale, CA) at 405 nm and absorbance was recorded. The highest serum dilution titer that resulted in an absorbance of at least twice as that of the naïve serum was recorded as the antibody-titer value. A schematic representation of ELISA protocol has been depicted in Figure IV-2.

XI: Tetramer staining for antigen-specific T cell enumeration

Within the past decade, the use of tetramer technology has allowed scientists to quantify antigen-specific T cells directly through the antigen-specific receptor. Previously, this was not possible, as T cells require both the antigen and appropriate MHC molecules to bind the antigen. Normally the interactions of the cells with the antigen were limited by this, and labeling the cells with the antigen alone was extremely difficult. By creating multimers, where four of the MHC-peptide complexes are bound to avidin or streptavidin by biotin, the strength of the interaction of the antigen complex and T cell is increased. (Figure IV-3) Additionally, fluorochromes can be added to the streptavidin to allow detection of T cells which bind the MHC tetramer complex. This allows for detection of cells that are specific for the antigen at interest.

To enumerate the antigen-specific CD8+ T cells, tetramer staining using MHC I SIINFEKL tetramer (Beckman Coulter, Fullerton, CA) was performed. For each treatment group, the mice were bled (100 µL) into ACK buffer and centrifuged immediately to prevent coagulation. Red blood cells were lysed using ACK buffer, and the cell suspensions were filtered through a 70mm cell strainer. The peripheral blood lymphocytes were counted and resuspended at 10^7 cells/ml. 100 µL of cells were plated per well in a 96 well plate, and blocked with 24G2 Fc receptor block for 15 minutes on ice. Cells were stained for 30 minutes with tetramer (OVA, MHC I SIINFEKL tetramer (Beckman Coulter, Fullerton, CA) then for 20 minutes for anti-CD8 FITC and anti-CD3 PE-Cy5. The cells were washed, fixed, and permeabilized with the Cytoperm/Cytofix kit (BD Biosciences, San Diego, CA) and resuspended in FACS buffer for flow cytometry analysis, collecting 10,000 events. The data was analyzed using FlowJo software (Tree Star, Stanford, CA).

As a positive control for enumerating antigen-specific CD8+ cells, a group of mice was vaccinated with 1 x 10^6 *Listeria monocytogenes* (LM)-OVA cells stably transfected to express OVA. *Listeria monocytogenes* (LM)-OVA is a chronic intracellular pathogen that proliferates rapidly in vivo, resulting in profound LM-OVA expansion within the first 24 h of infection, culminating in the generation of a potent $CD8^+$ T cell response.

XII: Prophylactic tumor challenge- I

The mice were vaccinated either by the i.p or i.m route with the groups as mentioned in the above section. Treatment was administered using 1mL syringe fitted with a needle (23 gauge). On day 28 after the first vaccination dose, prophylactic tumor challenge study was commenced. Mice were shaved and injected with 5 x 10^6 EG.7 cells (passages 9 – 13) in 100 uL of PBS subcutaneously (s.c.) into the dorsal right flank. Injections were performed using insulin syringes. Tumor measurements were made using

a digital caliper (0 – 150 mm: Cat # 111-101B; Tresna, Guangxi Province, China). Tumor outgrowth was measured twice weekly, with tumor volume calculated as described by Shariat et al.(122)

$$\boldsymbol{volume}\ (\boldsymbol{v}) = \boldsymbol{length\ x\ width\ x\ depth\ x}\ \left(\frac{\boldsymbol{\Pi}}{\boldsymbol{6}}\right) \qquad \text{(IV-1)}$$

Survival of the mouse treatment groups was also monitored. Mice were sacrificed for ethical reasons if they appeared ill from tumor burden or if measurements exceeded 25 mm in any direction. Each experimental group consisted of 3 mice. All animal experiments were conducted in accordance with the procedures outlined in the University of Iowa's Guidelines for Care and Use of Experimental Animals.

XIII: Prophylactic tumor challenge – II

Mice were vaccinated by the i.p route with each of the six groups at the same doses mentioned above. The same vaccination protocol of prime and 14 day boost was followed. On day 60 following prime vaccination dose, prophylactic tumor challenge study was commenced. In these studies, the EG.7 tumor cells were resuspended in PBS at a concentration of 5 x 10^6 cells in 100 µL. The cells were injected subcutaneously into the right flank of the mouse. Tumor outgrowth was measured twice weekly, with tumor volume calculated as mentioned above. Survival of the mouse treatment groups was also monitored. Mice were sacrificed for ethical reasons if they appeared ill from tumor burden or if measurements exceeded 25 mm in any direction. Each experimental group consisted of 3 mice. All animal experiments were conducted in accordance with the procedures outlined in the University of Iowa's Guidelines for Care and Use of Experimental Animals.

XIV: Therapeutic tumor challenge

The EG.7 tumor cells were resuspended in PBS at a concentration of 1 x 10^7 cells in 100 µL. The cells were injected subcutaneously into the right flank of the mouse. This

was considered as Day 0 for the therapeutic study. On day 3, mice were treated with the following six groups by subcutaneous (s.c) route with 4 mice in every group.

1. OVA-loaded PLGA MP (100 µg OVA/mouse)
2. OVA + CpG co-loaded PLGA MP (100 µg OVA + 50 µg CpG/mouse)
3. OVA + poly I:C co-loaded PLGA MP (100 µg OVA + 50 µg polyI:C/mouse
4. OVA + CpG + poly I:C tri-component PLGA MP (100, 45 and 40 µg of OVA, poly I:C and CpG respectively/mouse
5. OVA , CpG and poly I:C each component entrapped separately in PLGA MP and admixed together prior to vaccination (100, 50 and 50 µg of OVA, poly I:C and CpG respectively/mouse
6. Naïve untreated mice serving as control.

Tumor outgrowth was measured twice weekly and tumor volume was computed. Survival of the mouse treatment groups was also monitored. Mice were sacrificed for ethical reasons if they appeared ill from tumor burden or if measurements exceeded 25 mm in any direction. Each experimental group consisted of 4 mice. All animal experiments were conducted in accordance with the procedures outlined in the University of Iowa's Guidelines for Care and Use of Experimental Animals.

In addition to the tumor volume measurements and survival curves, tumor growth rate constant was also computed for both the prophylactic and therapeutic treatment groups. A tumor growth model is a mathematical expression describing the size of a tumor with respect to time. Tumor growth rate constant was calculated from the slope of the exponentially fit tumor growth curves. This model assumes that the rate of increase in the volume (or number of cells) of a tumor is proportional to the volume (or number of cells) at that time. If the volume of a tumor, at time t is denoted by V (t) and a constant of proportionality by γ, then mathematically:

Whose solution is given as:

$$\boldsymbol{V(t) = V_0 e^{\gamma t}} \qquad \text{(IV-2)}$$

Doubling time of tumor cells at any given point in time is calculated as:

$$\boldsymbol{Doubling\ time} = \mathbf{ln}(\mathbf{2})\ /\boldsymbol{\gamma} \qquad \text{IV-3)}$$

This analysis provided a good means of delineating the various treatment groups by providing a direct comparison of tumor growth progression as a function of the treatment method. For the therapeutic tumor challenge tumor growth analysis, a constraint was placed on the initial values of tumor volume at day 0. This value was obtained by pooling the tumor growth volumes of several naïve mice (n = 10) and fitting the tumor growth data to an exponential tumor growth model. This value was calculated to be 50 mm^3.

Additionally, in the rare event of a mouse showing sudden tumor regression, the data was omitted for analysis purposes. This method of tumor growth analysis was used as a preliminary indicator and as initial attempt to study the effect of immunotherapeutic treatments. The results from this study were used to study only trends and were not used to draw any statistically robust conclusive evidence.

XV. Enumeration of regulatory Tcells (T_{regs})

$CD4^+Foxp3^+$ lymphocytes (T_{regs}) were detected using the mouse/rat-specific Foxp3 Staining Set (eBioscience, San Diego, CA), according to manufacturer's protocol. Briefly, PBLs were harvested 14 days after immunization and PBL suspensions prepared as described in section XI above. For each sample, 10^6 PBLs were used and all steps in the staining procedure were performed on ice and in the dark. Cells were first blocked with mAb supernatant from the 24G2 hybridoma (ATCC), followed by staining with CD4-FITC and CD3-PECy5 mAbs (eBioscience, San Diego, CA). Cells were then washed and incubated in Fixation/Permeabilization working solution for 30 min. Following fixation, cells were washed and stained with Foxp3-PE mAb (eBioscience, San Diego, CA). After staining, cells were resuspended and stored in FACS buffer at 4°C until flow cytometric analysis was performed, as described.

XVII. Statistical analysis

Group data are reported as mean ± standard deviation. Differences between groups are analyzed by one way analysis of variance with a Tukey post-test analysis. Levels of significance were accepted at the $p < 0.05$ level. Statistical analyses were performed using Prism 5.0 software (Graphpad Software, Inc., San Diego, CA).

Results

I. Characterization of the various microparticle formulations

The mean hydrodynamic diameter of the microparticles ranged between 800 nm and 2.0 µm with a polydispersity below 0.3 and a mean particle size of 1.5 µm. Table IV-1 lists the formulations and the entrapment efficiencies (EE) of the encapsulated components. Based on the BCA assay the EE of OVA ranged between 68-72% when entrapped alone or in combination with either poly I:C or CpG or both. The average loading of OVA was 18 µg per mg PLGA particles in the single and dual-component carriers and approximately 15 µg in the tri-component carrier. The EE of poly I:C and CpG were 45 and 41 % respectively in the co-delivery carriers. The amount of poly I:C and CpG loaded was approximately 8 µg per mg PLGA particles. In the tri-component system, the surface modification step resulted in partial loss of initially loaded OVA and poly I:C resulting in a net loading of 15 and 6 µg of OVA and poly I:C respectively. The net amount of CpG adsorbed was approximately 5-6 µg per mg PEI-modified PLGA particles. The i*n-vitro* release profiles of the various formulations have been shown in Chapter 2. An initial rapid release due to the burst effect is usually followed by a sustained release because of the gradual degradation of polymer. All the three components showed an initial burst release followed by a more controlled release. CpG is the smallest of the three components and expectedly showed the fastest release exhibiting nearly 50 % release at the end of 5 days when the microparticles were prepared by the

sonication method (Figure II-16). In contrast, OVA and poly I:C showed about 30 and 40% release respectively (Figure II-14 and II-15).

II. Gel electrophoresis

The result from gel electrophoresis has been depicted in Figures IV-4A and IV-4B . Lanes in Figure IV-4A represent soluble poly I:C and CpG extracted from the co-delivery carriers. It can be seen that poly I:C and CpG both retain their structure and are not fragmented into smaller units as seen by the comparable band intensities and position to that of the standard solutions of CpG and poly I:C in PBS, pH 7.4. These results indicated that the double sonication method was a suitable fabrication technique for preparing the microparticles. In addition to the method of manufacture, we speculate that ssDNA could also be degraded in the release media by a possible acidic microenvironment created by PLGA degradation. Hence release samples were collected at the end of 15 days to compare the band intensities of released CpG to that of the standard solution of CpG in PBS. The results in Figure IV-4B indicate no damage or base-pair reduction to either CpG or poly I:C upon release.

III. PLGA based particulate carriers are efficiently taken up by DCs

To track the cellular uptake and distribution of particulate antigen/adjuvant systems, OVA loaded or CpG-loaded PLGA MP were used for the intracellular trafficking studies. OVA or CpG and lysosomes were labeled with red and green fluorophores respectively as described in sections II, III and IV in the materials and methods section . At 4 hours post-incubation, most of the particles were successfully internalized in the BMDCs. CpG-loaded PLGA MP were taken up by cells and localized in vesicular structures as seen by yellow fluorescence due to the green staining of lysosome and red CpG signal in close proximity (Figures IV-5A and IV-5B). OVA-

loaded PLGA MP were also found in the endosomes (Figure IV-5C). PLGA MP showed uniform endocytosis and were found to be evenly distributed in a large group of cells.

The results from this study suggested efficient uptake of particulate antigens suggesting the ability of these systems to be used as potential vaccine carriers. Localization of the particles in the endosomes indicates the ability of the CpG to engage with its specific receptor (TLR9) and elicit a co-stimulatory or a danger signal to boost the immune response.

These results clearly demonstrated the presence of MP in the endosomal compartments known to house TLR 3, 7, 8 and 9 and functionally the Ag processing and presentation machinery. Hence we can conclude that upon proteolytical degradation, the entrapped Ag and adjuvant give rise to Ag-presenting activated APCs.

IV. Co-delivery of antigen and adjuvant(s) induces DC activation with increased expression of DC maturation surface markers

The efficiency of the antigen presentation via the MHC class I or II pathways alone is not enough stimulation for proliferation of CD4 T-helper and CD8 T cells. The antigen-specific clonal expansion of naïve T cells requires a second or a co-stimulatory signal which must be delivered to the same antigen presenting cell on which the T cell recognizes the antigen. The best characterized co-stimulatory molecules are CD80 and CD86 (commonly referred to as B7 molecules) that are up-regulated upon DC activation. T cells possess CD28, yet another member of the immunoglobulin family that possess receptors for these molecules. Binding to these CD28 receptors by the B7 molecules is absolutely essential for stimulation of T cells.(123)

To determine the effect of particles on DC activation, BMDCs were incubated with the OVA, OVA + CpG, OVA + poly I:C, OVA + CpG + poly I:C and empty PLGA microparticle vaccination formulations and were assessed for DC maturation surface markers. Soluble CpG was used as a positive control for this study. In the course of

natural infection, CpG sequences in bacterial DNA may similarly enhance Ag processing by inducing DC maturation. Previous studies by Kreig et al. have shown that this TLR9 adjuvant mimics the bacterial infection signal and functions as a microbial product. This is known to activate DCs and induce enhanced expression of CD80 and 86 surface markers resulting in DC maturation.(65) After 48 hour incubation, BMDCs were stained with Abs against the co-stimulatory molecules CD80 and CD86 and analyzed by flow cytometry. CD80 and CD86 expression on DCs was elevated to the highest degree after treatment with the OVA + poly I:C, OVA + CpG and OVA + CpG + poly I:C tri-component microparticles comparable to that of soluble CpG used as a positive control.

However, the most notable result here was that the particle formulations resulted in a significant DC activation at a concentration 5-fold lower than the soluble CpG. With respect to the tri-component particles the extent of CD86 up-regulation was greater than the co-delivery carriers at half the dose of the individual adjuvants which was indicative of an additive immunostimulatory effect (Figures IV-6A and IV-6B). Soluble OVA peptide was less successful at promoting co-stimulatory marker expression even at concentrations five times higher than that present within the microparticles. The interesting aspect of this study was that even empty microparticles were able to induce DC activation moderately thereby showing that the carrier itself functions as an adjuvant. These results were in agreement with some previously conducted studies demonstrating the role of PLGA microparticles and films in augmenting the process of DC maturation.(124) However, the results from our study suggest that while PLGA microparticles alone may not be enough to cause a significant extent of DC maturation in vitro as measured by cell surface marker expression. An increase in antigen dose or co-delivery of an immune modulator like CpG or poly I:C may enhance the potential immunostimulatory capacity of PLGA.

The study was repeated to study the effect of antigen/adjuvant concentration on the ability to promote DC maturation**.** It can be seen from Figure IV-7 that even at

concentrations as low as 1.5 – 2 µg, microparticles entrapping OVA and CpG/poly I:C were able to successfully induce DC activation and the co-stimulatory molecules surface expression is a function of antigen and adjuvant concentrations. The repeat studies also exhibited an additive adjuvant effect as demonstrated by the ability of the tri-component carrier to successfully induce strong DC activation signals at lower antigen and adjuvant concentrations (Figure IV-7). Additionally, it can also be observed from Figure IV-7 that CpG functions more effectively when entrapped in a particle form in comparison to the soluble form. The particulate carrier of CpG induces a two-fold increase in CD86 surface expression at a four-fold lower concentration than the soluble form. These results also indicate the importance of the CpG motif sequence in eliciting DC activation as the scrambled sequence of the oligonucleotide failed to generate any positive CD86 up-regulation signal (Figure IV-7). These findings further established the role of particulate carriers for co-delivery of antigen and adjuvant to generate a strong immune response.

V. Prophylactic tumor studies-I

VA. Co-delivery of antigen and adjuvant(s) increases the population of antigen-specific cytotoxic T-lymphocytes (CTLs)

To test the ability of the co-delivery and tri-component carriers in enhancing the immune response over delivery of antigen alone, we needed to fully characterize the *in-vitro* and *in-vivo* responses. In addition to the effect of treatment, the impact of route of vaccination was also studied. To investigate the population of OVA-specific CD8+ T cell population in immunized mice, tetramer staining was performed 21 days after the prime immunization (7 days after the boost). Peripheral blood lymphocytes were harvested and processed as previously described and then stained for CD8, CD3, and OVA tetramer. Figure IV-8A and IV-8B shows the representative gating on the CD3+ CD8+ population, and then FL1 vs. FL2 identifying cells double positive for FITC CD8 and PE tetramer for the various treatment groups given i.p and i.m respectively. The fluorescence plots are

representative plots of one mouse from every group. The gates were drawn based on the % OVA-specific CD8+ T-lymphocytes that were obtained in the mice that were treated with LM-OVA as explained in section XI under materials and methods section. Figure IV-9A shows the comparison between the various treatment groups by comparison of the % of antigen-specific CD8 T-lymphocytes. Figure IV-9B delineates the different treatment groups more clearly by showing the fold increase in the population of CTLs when the mice were vaccinated with carriers entrapping both the antigen and adjuvant in comparison to vaccination with antigen alone.

In our study OVA + either CpG or poly I:C when administered in the co-delivery carrier significantly increases the tetramer frequency compared to delivery of OVA in microparticles alone. The highest mean frequency of CTLs was obtained in the mice treated with microparticles co-entrapping OVA + CpG and OVA + CpG + poly I:C. Additionally, the co-delivery and tri-component microparticle groups showed a 3-4 fold increase in the population of CTLs in comparison to treatment with OVA alone. Although, these groups showed significantly higher frequency of CTL's than OVA, they were not significantly different from one another. Conversely, the i.m. vaccination did not generate a strong T cell immune response. Although the mean values of CTL population did seem marginally superior in the co-delivery and the tri-component microparticles groups, statistical analysis indicated no significant difference. From these studies, we concluded that the i.p. route of vaccination was the most potent at generating a strong T cell mediated immune response. Additionally, these results were also in agreement with *in-vitro* DC activation data, suggesting that a simultaneous trigger arising from the antigen and the adjuvant is essential for maximum immunostimulatory responses.

Given the many types of cell populations that may modulate the immune responses, a tumor challenge study was the next step to corroborate our findings from this CTL enumeration study.

VB. Co-delivery of antigen and adjuvant(s) elicits a Th-1 polarized immune response

In order to determine whether type-1 polarized immune response was generated upon antigen-adjuvant co-delivery, anti-OVA serum antibody titers (IgG1 and IgG2a) were analyzed. To examine OVA-specific Th-1 and Th-2 antibody responses induced by microparticles loaded with OVA, OVA + poly I:C, OVA + CpG, OVA + poly I:C + CpG in mice, we measured anti-OVA IgG isotype levels. For that, levels of IgG1 and IgG2a were assayed by ELISA 14 and 28 days after the prime vaccination. To better establish the influence of each treatment group on the specific IgG response, we measured the titers of anti-OVA IgG1 (which has been associated with Th-2 responses) and IgG2a (which has been associated with Th-1 responses.

We found that soluble and particulate carriers stimulate a different pattern and level of anti-OVA IgG isotype titers. In addition, the presence of adjuvants and the route of vaccination also caused a significant impact on the serum antibody titers. Figures IV-10 and IV-11 depict the serum anti-OVA IgG2a and IgG1 levels when the mice were vaccinated prophylactically by the i.m and the i.p routes respectively. The results indicated that the highest anti-body titers were obtained on day 28, 14 days after the boost dose of vaccination in both the cases. Examining the IgG2a and IgG1 responses for the i.p. route, it can be seen that microparticles co-loaded with OVA + CpG and OVA + poly I:C resulted in significantly higher IgG2a antibody titers (15-20 fold higher) as compared to mice that were vaccinated with OVA microparticles alone. The highest IgG2a titers were generated by the tri-component particles carrying OVA + CpG + poly I:C. The antibody titers were 3-4 fold higher when the two adjuvants were administered together with the antigen in comparison to each of them co-delivered individually with OVA. This indicated a synergistic effect between poly I:C and CpG. These observations indicated a strong induction of Th-1 response upon co-delivery of a TLR adjuvant with the antigen.

However, when the same combination of OVA + CpG + poly I:C was administered in a soluble form, this group failed to elicit a high IgG2a response.

A stronger IgG1 response was generated when mice were vaccinated with microparticles entrapping OVA alone with the IgG2a/IgG1 ratio being 0.45 (Figure IV-12A). Although, the other groups did generate a strong IgG1 response, the ratio of IgG2a/IgG1 varied between 1.5 – 3 when either CpG or poly I:C or both were present along with the OVA in microparticles. This indicated a significant shift in IgG isotype favoring a Th-1 biased immune response. Although the overall antibody response was lower in the group that was vaccinated with the soluble combination of OVA + CpG + poly I:C, the IgG2a/IgG1 ratio was 1.33 suggesting conclusively that CpG and poly I:C contribute significantly in causing a pronounced increase in Th-1 polarized immune response. Figure IV-12B shows a similar trend in Th-1/Th-2 isotype shift upon vaccination of the various microparticle groups by the i.m. route. However, the overall strength of anti-body response was lower in comparison to the antibody titers attained by the i.p route of vaccination. The presence of poly I:C and in particular CpG caused a significant increase in serum IgG2a titers, however the synergy between CpG and poly I:C was not evident when the mice were vaccinated by the i.m route. The most significant part of the result was that an enhanced shift in Th-1/Th-2 isotype was maintained. The IgG2a/IgG1 ratio was in the range of 1-3, despite the overall lower antibody response. When OVA was administered alone in a microparticle carrier, the mice showed a Th-2 biased response with the fraction of IgG2a/IgG1 response being 0.28.

These findings better illustrated the role of CpG and poly I:C in inducing a Th-1 polarized immune response and were in agreement with the some of the previous data generated in the lab.

VC. Co-delivery of antigen and adjuvant(s) significantly benefits survival and retards tumor growth in an EG7 prophylactic model

Figure IV-13 gives a summary of tumor growth curves for the various treatment groups. It can be seen from the growth curves that the chosen tumor model and tumor cell-line resulted in consistent growth within mice from the same group with small inter-animal variability. It can also be observed that mice treated with microparticles co-entrapping OVA + poly I:C or OVA + CpG or OVA + CpG + poly I:C resulted in significantly smaller tumor volumes. Figure IV-14A depicts the mean tumor volumes of each of the vaccination group and the untreated naïve mice group. It was observed that the group that received OVA alone in microparticles was unable to resist tumor growth effectively and showed a similar growth pattern as that of the naïve untreated mice. In sharp contrast it is evident that tumors were significantly smaller for the groups treated with OVA + poly I:C or OVA + CpG or OVA + CpG + poly I:C. Figure IV-14B shows tumor growth rate comparison between the various vaccination groups. As explained in the methods section, the tumor growth rate constant was computed using the exponential growth model. Tumor growth was seen to be significantly influenced by the presence of a co-entrapped adjuvant component in the vaccine. The co-delivery and tri-component groups resulted in a 2-fold slower tumor progression rate in comparison to the naïve mice. There was no statistically significant difference between the co-delivery and the tri-component groups resulting in a mean tumor growth rate constant of 0.04 $days^{-1}$ and a mean tumor volume between 1200- 1500 mm^3 at the end of day 60.

Along with tumor progression, survival time is an important parameter in determining the efficacy of a vaccine for tumor immunotherapy. There was a marked difference in the survival rate and median survival times between the different treatment groups. It can be seen from Figure IV-15 that mice that were treated with microparticles entrapping OVA alone succumbed by 20 days following tumor challenge, while mice treated with microparticles co-entrapping OVA + poly I:C survived up to day 60. In the

group that was treated with microparticles co-entrapping OVA + CpG one out of the three mice survived beyond day 60 while in the tri-component microparticle group loaded with OVA + CpG + poly I:C, two out of three mice in the group survived beyond day 60. Table IV-2 provides a summary of the median survival times of the various groups. It can be seen that co-delivery of OVA + poly I:C resulted in doubling of survival time in comparison to naïve untreated mice or mice treated with OVA alone. The survival time was 3 times longer in the mice treated with OVA + CpG with a median survival time of 60 days, while the tri-component groups resulted in the longest survival time of over 60 days.

These observations co-related well with the population data of cytotoxic T-lymphocyte populations and Th-1 antibody titers. Mice vaccinated with OVA + CpG and OVA + CpG + poly I:C MP groups, showed the maximum population of CTLs, anti-OVA IgG2a titers and also demonstrated the longest survival times. These studies provided a promising conclusion to our hypothesis that co-delivery of adjuvants with the antigen within the same carrier could serve as a promising carrier in tumor immunotherapy.

VI. Co-delivery of antigen and adjuvant(s) significantly benefits survival and retards tumor growth in an EG7 prophylactic model indicative of immunogenic memory

We wanted to test the long-term protection afforded by our immunization formulations in an *in-vivo* tumor challenge model; 2 months after prophylactic vaccination. The time point for tumor challenge was taking into consideration degradation profiles of the particulate formulations and tetramer kinetics tracing T cell population following immunization. Our *in-vitro* release data indicated that most of the entrapped components exhibited nearly complete release by the end of 45 days and is expected to be accelerated *in-vivo* Additionally tetramer kinetics data upon prophylactic

vaccination indicated a decline in the population of systemic antigen-specific CTLs day 28 onwards. Hence the hypothesis of the current study was to demonstrate the ability of our immunization formulations to induce an immunogenic memory that protects against a tumor challenge. Mice were immunized with the aforementioned microparticle based vaccination groups by the i.p. route. The mice were challenged 60 days later with 5×10^6 EG.7- OVA cells which were injected subcutaneously on the right flank. Tumor outgrowth was measured twice weekly, and survival was monitored to study the effect of various treatment groups on survival rate. Mice were sacrificed if they appeared ill from tumor burden or if the tumor exceeded 25 mm in any direction. The survival graph of this representative experiment has been shown in Figure IV-16. In this representative experiment, all the mice that were immunized with OVA alone developed tumors by day 70 after prime immunization (day 10 after tumor challenge) and had to be all sacrificed by day 82. Mice that were vaccinated with OVA + poly I:C showed better tumor protection and remained tumor free until day 75 and showed a mean survival time of 87 days. OVA + CpG group showed better protection with 2 mice in the group remaining tumor free until day 82 and a mean survival rate of 66 % at the end of day 87. The best protection was afforded by microparticles loaded with OVA + CpG + poly I:C in which all the mice in the group remained tumor free until day 82 with 100% survival rate. After day 82, they developed small tumors. These results indicated the existence of a possible synergistic anti-tumor effects between CpG and poly I:C improving mouse survival. However, a repeat study with a larger sample size would prove the synergy more conclusively. Mice vaccinated with microparticles co-loaded with OVA + CpG and OVA + poly I:C also showed superior survival times in comparison to mice immunized with OVA microparticles alone. The soluble form of the tri-component carrier with OVA + CpG and poly I:C showed only a 33 % survival rate.

In terms of tumor growth kinetics, no statistically significant difference could be detected between the dual and the tri-component groups up to day 82. Post day 82, the tri-

component group showed the best tumor protection that indicated the induction of a strong immunogenic memory.

VII. The co-delivery of antigen and adjuvant(s) significantly benefits survival and slows tumor growth progression in a therapeutic model

Figure IV-17 gives a summary of tumor growth curves for the various treatment groups. It can be seen from the growth curves that although the tumor growth seemed consistent amongst mice within the same group, occasionally one out of the four mice in the group showed faster tumor progression than the others. In such an event, if the data did not seem to follow the exponential growth kinetics it was considered as an outlier for the purpose of statistical and treatment effect analyses. Table IV-3 gives a summary of the tumor growth rate constant between groups and a comparison of doubling times that can be considered as an appropriate marker for tumor progression amongst patients. As explained in the experimental section, doubling time was computed as given in equation IV-4.

From the tumor growth curves and exponential tumor model, it can be observed that the untreated mice showed the fasted doubling time of 3.03 days. Mice that were treated with microparticles entrapping OVA alone did not show any improvement in tumor growth rate or progression and the mice behaved similar to that as the naïve mice. Addition of an adjuvant including CpG or poly I:C afforded better protection. Microparticles co-loaded with OVA + CpG showed a 1.7-2 times improvement in doubling time, whereas OVA + poly I:C and OVA + CpG + poly I:C resulted in slowest tumor growth progression with doubling times of approximately 6.1 and 6 days respectively; a 2-fold improvement in doubling time of tumor cells as compared to the OVA microparticles group. It can be seen from Table IV-3 that OVA+ poly I:C and OVA + CpG + poly I:C resulted in a 1.5 fold reduction in tumor growth rate as compared to the untreated mice or mice that were treated with OVA alone. Although, OVA + CpG

afforded some degree of protection, better than the naïve and the OVA microparticles treated group, the overall efficacy was lower than the two most beneficial groups containing poly I:C with or without CpG in combination with OVA.

Along with tumor progression, survival time was also computed for the various treatment groups and has been shown in Figure IV-18. For the purpose of this study an aggressive tumor challenge regime was followed by administration of 10^7 EG.7 tumor cells. The purpose of such a challenge was to study the efficacy of various treatment groups in the presence of a large tumor burden and the maximum ability to prolong survival. It can be seen from Figure IV-19 that most mice that were treated with microparticles entrapping OVA alone succumbed by day 17 post tumor challenge, similar as that of the untreated mice. Mice that were treated with OVA + CpG showed 100% survival up to day 25 and 25 % survival at the end of day 28. One of the mice in the OVA+ poly I:C group showed a sudden sharp rise in tumor volume and succumbed by day 17, while the remaining three mice survived up to day 25 showing an overall survival rate of 50% at the end of day 28. The tri-component model showed a similarity in trend as that of the OVA + poly I:C group with 75% survival rate at the end of day 25 and 50 % survival rate at the end of day 28. The improvement in survival times was not as significant as seen in the prophylactic studies. One reason attributed to this was the doubling in tumor burden at day 0 in comparison to that of the prophylactic studies. This did not allow a sufficient time gap for the treatment groups to prove efficacious. The naïve mice showed a doubling time of 3 days, which causes a tumor burden of 2×10^7 cells at the beginning of treatment. As mentioned earlier, the purpose of this study was to distinguish the differences; however small they might be amongst treatment groups under high tumor burden conditions.

VIII. Co-delivery of antigen and adjuvant(s) does not impact the population of immune-suppressant T-lymphocytes (Tregs)

Regulatory T cells (T_{reg}, sometimes known as suppressor T cells) are a specialized sub-population of T cells that act to suppress activation of the immune system and thereby decrease the sensitivity and strength of immune response. Regulatory T cells come in many forms, including those that express the CD8 transmembrane glycoprotein (CD8+ T cells); those that express CD4, CD25, and Foxp3 (CD4+CD25+ regulatory T cells and other T cell types that have suppressive function. These cells are involved in shutting down immune responses.(12) Chemotherapeutic agents like cyclophosphamide function by down-regulating the T_{reg} cells and thus increase the sensitivity of the tumor cells to any form of cancer therapy. In order to examine the effects of our immunization groups on the T_{reg} cell population, the peripheral lymphocytes were isolated from the surviving groups of mice at day 20 and stained with T_{reg} cell-specific antibodies to enumerate them by FACS. The cell population has been depicted in Figure IV-19. As a control, cells from a naïve tumor-free mouse were also isolated to elucidate the normal population of such cells in a normal mouse devoid of any tumor and treatment. It can be seen that none of the treatment groups seem to down-regulate the suppressor T cells and the population of these cells were all comparable to that of the naïve mouse.

Discussion

Until recently, tumors had been considered as a non-rewarding target for tumor immunotherapy as they are thought to be poorly immunogenic in nature. However, more recently it has become clear that tumor cells express specific tumor antigens and these can be harnessed for prophylactic and therapeutic immunotherapy purposes (10, 125, 126). A number of mechanisms may result in a tumor being tolerated by the host despite expression of defined endogenous TAAs or, as is the situation with the EG7 tumor model, the expression of a xenogenic protein such as chick ovalbumin (OVA). The

involvement of T cells in generating an anti-tumor immune response is crucial and the ability to trigger a cell-mediated immune response by fabricating appropriate delivery systems formed the foundation for this research study (121, 127). The interplay between the innate and adaptive immune response involving the T cells determines the type of CD4 T-lymphocyte pathway that is actively engaged. An antigen encounter by the naive T cells in a non-infectious milieu leads to a Th-2 type T cell response that promotes a cytokine environment rich in IL-4, which inactivate macrophages, promote angiogenesis and thus indirectly promote tumor growth. In contrast, the same antigen signal in an infectious context is prone to induce a proinflammatory Th-1 T cell response that entails a cytokine environment rich in IL-12. This results in increased production of IFN-γ and an increased cytotoxic T-lymphocyte (CTL) population and activity that promotes anti-tumor immunity (121). In this context we considered two adjuvants for this study, CpG a TLR9 adjuvant that mimics a bacterial infection danger signal and poly I:C a TLR3 adjuvant that provides a viral infection signal.

Amongst the two adjuvants, poly I:C has not been utilized to a large degree in anti-tumor immunotherapeutic studies. Although, the potential of this adjuvant to generate a cell-mediated immunity has been reasonably well elucidated in *in-vitro* studies (128), a study describing its complete potential *in-vivo* in conjunction with an antigen has not been well characterized. Given the success ratio of particulate antigens to induce better immune responses in various models studied by several groups, PLGA was the rational choice of carrier in this study. Additionally, PLGA is FDA approved, making it a much better candidate for therapeutic tumor vaccines.

The first and the most critical step in the immunostimulatory cascade for tumor therapy is the activation of DCs. Most studies so far have analyzed DC activation induced by a single TLR adjuvant. However, pathogens express several TLR agonists that may engage different TLRs at different times and in distinct cellular compartments. Additionally, most studies thus far have only explored the activation effects of soluble

form of these adjuvants. In our study, the effects of particulate OVA + poly I:C, OVA + CpG and OVA + CpG + poly I:C on the maturation of immature DCs were investigated and compared with the effects of a high concentration soluble CpG which is known to induce maturation of DCs. Our results demonstrated that treatment of immature DCs with dual and tri-component particles results in a significant extent of DC maturation with stable and high expression of the co-stimulatory molecules, CD80 and CD86. Interestingly, the few studies that have been done so far by some groups, have shown poly I:C to be a potent DC stimulator only at a minimum dose of 10μg (128).

Our studies show that co-entrapping poly I:C with OVA in a particle form makes it a strong DC activator at doses as low as 2 μg. It is postulated that poly I:C and CpG induce DC maturation that can in turn generate a cytokine profile rich in IL-12. IL-12 is an important initiator of the Th-1-like T cell responses involved in anti-tumor immunity (38).

The combination of CpG and poly I:C resulted in a greater surface expression of CD80 and 86 in comparison to either CpG or poly I:C co-entrapped individually with OVA. The effect however seemed additive than synergistic. In order for poly I:C and CpG to work in combination, a simultaneous induction of TLR3 and TLR9 receptor is essential (81, 129). In some cases, after initial TLR stimulation, DCs may become mildly refractory to subsequent stimulation by the same or another TLR adjuvant. From our results, it seemed that a combination of poly I:C and CpG induces a strong initial stimulation and perhaps hits a limiting degree of stimulation at the individual doses used in the tri-component carrier in an *in-vitro* assay condition.

Alongside the therapeutic components, understanding of material (carrier/vehicle) adjuvant effect is essential for the effective design and selection of appropriate materials for specific tumor therapy applications. Our results indicated a modest adjuvant activity of PLGA75:25 (MW 30000 Da) resulting in up-regulation of the CD80 and 86 surface markers upon incubation of the murine BMDCs with empty PLGA particles. These

results are consistent with a study done by Yoshida and co-workers whose study showed that treatment of murine DCs with PLGA MPs or films resulted in slightly increased CD80 and CD86 when compared with immature dendritic cells (iDCs).(124) The particulate carriers also demonstrated an increase in the phagocytic ability of the DCs demonstrated by the fact that particulate CpG and poly I:C promoted a stronger surface marker expression than soluble TLR ligands.

A few other groups including ours have demonstrated the potential application of OVA-CpG microparticle formulations for antigen delivery (66, 119, 130, 131). We wanted to explore this potential further by studying the role of antigen-specific cellular immune responses in the settings of real tumor immunology. One of the main goals was to analyze antibody response- mediated cellular immunity and the effect vaccination route on such responses. In immune responses to viral and bacterial infections, IgG2a and to a lesser degree IgG1 are dominant. Coutelier et al. analyzed the isotype distribution in antiviral immune responses using a panel of murine DNA and RNA viruses representative of various genera (132). In most cases a striking dominance of IgG2a production appeared. IgG2a could be advantageous for clearing tumors as these are considered to be better mediators of antibody dependent cytotoxicity (cellular immunity). IgG isotype markers are good predictors of T cell mediated Th-1 and Th-2 type immune responses. Mosmann et al. have postulated that if T-helper cells involved are of the Th-2 type, which produce the cytokine IL-4, this induces switching to IgG1 (133). Conversely, in the case of involvement of Th-1 type immune responses involving production of IFN-γ, this induces switching to IgG2a. As expected, vaccination in the absence of a co-stimulatory signal by an adjuvant, the antibody response showed an IgG1 shift with poor IgG2a titers. In contrast addition of either poly I:C or CpG or both along with OVA within the same microparticulate carrier caused a distinct shift in isotype with a marked increase in IgG2a over IgG1 titers. The overall immune response was IgG2a or Th-1 polarized. When the particles were administered by the i.p route a distinct synergistic

effect was observed wherein the IgG2a response was more than double as compared to the titers when each of the adjuvant was co-entrapped separately with OVA within PLGA MP. Thus, the synergistic TLR stimulation may represent a "combinatorial danger signal" that ensures engagement of multiple TLR ligands ensuring that a powerful anti-tumor immune activity is generated. Synergistic TLR stimulation represents a clinical situation, as pathogens may contain several TLR agonists that trigger TLRs in different cellular compartments. The integration of continuous multiple danger stimuli afforded by the particle based vaccines might allow a more effective response to invading tumor antigens than to soluble TLR adjuvants and antigen. For example, poly I:C may trigger TLR3 and prime DCs for a subsequent triggering of TLR9 by CpG. The super-induction of Th-1 responses was more evident *in-vivo* and less evident *in-vitro* as seen in the DC up-regulation studies. The TLR synergy was perhaps not distinguishable *in-vitro* indicating that DC up-regulation pathway has an induction threshold. The i.m. route too caused a distinct shift favoring IgG2a responses. However, the synergistic effect between poly I:C and CpG was less pronounced. CpG as an adjuvant exhibited better immunization potential when administered by the i.m. route as compared to poly I:C. The overall titers of antibody responses were however the greatest when the vaccination route was i.p. Intraperitonial route is almost analogous to a systemic intravenous route of administration with the capability of generating instantaneous uptake by APCs and inducing an immune response as evidenced by our study. The onset of action by the intramuscular route depends on the extent of uptake by the local APCs and the rate of systemic draining for antigen recognition and antibody response causing a delay in reaching the highest antibody titers. Intramuscular is often the preferred route for long-term immune responses enabling maintenance of high antibody titers over prolonged periods of time. A repeat study with serum sampling at time points beyond 28 days will elucidate this hypothesis better helping understand the underlying impact of vaccination route.

While estimating immune responses does forms an important aspect of testing vaccines, the real success of immunotherapy is the ability to translate these responses into protective tumor immunity. The most significant advantage of immunotherapy for cancer is the ability to generate a systemic response that can treat metastases or future tumor reoccurrences that are the limiting factors associated with conventional therapies. A prophylactic tumor vaccine could be a follow-up/maintenance therapy to tumor elimination by either chemotherapy or a surgical procedure to prevent or minimize and slow-down future out-break and rapid proliferation of tumor cells (134). When naïve mice devoid of any immunization are challenged with EG.7 tumor cells subcutaneously, mice usually succumb to the enormous proportion tumors within 2 – 2.5 weeks. Despite expression of a tumor associated antigen, untreated immunocompetent mice do not generally reject the tumors. Hence these formed the right control group to test the tumor protection potential of the various vaccination groups developed in this study. We have for the first time shown the beneficial potential of co-delivery of OVA and poly I:C in a particulate carrier in providing strong anti-tumor immunity and improving the life expectancy in murine tumor models. The two adjuvants; CpG and poly I:C showed equivalent benefit in slowing tumor growth rate and the tri-component group behaved in a similar pattern as well. However, they impacted the median survival times differently.

While co-delivery of poly I:C with OVA doubled the median survival time in comparison to the naïve group, CpG co-delivery with OVA provided further protection by improving the life-span by 3-fold. It was interesting to note that the best tumor protection was provided by the tri-component group wherein CpG and poly I:C helped resist tumor outgrowth until 21 days post challenge and improved survival time significantly with 67% survival rate amongst mice in this group at the end of day 60 after tumor challenge.

Mechanistically, this could be explained by strongest IgG2a; Th-1 polarized immune response generated by microparticles co-loaded with OVA + CpG and OVA +

poly I:C and OVA + CpG + poly I:C. The two adjuvants showed equivalent benefit in slowing tumor growth rate and the tri-component group behaved in a similar pattern as well. OVA in combination with either CpG or poly I:C or both demonstrated a 3-4 fold increase in the population of antigen specific CD8 T-lymphocytes in comparison to vaccination with OVA microparticles alone. Typically, CD8+ T cell responses cannot be effectively generated against pathogens that fail to infect DC, as well as cellular pathogens that are not present in the intracellular compartment within the DCs. DC therefore require a co-stimulatory signal generated by the presence of pathogen-associated molecular pattern (118, 121, 131). Our current co-delivery approach allows exogenous antigen and the pathogen associated adjuvant to access the MHC class I peptide loading machinery and stimulate CD8 T cell differentiation. In addition to providing anti-tumor immunity upon tumor challenge immediately post vaccination, the dual and tri-component co-delivery PLGA carriers showed potential to induce immunogenic memory to delay tumor growth and improve survival when mice are challenged nearly 2 months after prophylactic vaccination. These results were strong indicators of systemic cell-mediated immunity being conferred by the presence of CpG and/or poly I:C co-delivered with OVA.

The next step involved development of a particle based therapeutic vaccine for tumor therapy. Mice were subject to high tumor burdens to study the maximum efficacy of the therapeutic carriers to prolong mice survival and decelerate tumor progression rate. Presence of CpG with OVA or in combination with poly I:C and OVA in microparticles helped prolong median survival times by 1.5 fold. Although the expected outcome was to provide a more robust tumor protection, the high initial tumor burden and the doubling rate of the aggressively growing EG.7 cells might have had a role to play in this diminished response. Our prophylactic studies have shown that it requires at least 14 days after prime immunization with particulate vaccines for strong cell-mediated immune responses to develop that include CTL activity and IgG2a responses. A large tumor

burden on day 0 that doubles by day 3, limits the vaccine ability to elicit a fully developed immune response before uncontrolled tumor proliferation. Despite this time lag in induction of a fully-developed immune response, the dual and tri-component carriers did prolong survival times and caused a 2-fold delay in tumor doubling rate. The absence of any synergistic effect between poly I:C and CpG could be attributed to the delay in development of a potent therapeutic immune response. Additionally, the overall response was depressed as compared to the prophylactic tumor study outcome. However even the small magnitude of positive shift in protection, leads us to believe that microparticles co-entrapping CpG and poly I:C may have caused the generation of cell-mediated immune response allowing longer lasting protection in comparison to OVA alone.

These results gave further impetus to this research study involving PLGA carriers to co-deliver antigen and TLR adjuvant. Our present study provides experimental evidence that these PLGA particulate carriers strongly activate DCs. These results from the prophylactic tumor challenge presented here advocate the use biodegradable PLGMP as a powerful delivery Devices for prophylactic tumor vaccination protocols that are based on exogenous antigen in combination with ligands for endosomally expressed TLR. The carriers also showed strong evidence for the generation of anti-tumor immunogenic memory along with potential for generating a synergistic adjuvant activity between poly I:C and CpG in a prophylactic setting. Our PLGA microparticle based vaccine system, co-delivering OVA, poly I:C and CpG, is a novel system aimed at exploiting the maximum benefits of each component in the carrier.

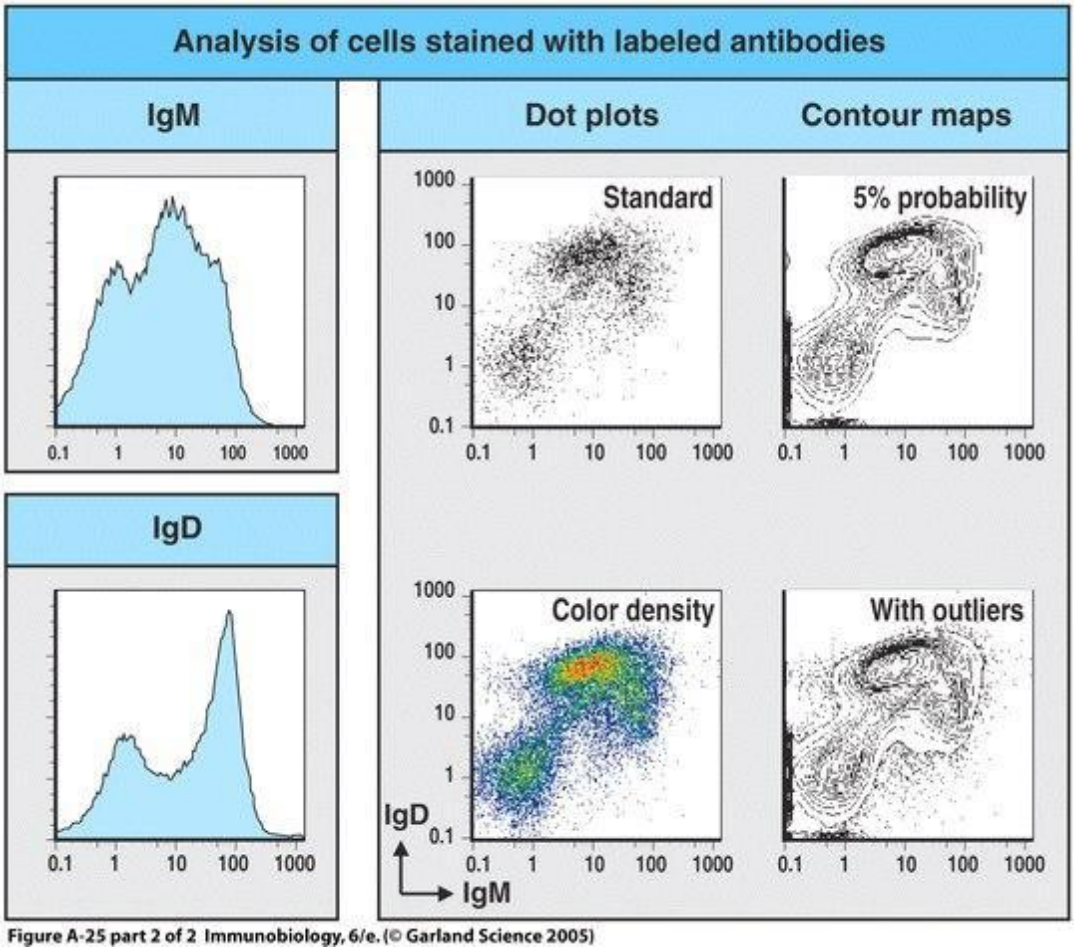

Figure IV-1: Flow cytometry (FACS) setup allowing cells to be sorted and quantified by their cell surface antigens. A mixture of cells can be labeled with fluorescent antibodies specific to different cell surface antigens. The labeled cells are forced through a nozzle into a single cell stream which passes through the laser beam. Laser beams delivering light at different wavelengths excite the fluorochromes and the emitted light is analyzed by computer. Additionally, the scattering of light allows identification of different cell populations, sorted by cell size and granularity. The cells that certain characteristics can be quantified and the level of expression can be measured, to compare effects of immunization on cell populations.[12]

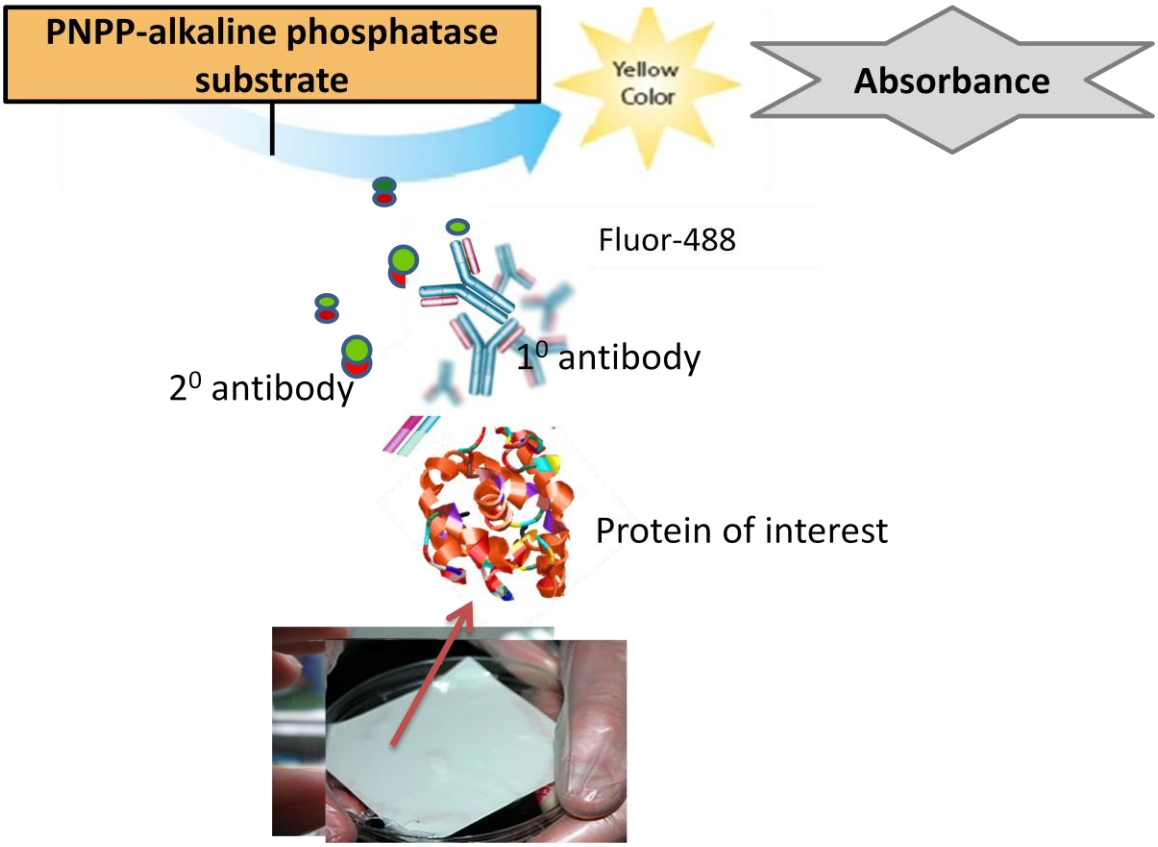

Figure IV-2: Schematic of ELISA assay. The antigen is immobilized on a solid support (usually a polystyrene microtiter plate) non-specifically (via adsorption to the surface). Thereafter the serum samples are added to the coated well plates. After the antigen of interest is immobilized the primary antibody is added, forming a complex with the antigen. This is followed by the addition of secondary or a detection antibody which is linked to an enzyme through bioconjugation. Between each step the plate is typically washed with a mild detergent solution to remove any proteins or antibodies that are not specifically bound. After the final wash step the plate is developed by adding an enzymatic substrate, 6-para-nitrophenyl phosphate (PNPP) to produce a visible signal, which indicates the quantity of antigen in the sample.

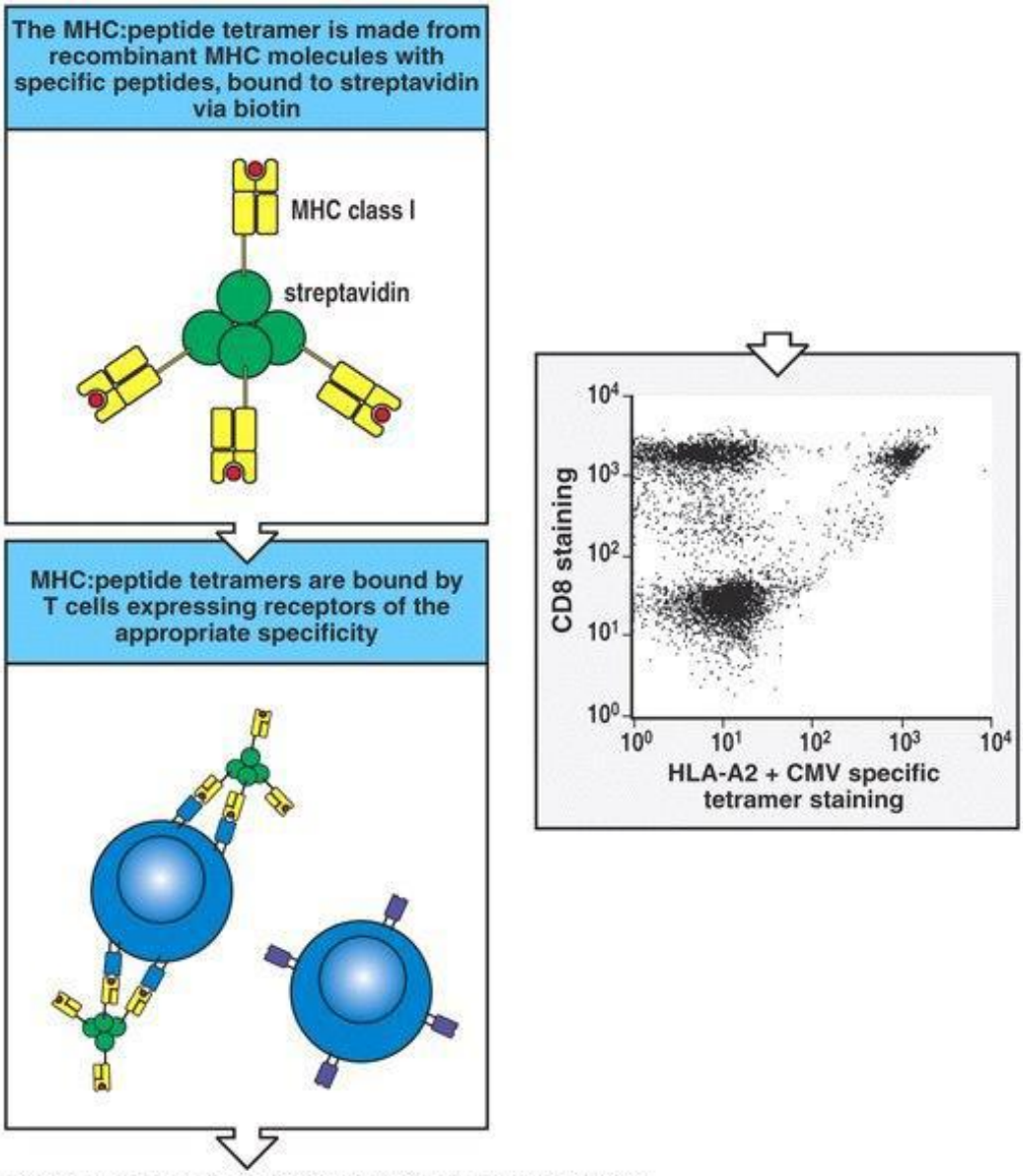

Figure IV-3: Tetramer staining principle to enumerate antigen-specific cell populations. The tetramer, providing four opportunities for MHC: peptide to bind the cell receptor, gives a stronger interaction of the complex with the cell. The tetramer complex is also bound with fluorochrome to allow analysis by flow cytometry. The bottom panel shows T cells stained with CD3 and CD8, and tetramer for HLA-A2 molecules. The CD3+ cells were gated on, and the figure shows a cell population in the upper right quadrant that is the tetramer positive CD8+ cells.

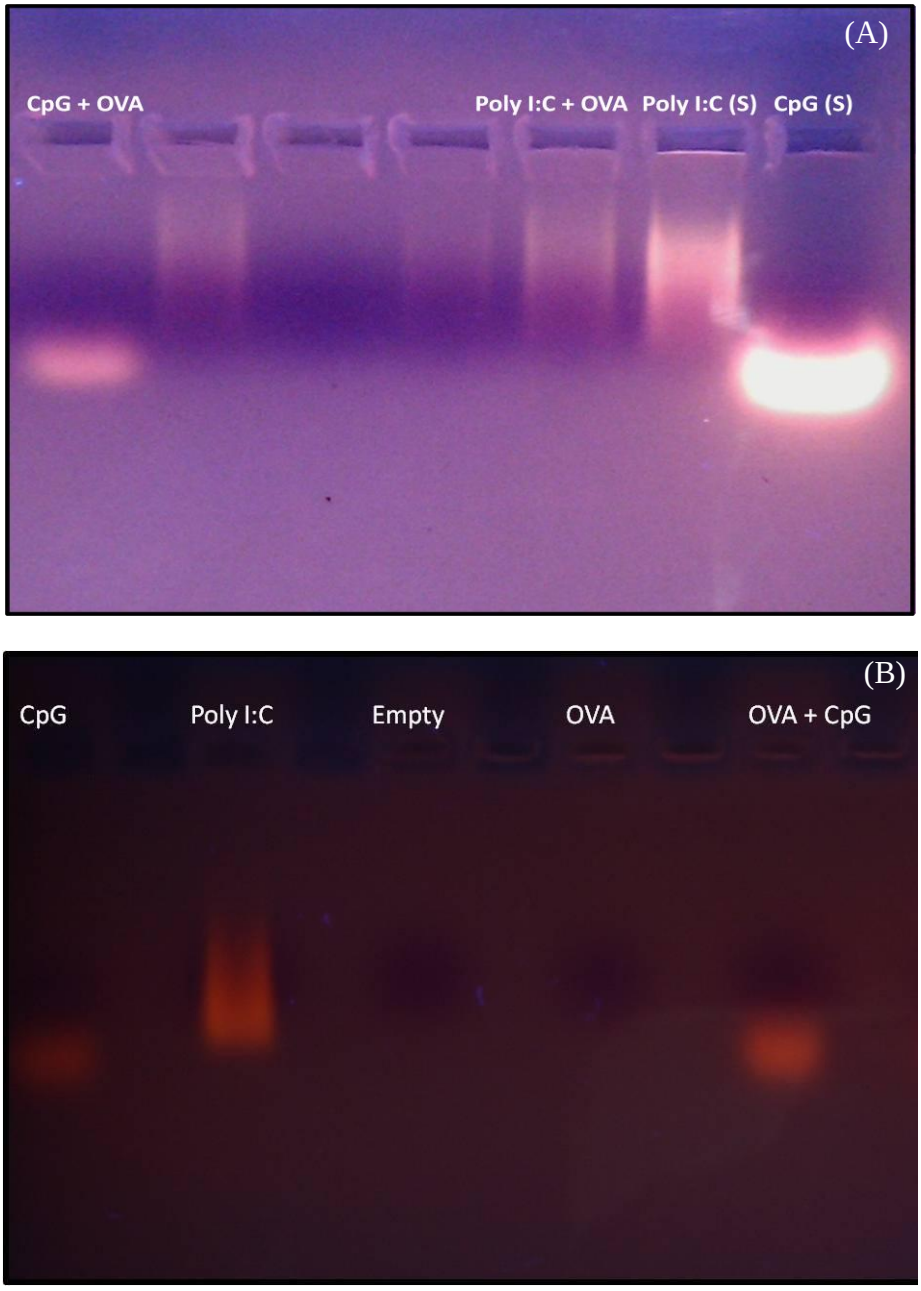

Figure IV-4: (A): Ethidium bromide gel electrophoresis showing intact structure of CpG (lane 1 from left) and poly I:C (lane 5) recovered from the dual-component PLGA 75:25 (MW 30000Da) microparticles as compared to standard soluble form (S) of poly I:C and CpG (lanes 6 and 7) and (B) CpG release at the end of 10 days from CpG-PLGA (lane 1), poly I:C release at the end of 15 days from OVA + poly I:C PLGA (lane 3) and CpG release at the end of 15 days from OVA + CpG PLGA (lane 9). It can be seen that empty particles and OVA PLGA do not cause any interference (lanes 5 and 7).

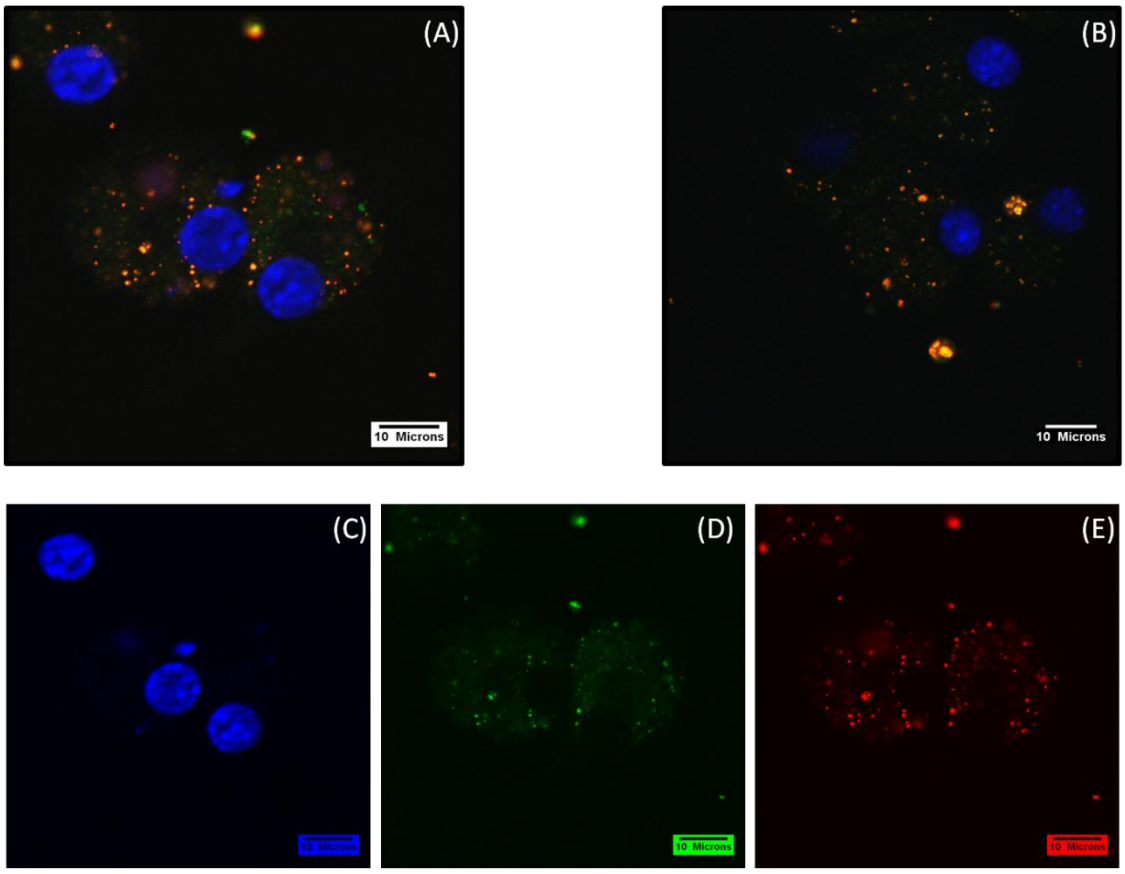

Figure IV-5: Composite confocal images demonstrating cellular uptake and lysosomal localization of (A) AlexaFluor-568-labeled CpG PLGA 75:25 (MW 30000 Da) microparticles and (B) NHS-rhodamine-labeled OVA PLGA 75:25 (MW 30000 Da) microparticles by bone marrow derived dendritic cells (BMDCs). The bottom images show the single channel images of (C) DAPI stained nucleus, (D) lysotracker green labeled lysosomes and (E) AlexaFluor-568-labeled CpG PLGA 75:25 (MW 30000 Da) microparticles.

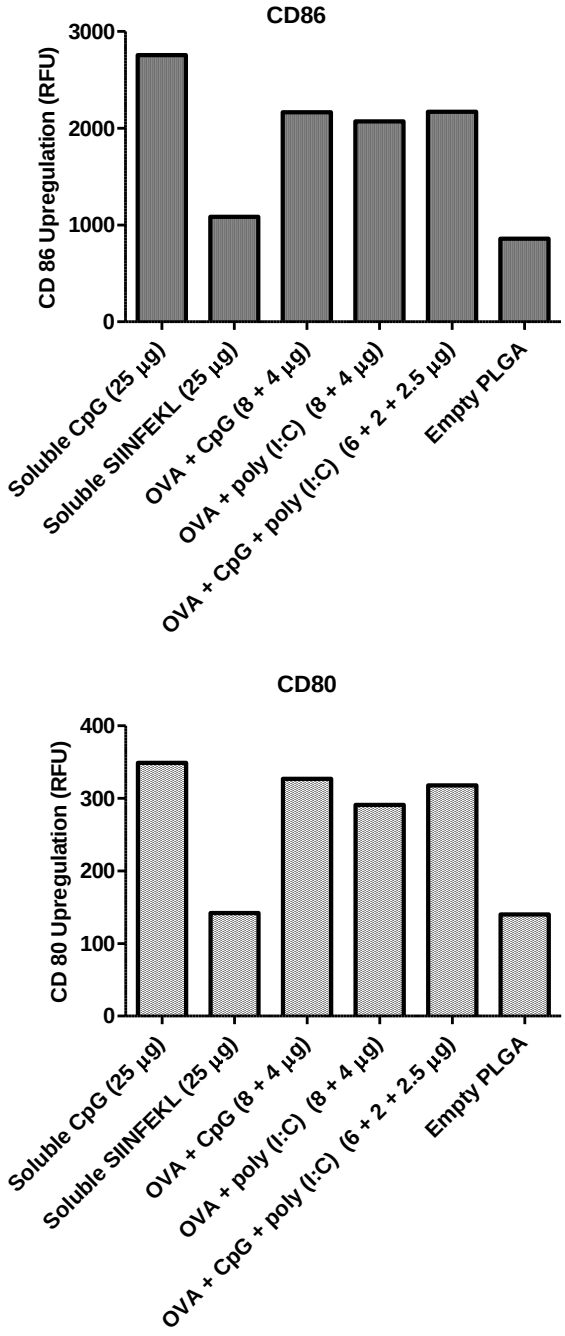

Figure IV-6: *In-vitro* dendritic cell (DC) up-regulation by various PLGA 75:25 (MW 30000 Da) based particulate vaccination groups measured as a function of magnitude of cell surface expressions markers like CD86 and CD80. Soluble CpG (25 µg) was used as a positive control for DC stimulation. (*n = 1*)

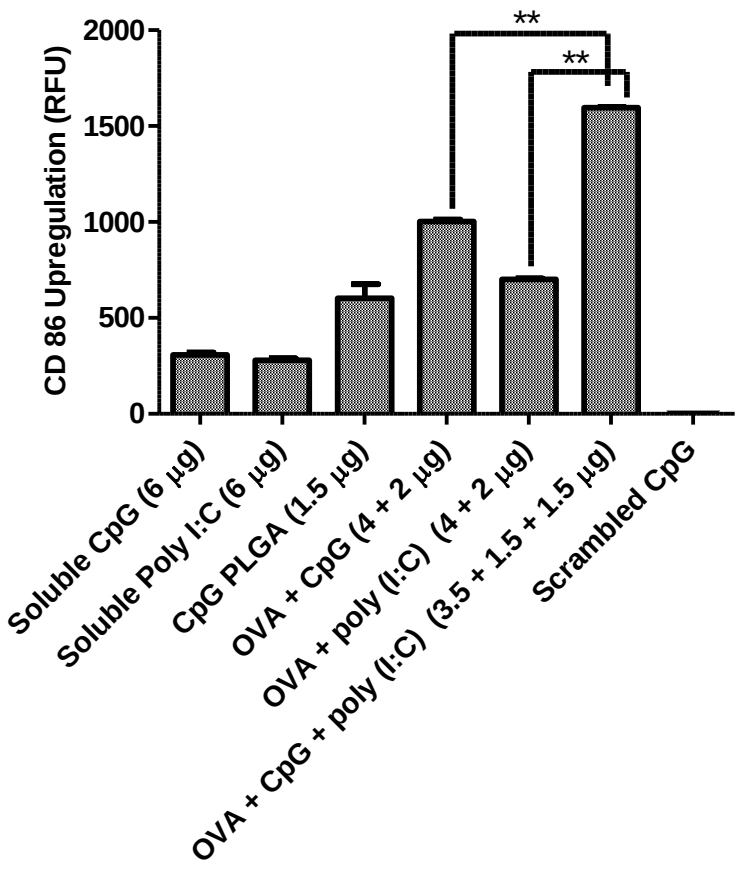

Figure IV-7: *In-vitro* DC stimulation to study the ability of PLGA 75:25 (MW 30000 Da) based particulate vaccines to up-regulate CD86 expression at low doses of CpG and poly I:C in dual and tri-component carriers. Non-stimulatory CpG that lacked the immunostimulatory CpG sequence motif was added as a negative control to the study. Data is represented as mean ± standard deviation (*n = 3*).

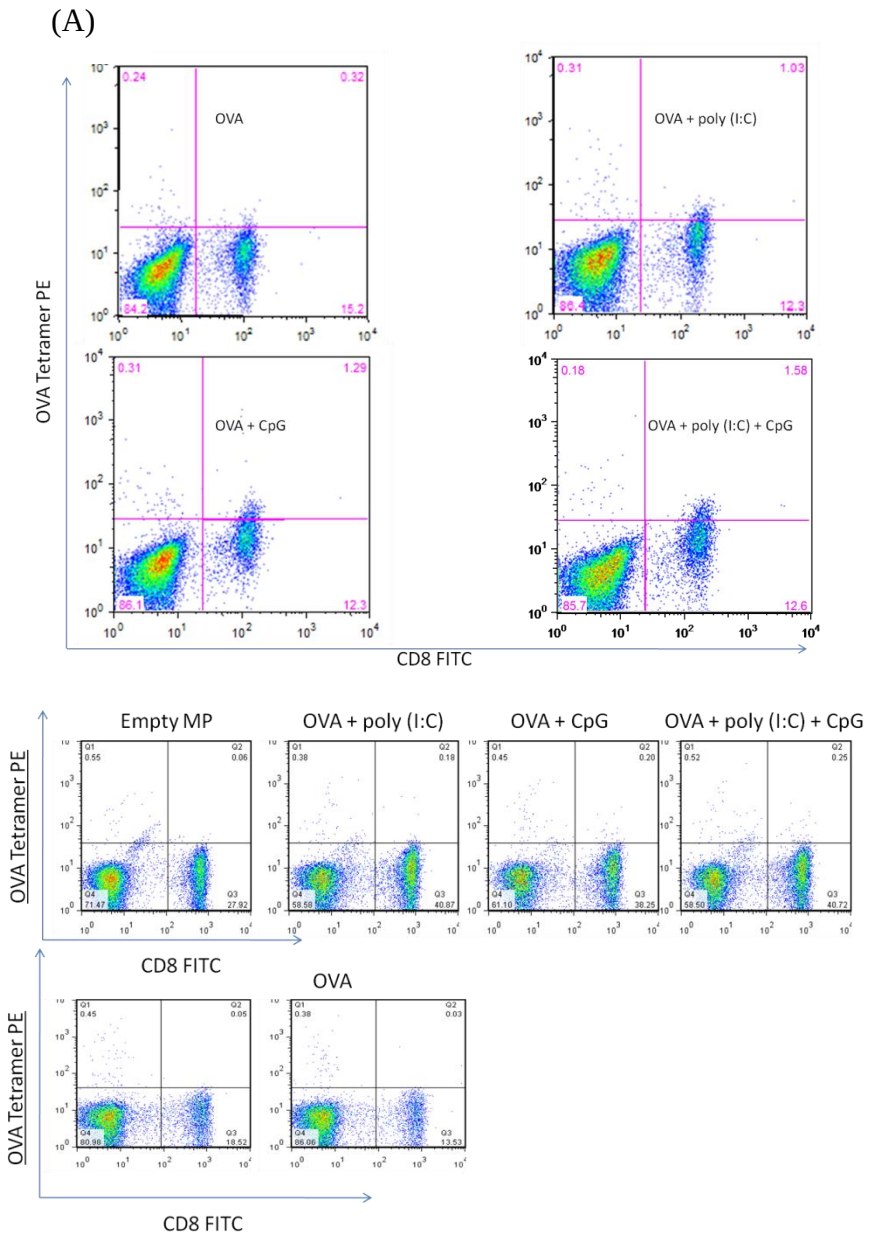

Figure IV-8: OVA-specific CD8+ T cells (upper right quadrant, Q2) were enumerated by tetramer staining and flow cytometric analysis on day 21 after immunization by i.p route (A) and i.m. (B) with OVA, OVA + CpG, OVA + poly I:C and OVA + CpG + poly I:C PLGA 75:25 (MW 30000 Da) MP. The dual and tri-component treatment groups resulted in $\geq$ 2-3 fold increases in tetramer+ CD8+ T cell frequency when vaccinated by i.p. route and about 2-fold increase the CTL population when vaccinated by i.m route. The plots are representatives of 1 mouse from each group of 3 mice.

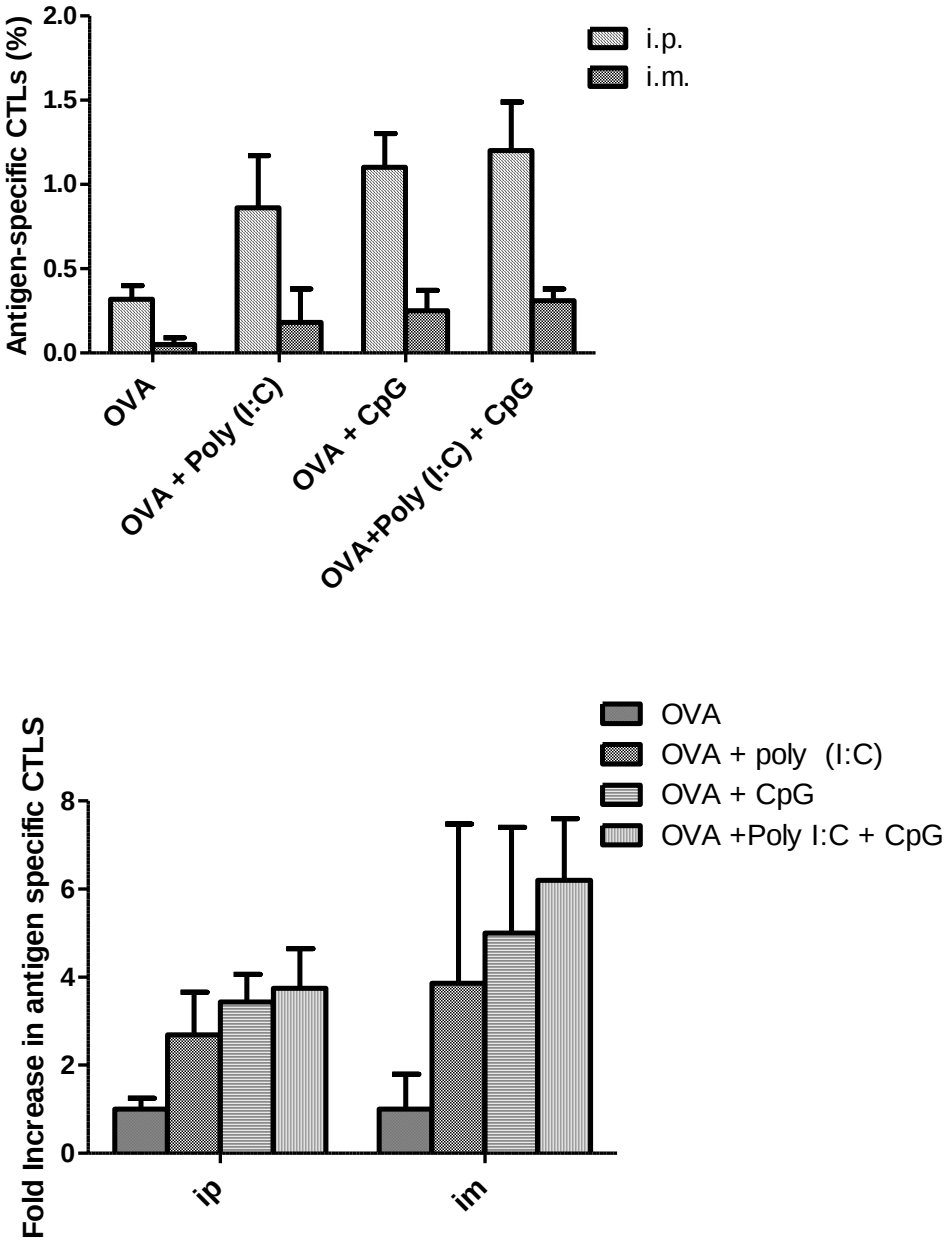

Figure IV-9: Effect of the route of vaccination on the population of antigen-specific cytotoxic T-lymphocytes; CD8+ (A) and the fold-increase in frequency of T cells (B) caused by the presence of adjuvants as compared to vaccination with OVA MP alone. OVA + CpG/poly I:C and OVA + CpG + poly I:C PLGA 75:25 (MW 30000 Da) MP elicited the highest antigen specific cytotoxic T cell population by both routes, the overall response being higher in case of i.p. Data is represented as mean ± standard deviation (*n = 3*).

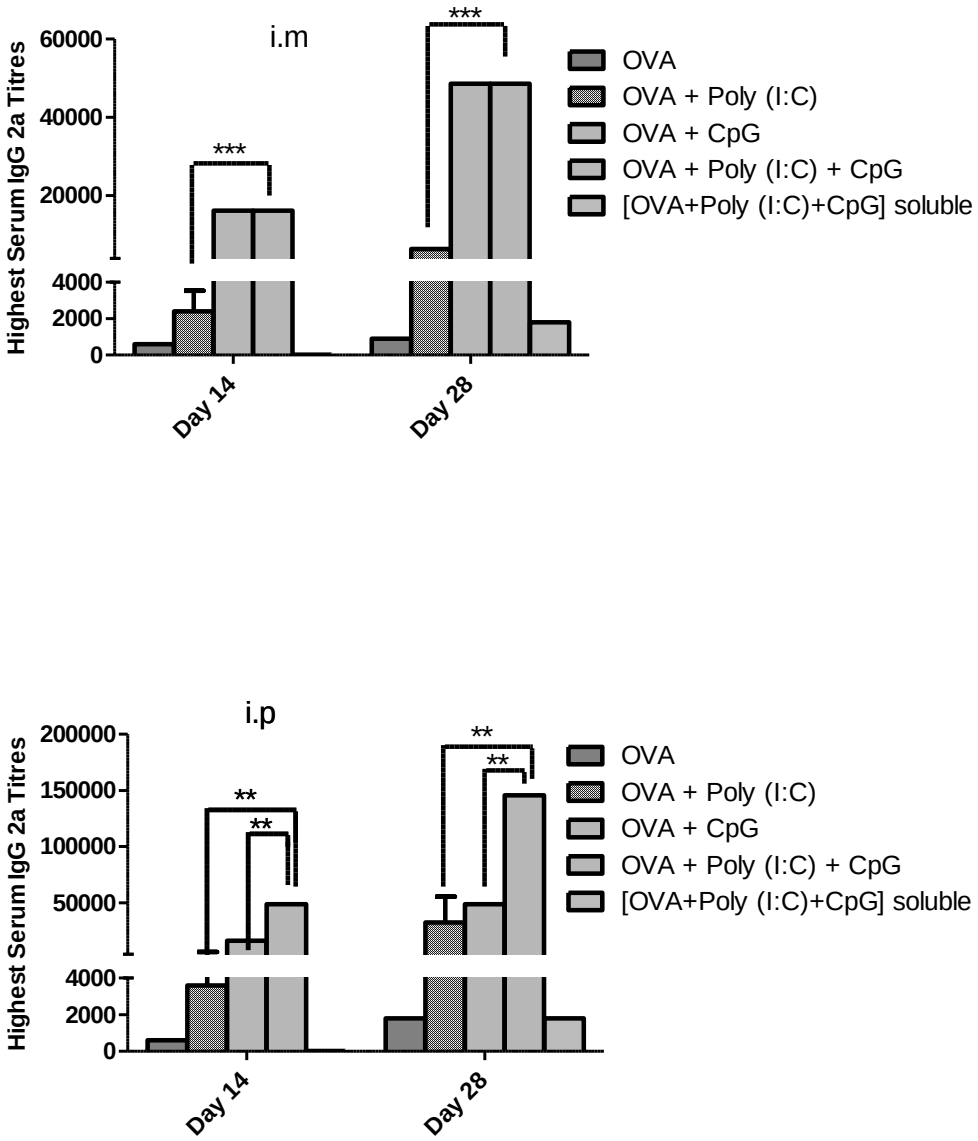

Figure IV-10: Anti-OVA IgG2a titers generated by various PLGA 75:25 (MW 30000 Da) MP based vaccine carriers entrapping OVA alone or in combination with either CpG or Poly I:C or both when administered by i.m and i.p route. Soluble OVA, poly I:C and CpG in combination was used as control to elucidate the effect of particulate form of carrier. Data is represented as mean ± standard deviation (*n = 3*).

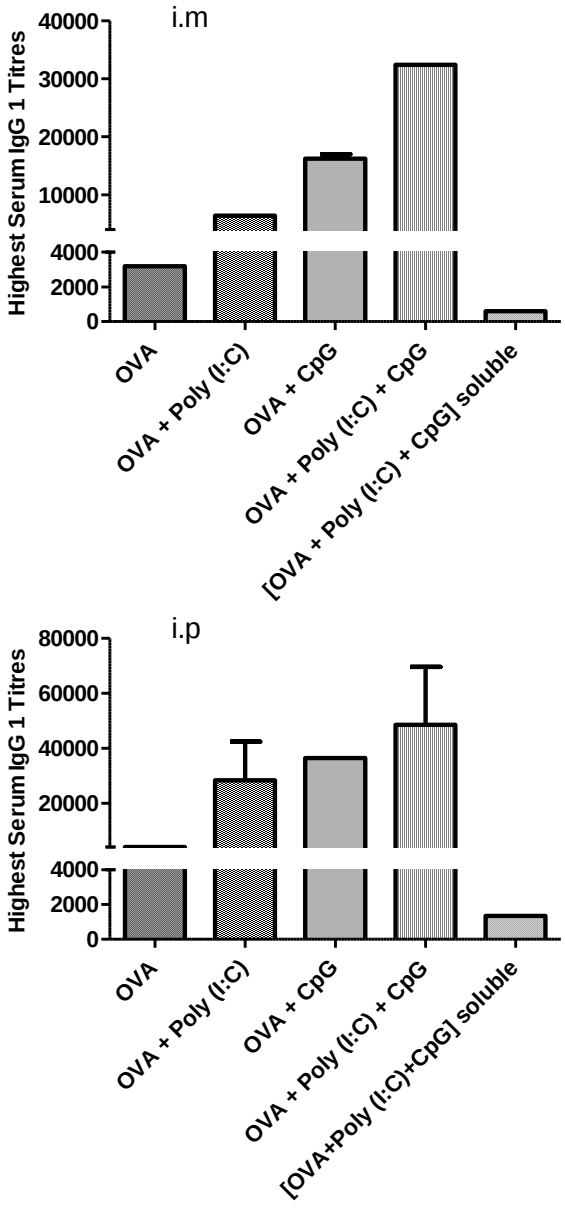

Figure IV-11: Anti-OVA IgG1 titers generated by various PLGA based vaccine carriers entrapping OVA alone or in combination with either CpG or poly I:C or both when administered by i.m and i.p route. Soluble OVA, poly I:C and CpG in combination was used as control to elucidate the effect of particulate form of carrier. Data is represented as mean ± standard deviation (*n = 3*).

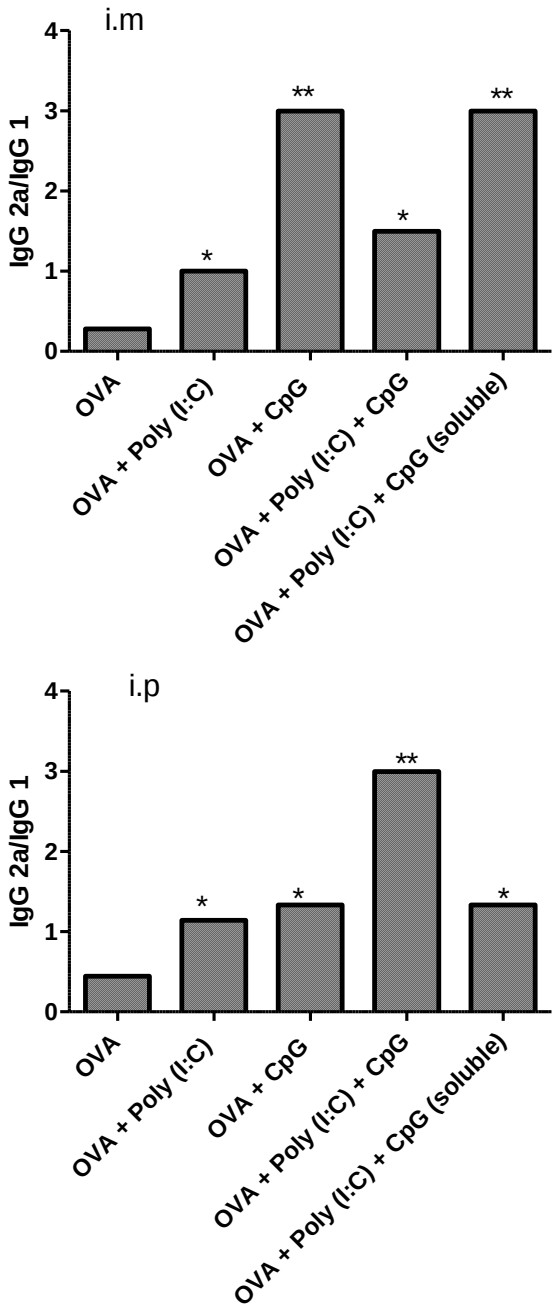

Figure IV-12: Ratio of IgG2a/IgG1 as marker for shift in T cell response (Th) isotype caused by addition of TLR ligands as adjuvants for co-stimulation along with antigen in PLGA 75:25 (MW 30000 Da) MP given by i.m (top) and i.p (bottom) routes. Addition of CpG and/or poly I:C with OVA causes a distinct shift in isotype to favor Th-1 response in soluble and particulate carriers. Data is represented as mean ± standard deviation (*n = 3*).

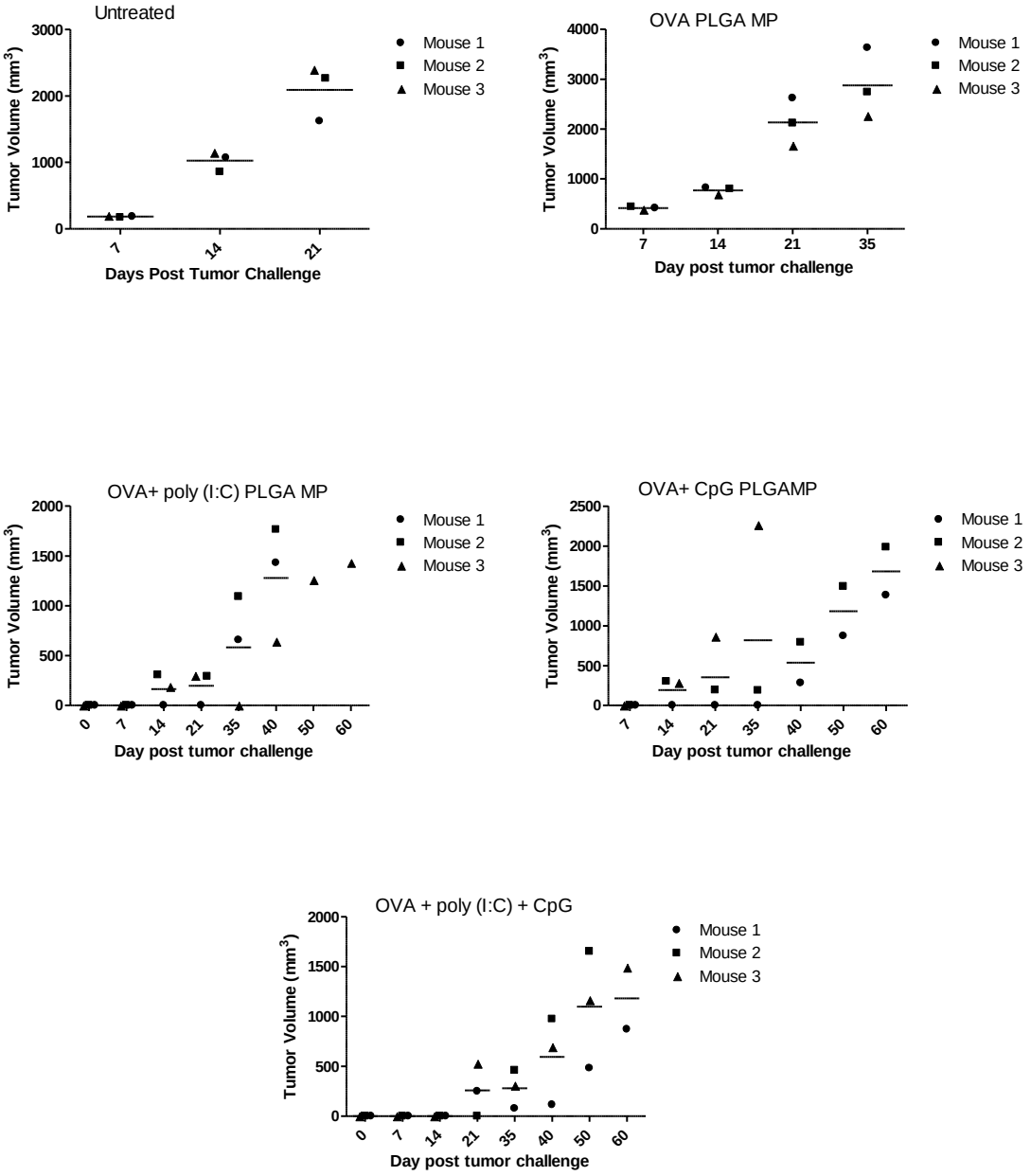

Figure IV-13: Effect of various PLGA 75:25 (MW 30000 Da) MP vaccination groups on tumor growth in a prophylactic murine tumor model. Each graph represents every group separately to trace inter-animal variability if any. All the mice were vaccinated by i.p route 28 days after prime immunization.

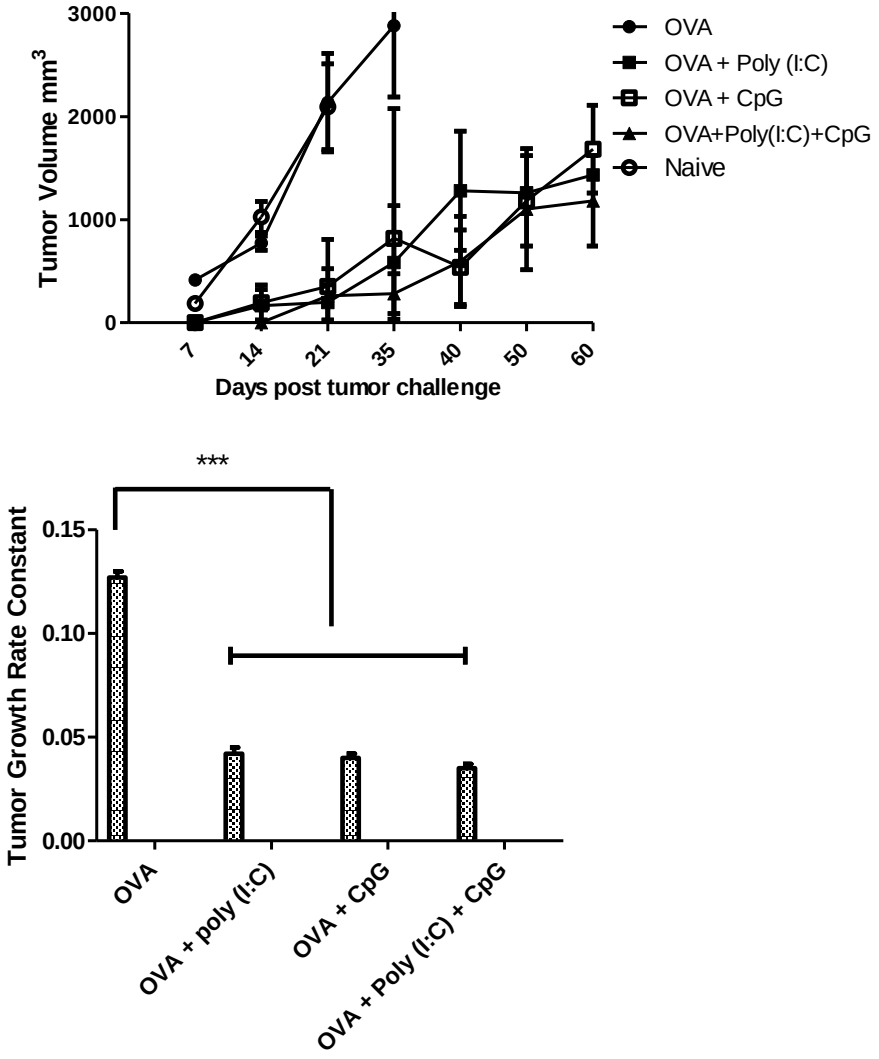

Figure IV-14: Comparison of mean tumor volumes (A) and tumor growth rate differences (B) between various PLGA 75:25 (MW 30000 Da) MP vaccination groups when administered by i.p route in a prophylactic tumor model 28 days after prime immunization. OVA + CpG and/or poly I:C showed the slowest tumor growth progression with a 2-fold improvement in tumor doubling rate as compared to mice treated with OVA alone. Data is represented as mean ± standard deviation (*n = 3*).

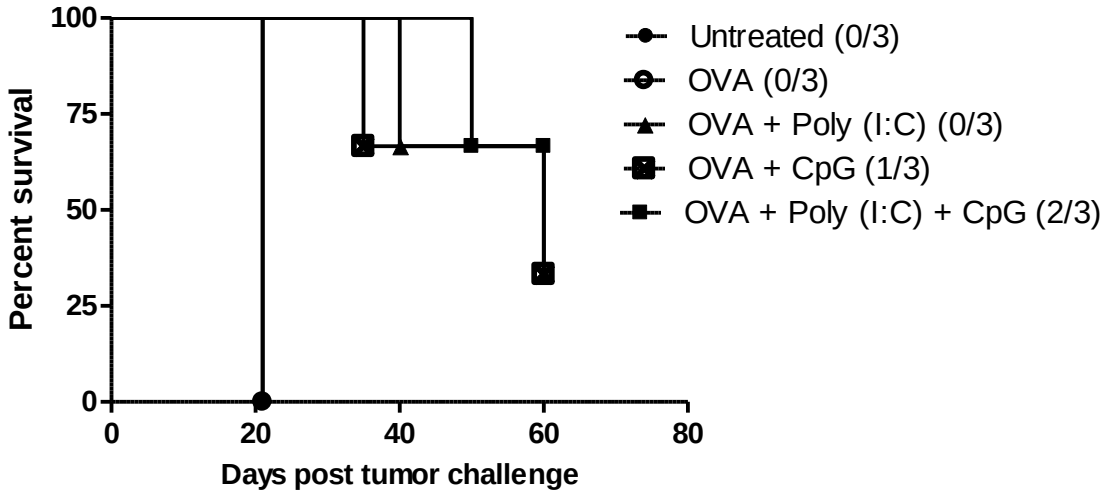

Figure IV-15: Survival Data: EG.7-OVA prophylactic tumor challenge. Mice were monitored twice weekly and sacrificed if tumor measurements exceeded 25 mm in any direction. The untreated mice grew tumors quickly and had to be sacrificed at earlier time points, demonstrating no antigen-specific protection and the ability for tumor cells to grow in the C57Bl/6 mouse model. All the other PLGA 75:25 (MW 30000 Da) MP vaccination groups exhibited different rates of tumor protection with the tri-component PLGA 75:25 (MW 30000 Da) MP group exhibiting the highest survival rate of 67%.

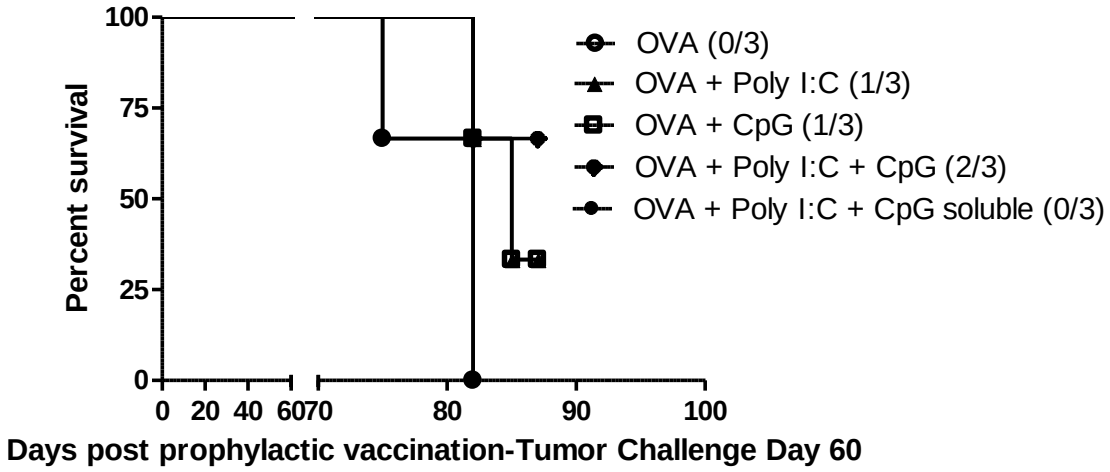

Figure IV-16: Survival Data: EG.7-OVA prophylactic tumor challenge to assess immunogenic memory. Mice were tumor challenged 60 days after prime immunization and monitored twice weekly and sacrificed if tumor measurements exceeded 25 mm in any direction. The mice treated with OVA PLGA 75:25 (MW 30000 Da) MP alone grew tumors quickly and had to be sacrificed at earlier time points, demonstrating no antigen-specific protection and the ability for tumor cells to grow in the C57Bl/6 mouse model. All the other PLGA 75:25 (MW 30000 Da) MP vaccination groups exhibited different rates of tumor protection with the tri-component group exhibiting the highest survival rate of 67%.

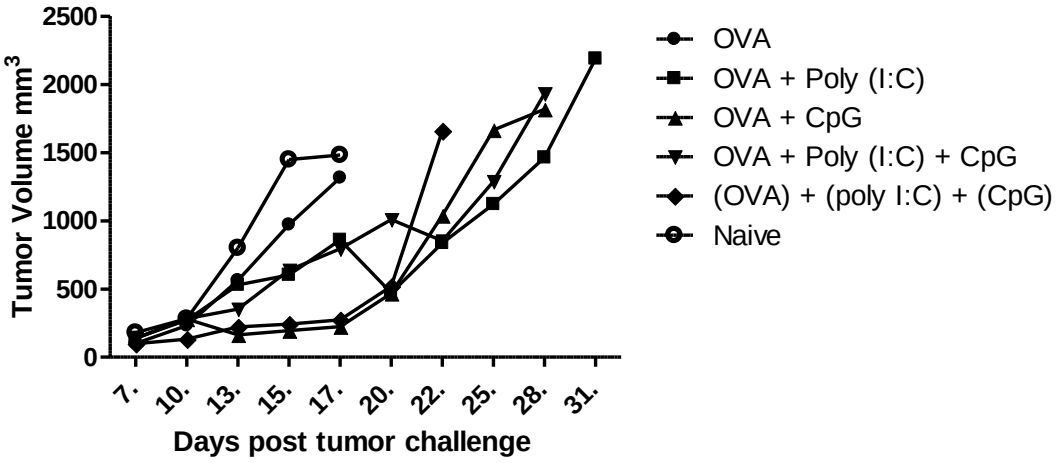

Figure IV-17: Effect of various treatment groups on mean tumor volumes in a therapeutic EG.7 tumor model. Mice that were treated with OVA PLGA 75:25 (MW 30000 Da) MP alone were comparable to untreated mice that showed rapid growth in tumors. The other treatment including OVA + either CpG or poly I:C or both groups showed some degree of resistance to prolific tumor growth. When PLGA 75:25 (MW 30000 Da) MP entrapping each component separately were admixed (◆), they did not provide equivalent tumor protection as that of the tri-component (▼).

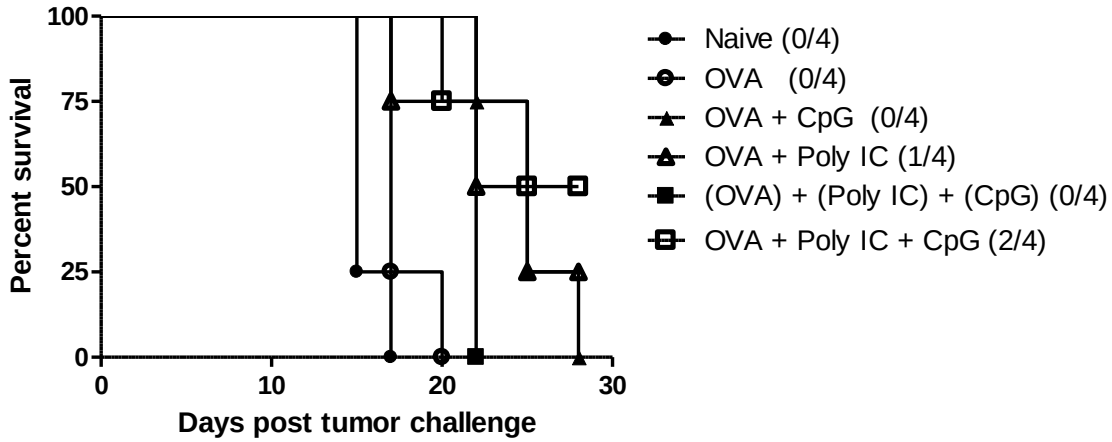

Figure IV-18: Survival Data: EG.7-OVA therapeutic tumor challenge. Mice were monitored twice weekly and sacrificed if tumor measurements exceeded 25 mm in any direction. The untreated mice grew tumors quickly and had to be sacrificed by day 17, demonstrating no antigen-specific protection and the ability for tumor cells to grow in the C57Bl/6 mouse model. All the other PLGA 75:25 (MW 30000 Da) MP vaccination groups exhibited different rates of tumor protection with the tri-component group exhibiting the highest survival rate of 50%. (n= 4 for every group).

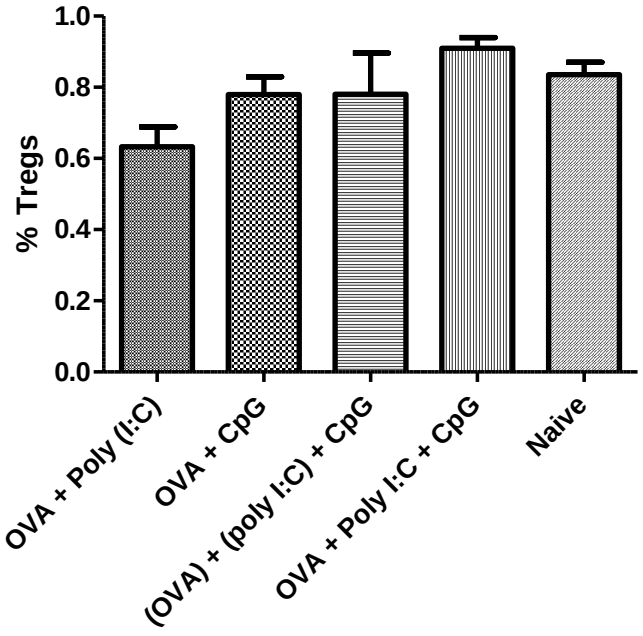

Figure IV-19: Effect of various treatment groups on the population of peripheral immunosuppressant T_{reg} cells 20 days after tumor challenge in a therapeutic tumor model. The treatment groups show no signs of down-regulation of T_{regs} and the population is comparable to that of naïve tumor-free mice.

Table IV-1: Entrapment Efficiency of various PLGA 75:25 (MW 30000 Da) MP based vaccination groups

Formulation	Average Entrapment Efficiency (%)	Average Loading (μg/mg PLGA)
OVA	72	18
OVA + Poly I:C	74 and 53	18 and 8
OVA + CpG	72 and 41	18 and 7
OVA + CpG + poly I:C*	60, 45 and 50	16, 6.8 and 6.5

* Denotes the microparticles were fabricated using PLGA 85:15 (MW 40000 Da) with a carboxylic acid terminal

Table IV-2: Median survival times of mice vaccinated with PLGA 75:25 (MW 30000 Da) MP groups in a prophylactic tumor model

Vaccination Group	Median Survival Time (Days)
Untreated	21
OVA	21
OVA + poly I:C	40
OVA + CpG	60
OVA + CpG + poly I:C*	> 60

* Denotes the microparticles were fabricated using PLGA 85:15 (MW 40000 Da) with a carboxylic acid terminal

Table IV-3: Tumor growth rate and tumor doubling times amongst various PLGA 75:25 (MW 30000 Da) MP based treatment groups in a therapeutic tumor model

Treatment Group	Growth Rate Constant (γ)	Doubling Time (Days)
Untreated	0.20-0.23	3.03
OVA	0.19-0.20	3.5
OVA + poly I:C	0.11-0.14	6.1
OVA + CpG	0.13-0.14	5.4
OVA + poly I:C + CpG*	0.13-0.14	5.2

* Denotes the microparticles were fabricated using PLGA 85:15 (MW 40000 Da) with a carboxylic acid terminal

CHAPTER V: PLGA MICROPARTICULATE CARRIER FOR COMBINATORIAL CHEMO-IMMUNOTHERAPY

Introduction

Conventional anti-cancer therapies include chemotherapy and radiotherapy. Radiotherapy is often integrated with surgical treatment. The most preferred treatment modality has been chemotherapy and it has met with considerable success in clinical research over the years. Anthracyclines (or anthracycline antibiotics) derived from Streptomyces bacteria is a class of drugs most frequently used in cancer chemotherapy (135). Doxorubicin and daunorubicin are the two main compounds from this class that find the maximum clinical utility. Doxorubicin is used for the treatment of solid tumors such as those arising in the breast, bile ducts, endometrial tissue, the esophagus and liver, osteosarcomas and non-Hodgkin's lymphoma. Daunorubicin is utilized primarily in acute myeloid leukemia (136). The mechanism of action of doxorubicin has been described in detail by Gewirtz (137). Three primary mechanisms of action have been identified for this class of compounds. The primary mechanism of action is by inhibition of DNA synthesis and cell proliferation by intercalating with the DNA of the rapidly dividing cells. The intercalation results in conversion of quinones to semiquinone free radicals that causes free-radical injury to DNA. Doxorubicin is also known to interact with DNA by intercalation and inhibition of macromolecular biosynthesis. This inhibits the progression of the enzyme topoisomerase II, which relaxes the supercoils in DNA for transcription. Doxorubicin stabilizes the topoisomerase II complex preventing the DNA double helix from being resealed thereby stopping the process of replication (137).

However, this class of chemotherapeutic compounds is associated with a high degree of tissue and cardiotoxicity. It is a fairly well elucidated fact that the cardiotoxicity of anthracyclines is associated with the generation of free radicals that interfere with mitochondrial function causing cell membrane lipid peroxidation.(137)

Owing to the challenges posed by conventional cancer treatment strategies there has been increasing interest in exploring newer and alternative strategies like immunotherapy for tumor treatment. While chemotherapy involves indiscriminate killing of tumor cells, immunotherapy is directed against specific tumor associated antigen (TAAs) expressing cells thus sparing healthy cells and tissues. Chemotherapy induces a "direct" apoptotic effect on tumor cells. Conversely, immunotherapy induces a "by-stander" effect. Upon antigen presentation, the APCs are activated which in turn direct the differentiation of T-lymphocytes into CTLs that can eradicate the tumor mass. While chemotherapy generates a local anti-tumor effect, immunotherapy has the potential to generate systemic effects that can treat tumor metastases and future reoccurrences (138, 139). A complete and a permanent cure to cancer involves a "direct" eradication of local tumor mass accompanied by a "by-stander effect" in which the immune system recognizes, attacks, and eradicates the remaining localized, circulating and metastasized tumor cells. Accumulating evidence suggests that a combination of therapies might be the best treatment modality for achieving long term cure for cancer (140).

Chemotherapy renders some degree of immunogenicity, a potential that can be exploited to its fullest by a combinatorial chemo-immunotherapy approach. The immunogenic potential of chemotherapy has been studied by a few groups and a summary of such findings and mechanisms is explained below. A proof of concept study for elucidating this finding was first put forth by Casares et al. in the Journal of Experimental Medicine (2005) (141). This study involved a prophylactic tumor cell vaccination therapy with three groups of colon carcinoma derived CT26 tumor cells treated with various combinations of chemotherapeutic agents. The first group of cells was subject to a 24 hour treatment with doxorubicin, the second group involved treatment with mitomycin, another class of antibiotic that induces cell death by necrosis. The third group of cells was subject to a 24 hour treatment with mitomycin followed by a 15 minute exposure to doxorubicin. The fourth group of cells was untreated. The results of

this study are presented in Figure V-1. Their studies showed that mice vaccinated with doxorubicin treated tumor cells showed the highest survival time and median survival rate. Their results suggested that anthracyclines (doxorubicin) induced immunogenicity of cancer cells in mice. This process was dependent on the induction of caspase-dependent tumor cell death leading to antigen uptake by DCs and to the activation of CD8+ cytotoxic T cells. This hypothesis has been schematically put forth in Figure V-2 describing the immune cascade triggered upon cell death induced by doxorubicin.

In another study, Levy et al. studied the ability of repeated administration of intratumoral CpG as a therapy model for B-cell lymphoma (142). CpGs are ssDNA fragments containing immune stimulatory sequence motifs similar to those found in bacterial DNA. DCs and B cells have a receptor for CpG that initiates an activating signal for these cells. The authors concluded that the therapeutic effect of CpG depended upon its injection directly into a site of dying tumor cells. This course resulted in a systemic CD8-dependent T cell immune response against the tumor (142). In another study by the same group, they showed that in a B cell lymphoma tumor model, intratumoral administration of immature DCs combined with cyclophosphamide (CTX) led to effective tumor regression (143). Some of these recent encouraging studies lead us to build a therapeutic intratumoral combinatorial chemo-immunotherapy model for treatment of lymphoma. Lymphoma is a malignancy which is responsive to active immunotherapy. Despite the success of passive immunotherapy with monoclonal antibodies (e.g. anti-CD20, rituximab), many patients with lymphoma still remain incurable (144). Therefore it is postulated that therapeutic vaccines against lymphoma might elicit long-lasting anti-tumor immune responses and prevent or prolong the time to recurrence.

Since this concept of combined benefit of chemotherapy and immunotherapy has not translated into extensive research, the fabrication of a delivery system that can co-deliver a chemotherapeutic agent and an adjuvant formed the premise of our current

study. The hypothesis and specific aims of this study is explained in detail in the following section.

Hypothesis and specific aims

Doxorubicin (DOX) induces local cell death by apoptosis (141). Co-delivery of CpG in a delivery system with DOX ensures simultaneous uptake by tumor cells. This results in a rapid deployment of phagocytic cells including DCs and macrophages to the tumor site. The tumor antigen is then presented by the phagocytic APCs in the context of the MHC class I pathway (140). We hypothesize that presence of CpG will provide a co-stimulatory signal inducing rapid activation of DCs creating a tumor cytokine milieu that is rich in IFN-γ. This in turn will result in CTL mediated eradication of residual tumor mass. The activation of CTLs might also trigger a systemic immune response and increase sensitization potential to future chemotherapy.

However, doxorubicin when injected in high and frequent doses in a soluble form poses problems due to acute cardiotoxicity and multidrug resistance as described in the first chapter. Hence researchers have tried to explore alternative delivery systems for doxorubicin that can reduce the frequency of administration and dose (145). The most successful commercial scale modification of the DOX biodistribution has been achieved by entrapping it in pegylated liposomes (Doxil, Johnson and Johnson) and non-pegylated liposomes (Enzon Pharmaceuticals for Cephalon). The research for alternative doxorubicin delivery strategies continues and microparticle technology may provide an interesting direction to this area of research.

The broad hypothesis of the current study is that immunotherapy will synergize with chemotherapy *in-vivo* augmenting the anti-tumor immune responses. Another advantage of this strategy is that it does not require *in-vitro* manipulation, unlike DC based vaccines. This treatment can thus be made available to a large numbers of patients.

Finally, the presence of an immunotherapeutic component can increase the sensitization potential of tumor cells to future chemotherapy (142, 143).

The specific aims of this study are listed as follows:

1. Fabricate doxorubicin (DOX)-loaded PLGA microparticles to study the effects of chemotherapy induced tumor regression.
2. Fabricate CpG-loaded PLGA microparticles to study the effects of adjuvant induced tumor regression.
3. Fabricate DOX + CpG PLGA microparticles to study the effect of a combinatorial vaccine therapy.
4. Study the effects of the following treatment strategies on a therapeutic B-cell lymphoma tumor model.
5. Study the effects of the same treatment modalities on a therapeutic T cell lymphoma tumor model.

On completion of these specific aims, we intended to explore the possibility of induction of systemic immunity triggered by the presence of CpG.

Materials and Methods

Materials

PLGA (75:25, Inherent viscosity, 0.41 dL/g) and PLGA (85:15, Inherent viscosity, 0.51 dL/g acid end group) were purchased from Lactel Absorbable Polymers (Cupertino, CA), poly (vinyl alcohol) (PVA, 87 – 89 % hydrolyzed, MW 30- 67,000 Da) was purchased from Sigma-Aldrich (St. Louis, MO). Doxorubicin hydrochloride (DOX) was purchased from Sigma-Aldrich. (St. Louis, MO). CpG-1826 was purchased from Coley pharmaceuticals (Dusseldorf, Germany). All other chemicals and solvents including dichloromethane (DCM) and acetonitrile used were of analytical grade.

Methods

I. Fabrication of Doxorubicin (DOX) or CpG loaded PLGA MP: Sonication method

The internal aqueous phase consisted of either doxorubicin HCl (5 mg) or CpG (2.5 mg) solubilized in 200 µL of 1% w/v aqueous solution of poly (vinyl alcohol) (PVA) as a surfactant. This was emulsified into an oil phase (2 mL) containing 6.67 % w/v PLGA (75:25 Inherent viscosity 0.41 dL/g) dissolved in DCM using a micro tip probe sonicator set at level 3 (Sonic Dismembrator Model 100, Fisher Scientific, Pittsburgh, PA). This primary w/o emulsion was then immediately sonicated into 4 mL of aqueous phase containing 1% PVA for 30 seconds at the same setting as above to generate the secondary emulsion. The secondary emulsion was then dropped slowly into a beaker containing 50 mL of 1% PVA and stirring was continued using magnetic stirrer until complete evaporation of DCM. The particles were collected by centrifugation at 5000 x g for 5 minutes, washed three times with DI water and lyophilized overnight (Labconco Freezone 4.5, Labconco, Kansas City, MO).

Effect of formulation additives including addition of (1 to 2%) w/v to the external phase during microparticle fabrication or pH modifiers like 50 mM sodium borate buffer (pH 8.5) on the entrapment efficiency of DOX was studied. When borate buffer was used, the pH of the external phase was adjusted to range between 8 and 8.5. CpG –loaded PLGA microparticles were prepared by the optimized method described in Chapter II and the same technique was followed for all the microparticle formulations entrapping CpG.

II. Characterization of microparticles

IIA. Particle Size

A suspension of the lyophilized microparticles in DI water at a conc. of 0.1-0.2 mg/mL was used to analyze the particle size using Zetasizer Nano ZS (Malvern, Southborough, MA). Microparticle morphology was assessed by scanning electron microscopy (SEM, Hitachi S-4000, Japan). Briefly, air-dried microparticles were placed

on adhesive carbon tabs mounted on SEM specimen stubs. The specimen stubs were coated with approximately 5 nm of gold by ion beam evaporation before examination in the SEM operated at 5 kV accelerating voltage.

IIB. Entrapment Efficiency (EE) and Loading Efficiency (LE)

The supernatant collected during centrifugation was used to analyze the free (un-entrapped DOX. The EE was then calculated as follows:

$$EE\ (\%) = [(\text{Initial amount of DOX} - \text{Free DOX in Supernatant}) / (\text{Initial amount of DOX})]\backslash\backslash] * 100 \quad \text{(V-1)}$$

The amount of DOX/CpG in the microparticles was calculated by directly measuring the amount of the actives in the particles. For analysis of doxorubicin, 5-10 mg of DOX-loaded particles was dissolved in 1 mL of dimethylsulfoxide (DMSO) and the solution was analyzed by fluorescence spectroscopy for a direct measurement of DOX content. For analysis of CpG, 5-10 mg of lyophilized CpG-loaded microparticles was dissolved in 200 µL DCM and the precipitated CpG was extracted by adding 10-fold excess phosphate buffered saline (PBS). The extraction procedure was repeated 2-3 times until no further active component could be detected in the aqueous extract. CpG content was analyzed by fluorescent spectroscopy as described in the analytical methods section.

Mass balance up to 95% was achieved between the two approaches. Hence for all further analysis, loading was directly assessed by extracting the active component from the particles.

IIC.Analytical Methods

Doxorubicin Hydrochloride (DOX)

DOX was analyzed by fluorescence spectroscopy. The excitation and emission wavelengths were set at 390 and 485 nm respectively and relative fluorescence intensity was used to calculate DOX concentration. The standard solution of DOX in a concentration range of 1-40 µg/mL was prepared by serial dilutions of a DOX stock

solution in both DMSO and water. The aqueous standards were prepared for analysis of DOX released during the *in-vitro* release studies and the DMSO standards served to quantify DOX loaded in the PLGA MP. The fluorescence intensity was then measured with a Microplate Reader (SpectramaxPlus 384, Sunnyvale, CA). Following the fluorescence assay of standard solutions of DOX, the standard curve of DOX in both DMSO and aqueous solutions was generated from the linear relationship between relative fluorescence intensity and concentration. All the measurements were done in triplicate.

CpG

CpG was analyzed by fluorescence spectroscopy by the use of Oligogreen, a fluorescent probe for the quantitative estimation of oligonucleotides. The excitation and emission wavelengths were set at 480 and 520 nm respectively and relative fluorescence intensity was used to calculate CpG concentration. The standard solution of CpG in a concentration range of 0.1 – 2 µg/mL was prepared by serial dilutions of a CpG stock solution in PBS. The Oligogree^{TM} detection reagent was prepared by a 200-fold dilution in either 1X TE buffer or PBS. The samples (100 µl) were pipeted into microplate wells (Microwell-plates, Nunc, Germany) and were mixed with 100 µl of detection reagent. This microtiter plate was incubated for 5 minutes at room temperature in dark. The fluorescence intensity was then measured with a Microplate Reader (SpectramaxPlus 384, Sunnyvale, CA). Following the fluorescence assay of standard solutions of CpG, the standard curve of was generated from the linear relationship between relative fluorescence intensity and the concentration of CpG. All the measurements were done in triplicate.

IID. *In-vitro* release profile

30- 40 mg of PLGA microparticles entrapping either DOX or CpG were suspended in 3 mL phosphate buffered saline (PBS, pH 7.4. The samples were shaken in

a water bath at 37 °C at 100 rpm. 200 µL of sample was withdrawn at pre-determined time intervals. The sample was centrifuged using a microcentrifuge at 5000 rpm for 5 minutes and the supernatant was used for release analysis. The microparticle sediment was redispersed in 200 µL in the same release medium and replenished back to the release sample container. Released DOX and CpG samples were assayed by fluorescence spectroscopy as described in the previous sections. All measurements were performed in triplicate.

III. Fabrication of a co-delivery carrier for DOX and CpG

The polymer of choice was an acid end-capped PLGA (85:15 with an inherent viscosity 0.5 dL/g . The method of fabrication for DOX-loaded PLGA particles remained the same as described in section I. The particles were analyzed for size and entrapment efficiency. Following lyophilization, the particles were modified using EDC-NHS for conjugation of a cationic polymer on the surface. Briefly, 100 mg of the particles were suspended in 3 mL MES buffer (pH 5.5). 20-fold molar excess of EDC and NHS over PLGA was used for modification. The calculated amounts of EDC and NHS were dissolved in 1 mL MES buffer each and was slowly added to the particles under constant stirring. Stirring was continued for 1 hour. The particles were then centrifuged and washed twice with PBS to remove any unreacted EDC-NHS. The particles were then suspended in 3 mL of autoclaved PBS. A 10-fold molar excess of cationic polymer, polyethyleneimine was used for surface conjugation and rendering an overall positive charge to the DOX-loaded PLGA particles. The cationic polymer was suspended in 2 mL PBS. The particles were then added drop wise into the PEI solution under constant stirring and the reaction was allowed to proceed at room temperature for 3 hours. The particles were then collected by centrifugation, washed and lyophilized overnight. The particles were then analyzed for DOX content to account for any loss of DOX by diffusion during the modification steps. PEI conjugation was confirmed by a change in

zeta potential from a slightly negative charge to a distinct positive charge. The particles were then incubated with a 1mg/mL solution of CpG for 4-6 hours to allow surface adsorption of CpG to the cationic particles. The particles were collected by centrifugation and the supernatant was analyzed for unadsorbed CpG by oligogreen assay to determine the amount of CpG adsorbed/mg of PLGA particles.

IV. Tumor cell lines and animals

6 to 8 week BALB/C and C57Bl/6 male mice were purchased from the National Cancer Institute (Bethesda, MD) and were maintained in filtered cages before use. A20, a BALB/c B cell lymphoma line and EG.7-OVA were used to measure *in- vivo* tumor growth in the prophylactic and therapeutic tumor models. A20 is a BALB/c B cell lymphoma line and these cells were stably transfected to express luciferin. EG.7 is an OVA-expressing thymoma cell line often used as a tumor model.

The cells were maintained in RPMI-1640 supplemented with 10% Fetal Bovine Serum (FBS), 1% sodium pyruvate and 0.05 mg/ml gentamycin in a humidified 5% CO_2-containing atmosphere.

V. Therapeutic tumor challenge in A20 tumor model

The A20 tumor cells were resuspended in PBS at a concentration of 1 x 10^6 cells in 100 µL. The cells were injected subcutaneously into the right flank of the mouse. This was considered as Day 0 for the therapeutic study. The treatment was initiated by intratumoral administration on day 20 when the tumors seemed uniformly palpable in all the mice. Every treatment group consisted of 4 mice. The treatment consisted of the following treatment groups:

1. DOX-loaded PLGA MP (50 µg of DOX/mouse)
2. CpG-loaded PLGA MP (30 µg of CpG/mouse)
3. DOX + CpG PLGA MP (50 and 30 µg of DOX and CpG/mouse respectively)

4. Naïve untreated mice serving as control.

Tumor outgrowth was measured twice weekly, using *in-vivo* imaging system; IVIS 200 (Xenogen Corporation, IN). The Xenogen IVIS-200 System is a high-sensitivity, low noise, *in-vivo* imaging technology platform that allows non-invasive visualization and tracking of cellular activity within a living organism, in real time by capturing bioluminescence images in an animal. Living Image® software was used for image display and analysis. Prior to tumor imaging, the mice were anesthetized using isoflurane. Luciferase was administered at a dose of 150 µg/mouse intraperitonially 10 minutes prior to imaging. The mice were then placed in a dark chamber and imaged for luminescence intensity. This technique relies on the principle of luciferase serving as an enzyme that catalyzes the conversion of luciferin to oxyluciferin. Luciferin is expressed by the proliferating tumor cells. The luminescence intensity is a function of substrate (luciferin) concentration which in turn is a direct reflection of tumor volume. The schematic for this technique has been shown in Figure V-3. Mice were sacrificed for ethical reasons if they appeared ill from tumor burden or if measurements exceeded 25 mm in any direction. Each experimental group consisted of 4 mice. All animal experiments were conducted in accordance with the procedures outlined in the University of Iowa's Guidelines for Care and Use of Experimental Animals adapted from the NIH guidelines for animal care and use.

VI. Therapeutic tumor challenge in the EG.7 thymoma tumor model

The EG.7 tumor cells were resuspended in PBS at a concentration of 2×10^6 cells in 100 µL. The cells were injected subcutaneously into the left flank of the mouse. This was considered as Day 0 for the therapeutic study. On day 3, mice were treated with the following five groups listed above by subcutaneous (s.c) route at the same location as tumor challenge with 4 mice in every group.

Tumor outgrowth was measured twice weekly, and tumor volume was computed using the following equation as described by Shariat et al.

$$\boldsymbol{volume}\ (\boldsymbol{v}) = \boldsymbol{length\ x\ width\ x\ depth\ x}\ (\boldsymbol{\Pi/6}) \qquad \text{(V-2)}$$

Survival of the mice following treatment was also monitored. Mice were sacrificed for ethical reasons if they appeared ill from tumor burden or if measurements exceeded 25 mm in any direction. All animal experiments were conducted in accordance with the procedures outlined in the University of Iowa's Guidelines for Care and Use of Experimental Animals.

VII. Tumor re-challenge in the EG.7 thymoma tumor model

The mice that survived the therapeutic tumor challenge study were re-challenged on day 50 after the first therapeutic tumor challenge. The EG.7 tumor cells were resuspended in PBS at a concentration of 2 x 10^6 cells in 100 µL. The cells were injected subcutaneously into the right flank of the mouse (opposite flank as the initial tumor challenge). Tumor outgrowth was measured twice weekly and tumor volume was computed. Survival of the mouse treatment groups was also monitored. Mice were sacrificed for ethical reasons if they appeared ill from tumor burden or if measurements exceeded 25 mm in any direction.

VIII. Statistical analysis

Group data are reported as mean ± standard deviation. Differences between groups are analyzed by one way analysis of variance with a Tukey post-test analysis. Levels of significance were accepted at the $p < 0.05$ level. Statistical analyses were performed using Prism 5.0 software (Graphpad Software, Inc., San Diego, CA).

Results

I. Standard Curve of Doxorubicin HCl assayed by fluorescence spectroscopy

A standard curve with definite concentration range in DMSO and water were studied in order to quantify DOX. As shown in Figure V-4, the relative fluorescence intensity increased linearly with respect to DOX concentration in DMSO of 1 to 40 µg/mL with an r^2 value of 0.99. The results indicated that this method developed for the detection and quantification of DOX is a suitable, reliable and robust method.

II. Standard Curve of CpG assayed by Oligogreen Quantification for ssDNA

The most commonly used technique for measuring oligonucleotides and ssDNA concentration is the determination of absorbance at 260 nm (A260). The major disadvantage of the absorbance method is the interference caused by contaminants commonly found in nucleic acid preparations decreasing the sensitivity of the assay. Hence we chose an alternative technique that involved the use of Quant-iT™ OliGreen® ssDNA reagent, an ultra-sensitive fluorescent nucleic acid stain for quantifying oligonucleotides and single-stranded DNA (ssDNA) in solution. As shown in Figure V-5, the relative fluorescence intensity increased linearly with respect to CpG concentration of 0. 1 to 2µg/mL with an r^2 value of 0.99. The results indicated that this method developed for the detection and quantification of CpG is a suitable, reliable and robust method.

III. Characterization of Doxorubicin-loaded PLGA MP

The structure of doxorubicin HCl is shown in Figure V-6. Literature values for the pKa of the amine functional group of DOX range from 7.2 to 8.3. The molecular weight of the drug is 579 g/mole. CpG carries an overall negative charge by the presence of a phosphate back bone and consists of 20 base pairs with an average molecular size of approximately 6000 g/mole. DOX-loaded PLGA microparticles exhibited smooth surface morphology as shown in Figure V-7 exhibiting a mean particle size of approximately 1.5

μm. Figure V-8 compares the entrapment efficiency in the presence of 1 % w/v NaCl as an additive in the external phase. It can be seen that upon the addition of sodium chloride, the EE increased 3-fold from 10% to 35%. This can be attributed primarily to common ion effect arising from the chloride ion that helps suppressing the salt solubility. The salt form of DOX (hydrochloride salt) exhibits a high degree of water solubility (~ 1-5 mg/mL). The high aqueous solubility pushes a large portion of DOX out of the primary emulsion into the aqueous phase during microparticle fabrication resulting in a poor loading efficiency. Presence of excess chloride ion in the external phase induces a common ion effect reducing the solubility of the salt. Addition of 0.5 to 1% NaCl in the external phase decreases solubility by common ion effect and thus improves the entrapment efficiency of doxorubicin within the microparticles. Alternatively, increasing the pH of the external aqueous phase during microparticle fabrication process up to 8-8.5 by use of a borate buffer also improved the entrapment efficiency of DOX up to 45%. The improvement can be attributed to the lower degree of ionization of DOX at pH 8.5 and hence an increase in the distribution co-efficient of DOX, facilitating more retention in the organic phase and better entrapment.

As shown in Figure V-8 the addition of NaCl also improved the entrapment efficiency of CpG which has been explained in detail in the previous chapters. The release profiles of DOX and CpG in PBS, pH 7.4 is shown in Figure V-9. It can be seen that both the compounds showed a burst effect followed by a more controlled release. The overall release of DOX was less owing to its reduced solubility at pH 7.4. However, *in-vivo* the release is expected to be higher owing to the slightly acidic conditions of the tumor environment resulting in an accelerated release.

IV. Characterization of DOX + CpG loaded PLGA Microparticles

DOX and CpG posed a challenge for co-entrapment within the same carrier due to their individual physico-chemical characteristics. Positively charged DOX and negatively

charged CpG instantly precipitated when these were mixed together to form the inner aqueous phase during microparticle fabrication. The requirement of a concentrated co-solution in the small volume of the inner aqueous phase made the process of simultaneous entrapment difficult. To overcome this limitation, we proposed the fabrication of cationic PLGA particles entrapping DOX with CpG adsorbed on the surface.

The particle size and zeta potential of the DOX-loaded cationic particles before and after modification with PEI has been shown in Table V-2. The magnitude of zeta potential of the PLGA particles prior to modification with PEI was not significantly negative. This can be attributed to the fact that during entrapment of DOX within PLGA particles, some amount of DOX also remains associated with the surface of the particles providing the initial burst release. The surface associated cationic DOX renders the particles with an overall lower magnitude of negative charge. However, it can be seen that upon PEI conjugation, the particles exhibited a distinct positive charge. It can be further observed that upon CpG adsorption on the surface, the particles revert back to being negatively charged as a result of the phosphate back-bone on CpG (Table 3).
It can be observed that after PEI modification, the particles retained 90 % of the entrapped DOX with only 10 % loss of entrapped doxorubicin during entrapment. The overall loadings of DOX and CpG are 8 µg and 5 µg respectively per mg of PLGA particles (Table V-III).

V. Therapeutic tumor challenge with A20 luciferin expressing tumor model

Figure V-10 traces the tumor growth by IVIS imaging of the untreated mice as a representative to show the increase in the luminescence intensity as a function of days post tumor challenge. The initial treatment modality involved intratumoral treatment initiation once the tumor reached at least 5mm in any direction. The tumor did not seem palpable up to day 20; however the luminescence intensity showed a progressive increase

over a period of time indicating cell proliferation *in-vivo*. The luminescence intensity showed consistency between groups with intensities in the range of 2-5 x 10^6 (photons/sec/cm^2/sr). Hence treatment was initiated on day 21 following tumor challenge. Figure V-11 traces the tumor growth amongst the 4 groups from day 1 until day 23 after treatment. It can see that the DOX + CpG group exhibited the lowest mean luminescence intensity at all the time points. Figure V-12 shows the mean tumor growth comparison prior to and after treatment in all the groups. Statistical analysis using ANOVA showed significant difference amongst groups only at day 23 following treatment. Microparticles co-loaded with DOX + CpG and particles entrapping DOX alone showed the best tumor protection amongst the 4 groups and were significantly different ($p<0.001$) from the untreated and CpG treated groups. Figure V-13 traces the survival rate amongst the 4 groups observed at day 23 after treatment (Day 44 after tumor challenge). The mice were sacrificed when the luminescence intensity hit a limiting value of 1 x 10^8 RFU and higher and visually the mice exhibited large tumors at this value.

Mice that were treated with DOX + CpG co-loaded microparticles showed 100% survival rate followed by the DOX group that showed 50% survival rate. Mice that were left untreated and those that were treated with CpG loaded microparticles showed only 25 % survival.

Although these results seemed promising, the data was not entirely conclusive as mice were susceptible to random tumor regression even without any treatment. One of the untreated mice showed sudden tumor regression after day 30 while one of the mice in the DOX group did not show tumor progression up to day 36 following tumor challenge. The tumor growth rate in all the mice was very slow with no trace of palpable solid tumors until day 20 following tumor challenge. The natural doubling rate of the tumor cells was very long making delineation between tumor groups difficult until very late in the treatment phase.

To make some sound and strong conclusions, the study was repeated with a 5-fold excess tumor cells in order to increase the tumor load at day 0 to increase the rate of tumor progression. The result of this study has been shown in Figure V-14 where the different groups have been compared prior to and following treatment. The groups showed no difference between treatments on day 7 and day 15 following treatment. The high tumor burden showed a large extent of metastasis making comparisons very difficult between groups and the inter-mouse variability was higher than the previous study.

Additionally, since the slow growing tumors were susceptible to sudden regression an exponential tumor model could not be used to compute tumor growth rate for any of the treatment groups. Additionally the model assumes a constant doubling rate and this assumption could not be held true in the case of certain mice in the groups that showed an uneven tumor progression curve.

In order to demonstrate our proof of concept for this delivery system more accurately, we decided to test the efficacy of the treatment groups in a previously established and robust tumor model with EG.7 cells.

VI. Treatment with DOX or DOX + CpG MP affords a better tumor protection in an EG.7 therapeutic tumor model

The primary objective of this study was to fabricate a microparticle based DOX + CpG combinatorial delivery system and study the ability of this treatment modality to confer anti-tumor immunity. Treatment was initiated on day 3 following tumor challenge by the subcutaneous route at the same location as the tumor challenge on the left flank. Figure V-15 traces tumor growth amongst groups' days 6, 8, 10 and 14 days following tumor challenge. At these time points, there was no significant difference between the treatment groups and the untreated mice or the mice that were treated with empty (blank) PLGA microparticles. The difference between the groups was appreciable starting day 20 onwards as seen in Figure V-16. Between days 20 and 27, microparticles loaded with

DOX alone and DOX + CpG group showed significantly smaller mean tumor volumes as compared the untreated, empty MP and CpG treated mice. Two mice from the DOX and DOX + CpG groups showed tumors that were not solid and palpable and did not progress over time indicating complete tumor regression following treatment. The remaining two mice in the group showed slower rate of tumor progression and were sacrificed by day 44 following tumor challenge.

Figure V-17 shows the survival curve for the various treatment groups. The untreated mice and mice that were treated with empty PLGA particles survived for the shortest time with median survival time of 24 days. CpG treated mice showed a median survival time of 27 days, while DOX and DOX + CpG group showed the best protection amongst the four groups with median survival time of 47 days and 50 % survival rate at day 47 following tumor challenge.

VII. DOX + CpG MP affords better tumor protection upon tumor re-challenge

The surviving mice in the DOX and DOX + CpG group were re-challenged with EG.7 tumor cells to examine the effects of any immunogenic memory that was established with the prior treatment. The mice were challenged on the opposite flank to the treatment, to ensure complete isolation from any residual treatment effects from localized microparticles. Figure V-18 shows the results from the tumor re-challenge study. One of the two surviving mice that were treated with DOX microparticles showed spontaneous tumor out-growth , while the other showed a slightly retarded growth but progressively grew over time and both the mice succumbed by days 33 and 39 respectively following tumor re-challenge. Mice that were treated with DOX + CpG microparticles showed no incidence of tumor until day 35 and showed an enhanced survival up to day 55 following tumor challenge. These results indicated the possibility of a systemic immune response induction triggered by CpG conferring enhanced tumor protection upon tumor reoccurrence.

In order to elucidate this response more clearly with a larger sample size, a model to study the induction of systemic immune response was designed that is described in the next section.

VIII. Systemic Immune Response Model

Mice were tumor challenged on left and right flank simultaneously with 5 x 10^6 EG.7 tumor cells suspended in 100 µL PBS. Treatment was initiated on day 3 on the left flank only by subcutaneous administration of either DOX or DOX + CpG PLGA microparticles. One group was mice were left untreated to serve as control. Tumor growth was monitored on both the flanks and tumor volume was computed. Survival of the mice was also monitored and the mice were sacrificed if the tumor dimension in any direction in either tumors was more than 20 mm. Each group consisted of 4 mice.

V. Results-systemic immune response model

The result from this study is shown in Figure V-19. The top graph represents the tumor volume comparison amongst groups on the left flank, where the mouse was treated locally. It can be seen that mice treated with microparticles co-loaded with DOX + CpG group showed the slowest tumor progression amongst the three groups at the treatment site. One out of the 4 mice showed complete regression of tumor by day 20 post-tumor challenge. The graph at the bottom shows the comparison of tumor volumes on the right flank that was not subject to any direct local treatment. The mice that were treated with DOX + CpG co-loaded microparticles displayed the lowest mean tumor intensity amongst the three groups. However, the tumor growth volumes between the three groups were not significantly different from each other.

However, the smaller cumulative tumor burden (comparing the tumor volumes on both the flanks) resulted in the mice treated with the DOX + CpG microparticles showing an overall enhanced survival. The mice in this group showed a median survival

time of 20 days post tumor challenge, while the DOX and untreated mice all succumbed by day 13 (Figure V-20).

Discussion

The past three decades have seen significant advances with respect to chemotherapy for the treatment of various types of cancer and the last decade has witnessed the emergence of immunotherapy as an alternative approach to cancer treatment. The next direction in tumor therapy is inching towards harnessing of combinatorial carrier that is superior to either of the aforementioned stand-alone therapies. Casares et al. showed the potential for chemotherapy to induce *in-situ* vaccination (141). Taking this idea forward, Levy et al. showed that a therapy comprising of DCs with systemically administered cyclophosphamide (CTX) was a potent vaccine as compared to a treatment with DCs alone (144). They proposed that the extended benefit was a result of CTX being able to retard the tumor allowing time for a T cell immune response to occur.

Giving this combinatorial therapy a different direction, we proposed that a combination of Doxorubicin (DOX) and CpG when administered together will accentuate the benefits of chemotherapy induced cell death. Microparticles entrapping either DOX or CpG or both were fabricated using an optimized double emulsion solvent evaporation technique. PLGA 75:25 was the polymer of choice given its hydrophobicity and degradation profile. Van et al. (146) showed a novel method based on nonresonant confocal Raman spectroscopy and imaging to study the degradation profile of PLGA 50:50 microparticles *in-vivo*. They found that the degradation of the microparticles was accelerated in the *in-vivo* conditions within the macrophages aided by the presence of ester catalytic enzymes within the phagosomes. Particles showed up to 40-50 % degradation within 2 weeks. Our study is aimed at delivering the entrapped components in a controlled manner up to 25-30 days. This is the approximate life-span of DCs and

macrophages. These aforementioned results coupled with our end goal made PLGA 75:25 the polymer of choice for this proof of concept study. Optimizing formulation variables and inclusion of additives helped improve entrapment efficiencies. This significantly improved the process efficiency of microparticle fabrication.

The fabrication of cationic PLGA microparticles entrapping DOX allowed CpG loading thus facilitating the fabrication of a co-delivery carrier without an untoward physico-chemical interaction between DOX and CpG. For the initial studies, we chose to use an A20 therapeutic tumor model. A20 is a B cell lymphoma cell line that owns both characteristics of tumor cells and B cells. Like B cells, the tumor cells possess TLR9 receptor (143). It has been shown that the up-regulation of the expression of MHC class II molecules and co-stimulatory molecules such as CD80 and 86 might enhance the antigen-presenting function of A20 B lymphoma cells enabling these cells to function as antigen-presenting cells *in-vivo* (143). As described in the earlier chapters, a CpG motif has been shown to be a potent immune adjuvant for amplifying B cell and T cell responses to poorly immunogenic antigens. Considering the above information we used the A20 cell model to investigate, whether the immunogenicity of mouse B lymphoma cells could be potentiated by CpG alone or in combination with DOX. Our results indicated that treatment with CpG alone did not render any tumor protection and the mice behaved similar to the untreated group of control mice. It has been shown that CpG can induce the proliferation of murine and human B cells. However, Chen et al. showed an improvement in the antigen-presenting ability of A20 tumor cells when they were incubated with CpG *in-vitro* (143). A study by Levy et al. using CpG as a therapeutic vaccine in an A20 tumor model showed only transient tumor regression with CpG therapy. Moreover, CpG in this study was administered intratumorally every alternate day with a total dose of 500 µg over five administrations (136, 142). Our study consisted of a single administration of 30 µg of CpG microparticles. The lower dose of CpG

coupled with its proliferative activity on A20 cells failed to elicit any anti-tumor immunity.

However, when CpG was administered with DOX, the co-delivery carrier was capable of conferring some degree of tumor protection with enhanced mouse survival rate. The molecular interaction between dying tumor cells (chemotherapeutic component derived) and induction of cell-mediated immunity by the presence of CpG results in a potent activation of T cells. This provided enhanced tumor protection and resulted in slower progression of the tumor cells. Immunogenic cell death is shown to induce the early membrane exposure of calreticulin, which determines phagocytosis of dying tumor cells by DCs (138, 147). CpG when present locally at the same microenvironment functions as an effective adjuvant for antigen immunization by eliciting a potent Th-1 type immune response for augmenting antigen-specific cytotoxic T cell activity.

Given the limitations of the above model as exemplified in the results section, we hoped to demonstrate this proof of concept more lucidly in another tumor model like EG.7 that is not subject to proliferation in the presence of CpG. The preliminary results from this study were promising as the DOX + CpG treated mice showed improved survival time, slower tumor growth and induction of immunogenic memory. It was interesting to note that DOX-loaded PLGA microparticles also showed potential to improve survival time in tumor challenged mice. Although the chemotherapeutic effects of DOX-loaded micro/nanoparticulate systems have been demonstrated *in-vitro,* such studies have been very rarely carried out in an *in-vivo* tumor model. A controlled delivery of chemotherapeutic agent is essential to overcome multi-drug resistance and improve patient compliance. Our results indicate the potential for a microparticulate delivery system of doxorubicin for chemotherapy. These results however need more studies for validation of this concept.

A repeat study was carried out to establish systemic anti-tumor effect of DOX + CpG. The underlying hypothesis of such a model was that systemic immune response

generated will increase the population of CTLs. Enhanced CTL activity can eradicate a distant tumor (right flank in the model) along with inducing anti-tumor immunity locally at the site of tumor challenge and treatment. Additionally, the distribution half-life of DOX is less than 3 hours limiting the possibility of DOX released from the subcutaneously administered PLGA microparticles accumulating in the distant tumor on the opposite flank. The results from this study reiterated the anti-tumor activity of DOX + CpG at the site of tumor challenge and treatment. The direct apoptotic effect of DOX on tumor cells at the site of treatment, immediately stimulates the cascade of immunostimulatory anti-tumor responses in conjunction with CpG. However, this model failed to elicit the envisaged systemic immune response. The reasons for this could perhaps relate to the design of this model. The primary reason was a high cumulative tumor burden that increases the pressure on the immune system. The high tumor burden does not allow enough time for the development of an anti-tumor immune response. Additionally, prophylactic studies have shown the requirement of a 14-day window to detect the presence of antigen-specific cytotoxic CD8+ T-lymphocytes that are markers for cell-mediated systemic immunity. A lag or a delay in the second challenge may present a better model to elucidate the pathway more clearly. The mice treated with DOX + CpG co-loaded microparticles did exhibit smaller mean tumor volumes at the distant tumor location. However they were not significantly distinguishable from DOX microparticles treated and untreated mice requiring modification of the model structure and a repeat study.

Our results indicate that doxorubicin microparticle carrier system holds promise to serve as potent chemotherapeutic system for cancer treatment. Such a delivery system also mitigates tissue toxicity and cardiotoxicity issues associated with solution based formulations of DOX that require repeated administration. It is important to underscore from these studies that microparticles co-loaded with DOX + CpG system showed great potential to induce a symbiotic anti-tumor response comprising of a direct apoptotic

component and a derived cellular immunity component. In general, we may speculate that chemotherapy synergizes with immunotherapy *in-vivo* by disrupting tumor cells and paves the way for enhanced T cell responses.

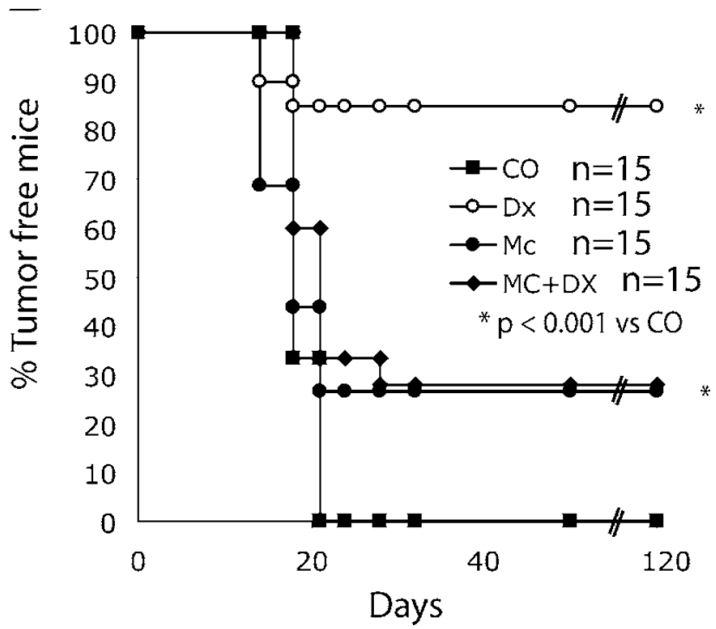

Figure V-1: Preliminary literature data indicating the immunogenic potential of anthracycline class of chemotherapeutic agents like Doxorubicin. Reproduced with permission from [138] Copyright© The Rockefeller University Press.

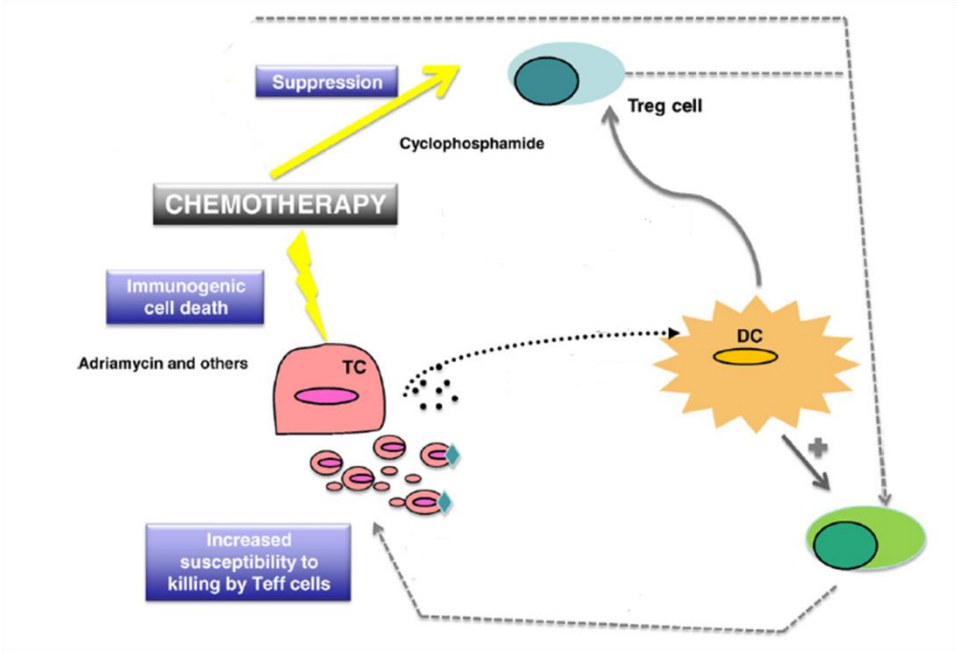

Figure V-2: Schematic representation of immune cascade stimulated upon tumor cell apoptosis by chemotherapeutic agents.

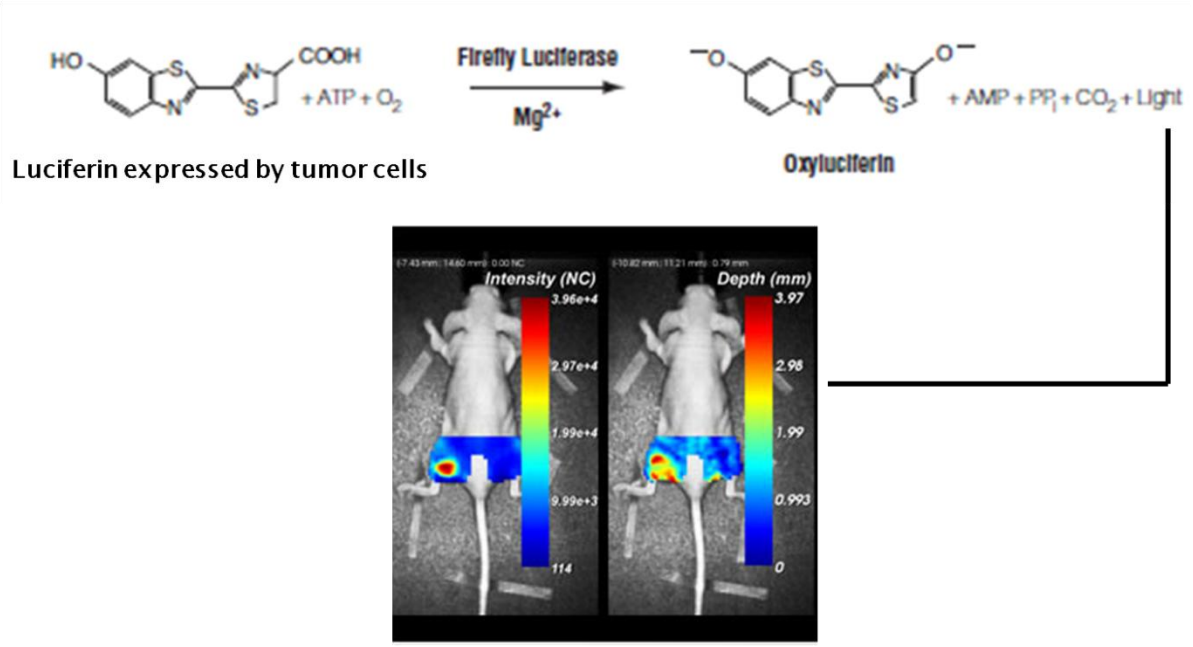

Figure V-3: A20 B-cell lymphoma therapeutic tumor model. A20 tumor cells are stably transfected to express luciferin. As these cells continue to proliferate *in-vivo* the luciferin concentration increases as the tumor volume increases. Luciferase substrate injected prior to tumor imaging catalyzes the conversion of luciferin to oxyluciferin that is accompanied by the emission of photon of light that is measured by a luminometer by the *in-vivo* imaging system (IVIS). The luminescence intensity captured is a function of substrate concentration that is a reflection of tumor volume.

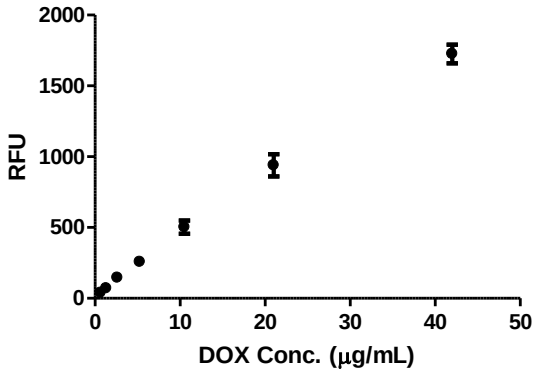

Figure V-4. Standard Curve of Doxorubicin HCl in DMSO analyzed by fluorescence spectroscopy. Data is represented mean ± standard deviation (*n = 3*).

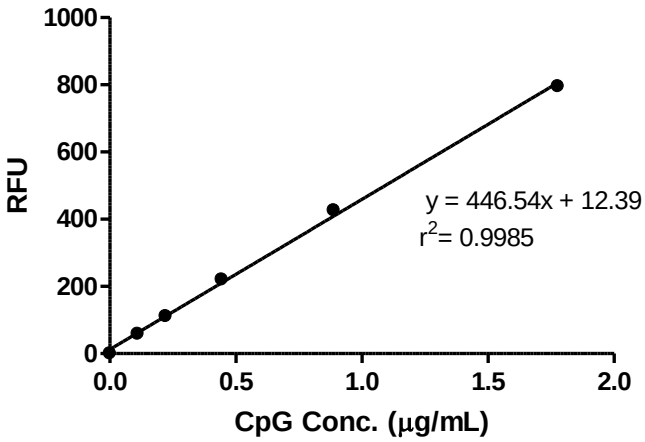

Figure V-5: Standard curve of CpG analyzed by Oligogreen assay for ssDNA. Data is represented mean ± standard deviation (*n = 3*).

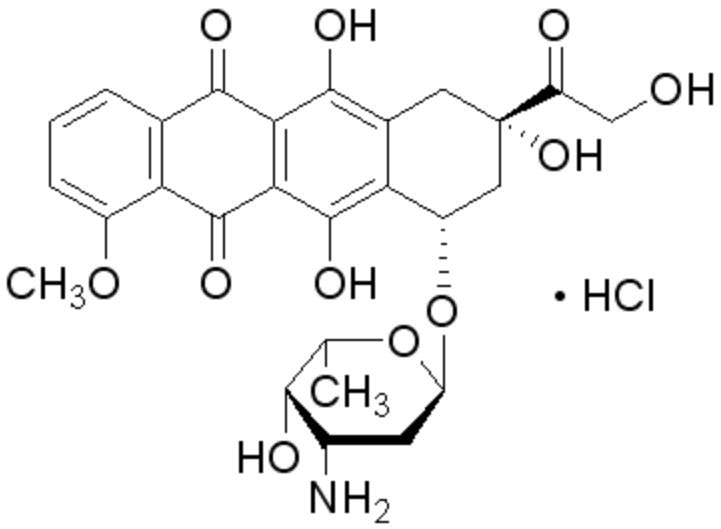

Figure V-6: Structure of Doxorubicin HCl.

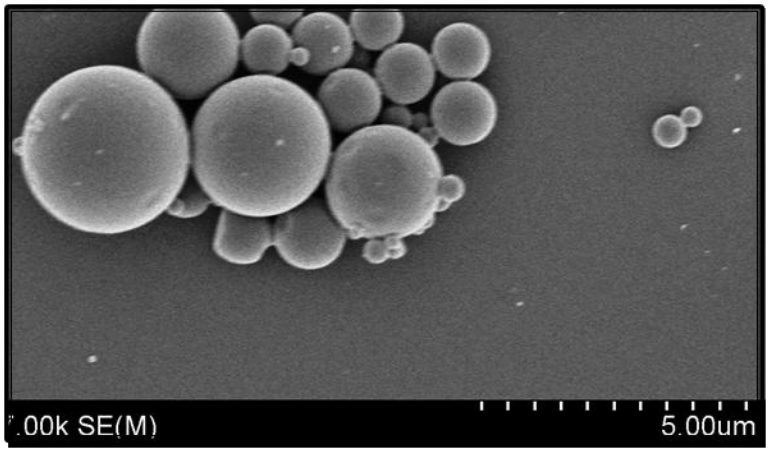

Figure V-7: SEM image of DOX-loaded PLGA 75:25 (MW 30000 Da) MP fabricated using double emulsion solvent evaporation technique.

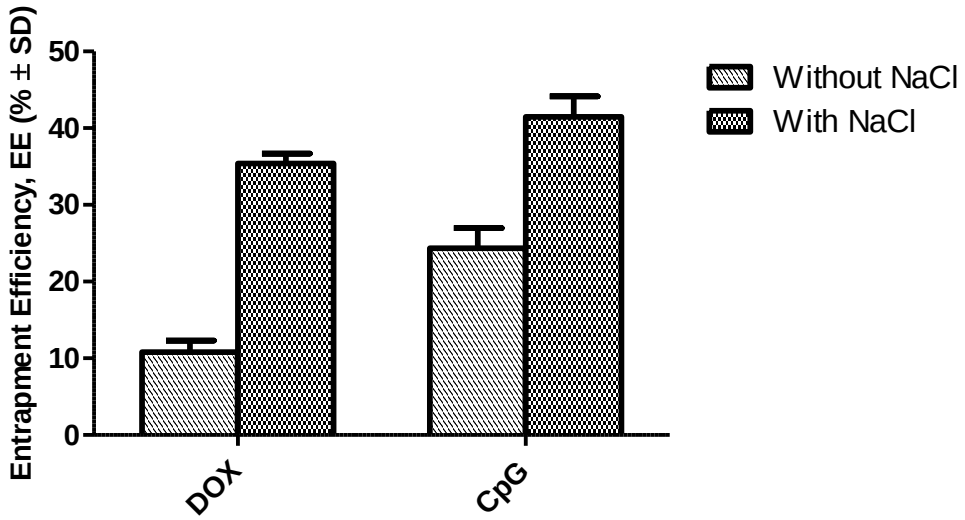

Figure V-8: Effect of addition of NaCl on entrapment efficiencies of DOX and CpG in the single component PLGA 75:25 (MW 30000 Da) MP. Data is represented as mean ± standard deviation (*n = 3*).

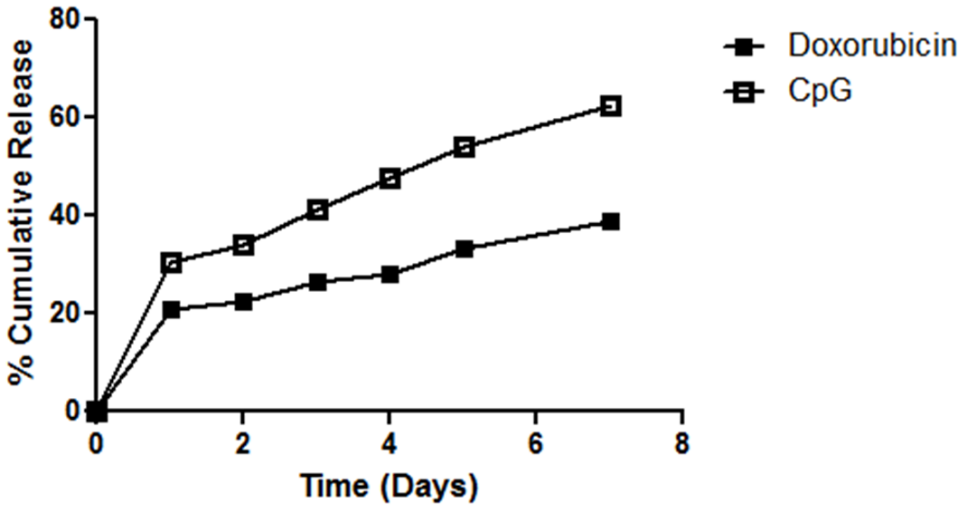

Figure V-9: Release profiles of DOX and CpG in PBS, pH 7.4 from the respective single component PLGA 75: 25 (MW 30000 Da MP.

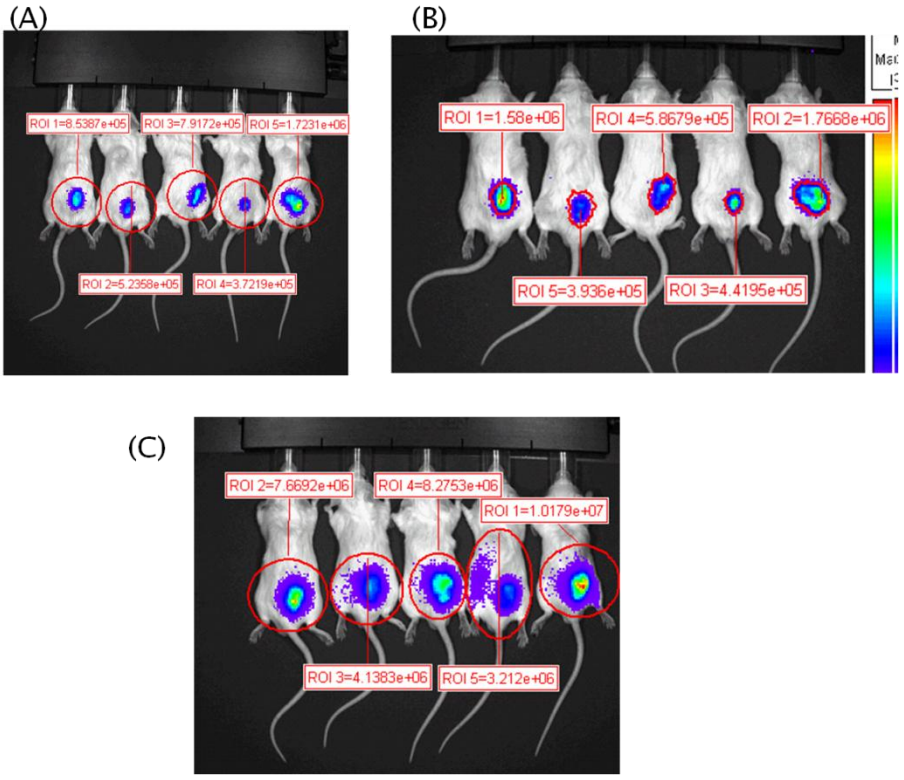

Figure V-10: Tumor growth progression (luminescence intensity) traced by IVIS following tumor challenge on (A) day 6, (B) day 9 and (C) day 15 following tumor challenge prior to any treatment initiation.

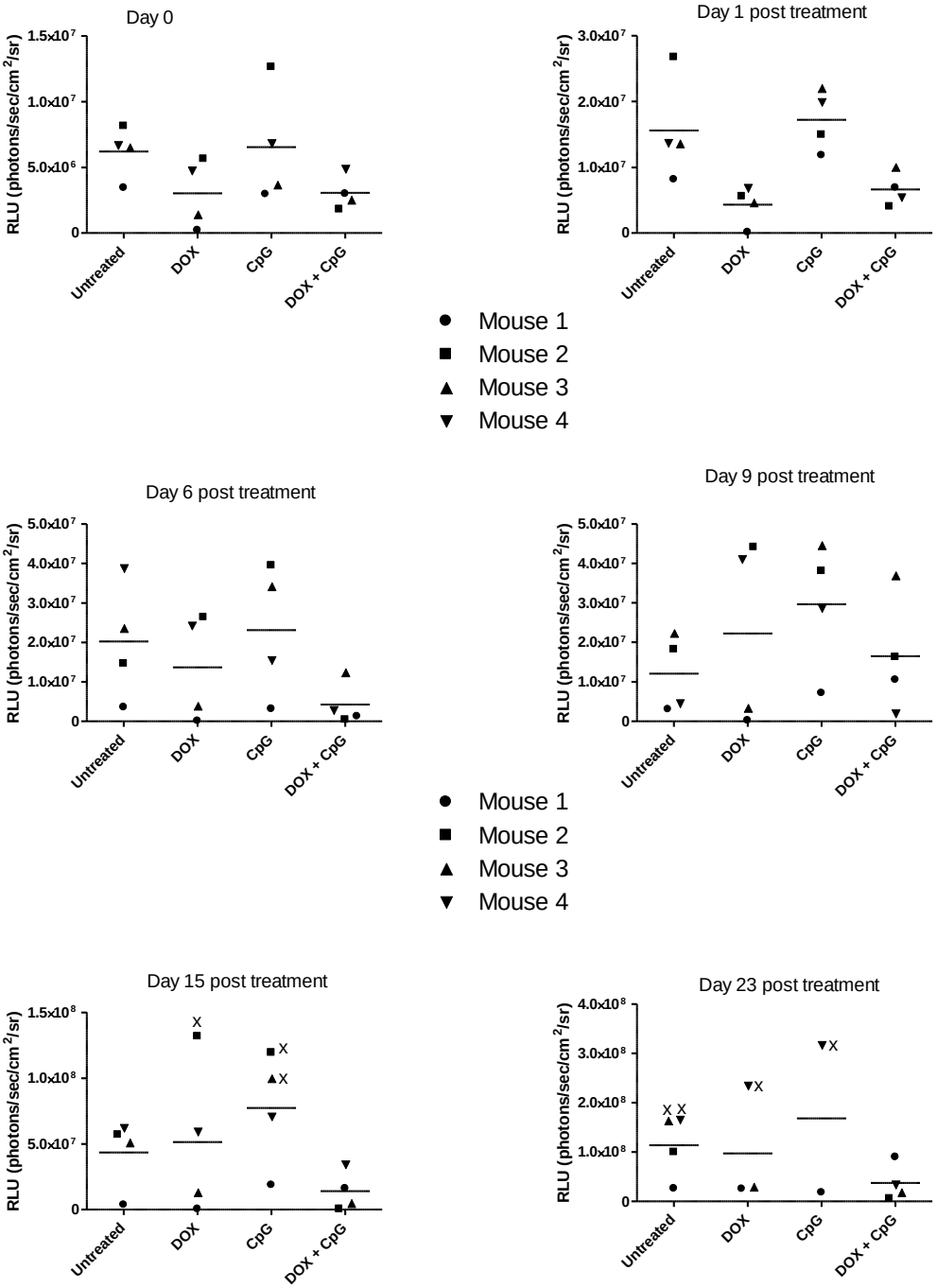

Figure V-11: Tumor growth curve comparison of the various PLGA 75:25 (MW 30000 Da) MP treatment groups monitored over time following treatment initiation.

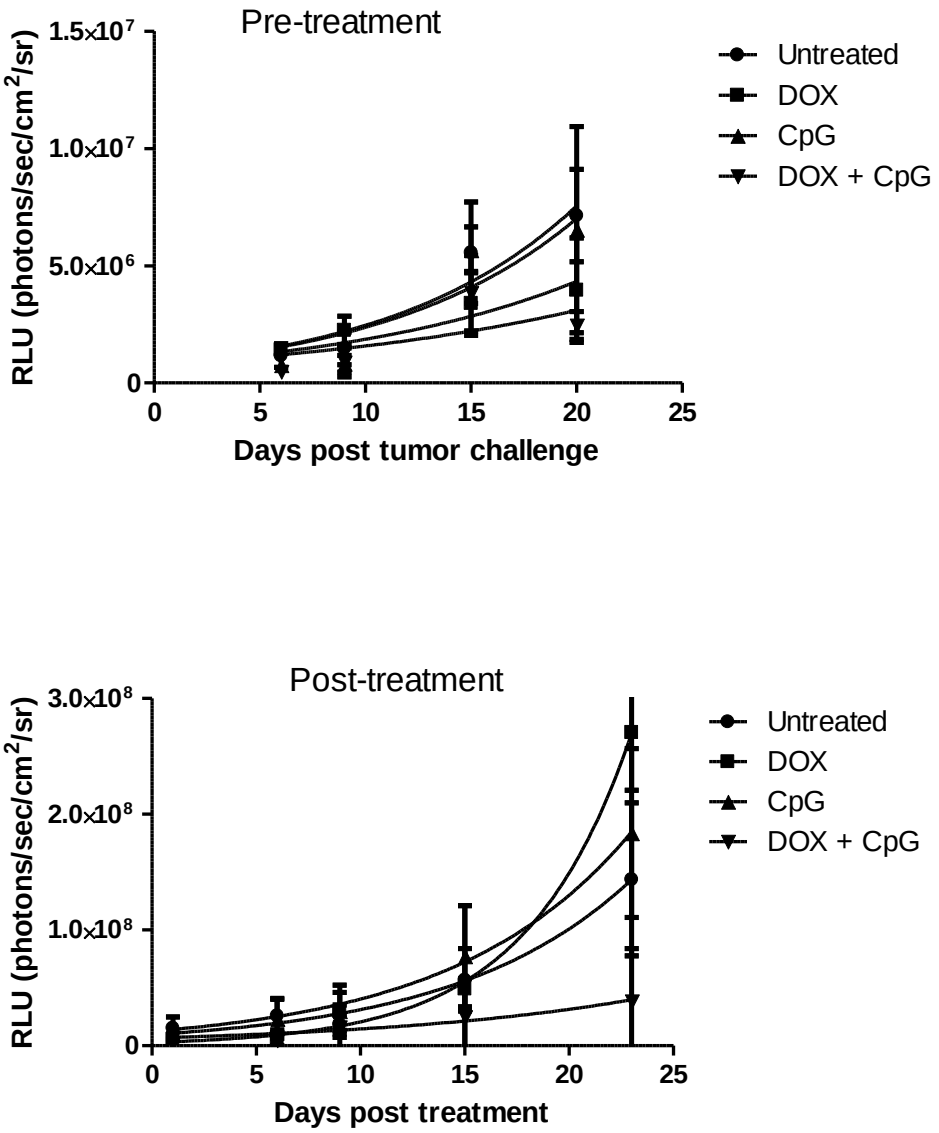

Figure V-12: Mean tumor growth comparison amongst various PLGA 75:25 (MW 30000 Da) MP treatment groups' pre and post treatment. Data is represented as mean ± standard deviation (*n = 3*).

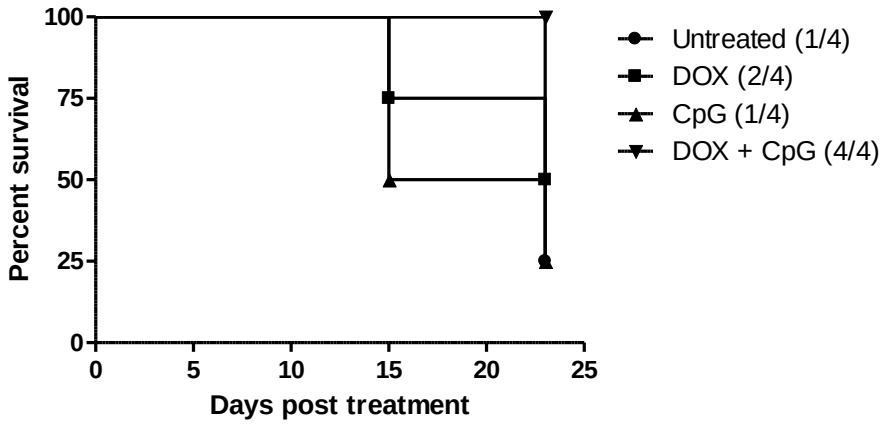

Figure V-13: Survival proportions amongst various PLGA 75:25 (MW 30000 Da) MP treatment groups in an A20 B-cell lymphoma therapeutic tumor model. (Numbers in parentheses indicate the number of surviving mice at the end of day 23 following treatment; day 44 following tumor challenge. (*n = 4*).

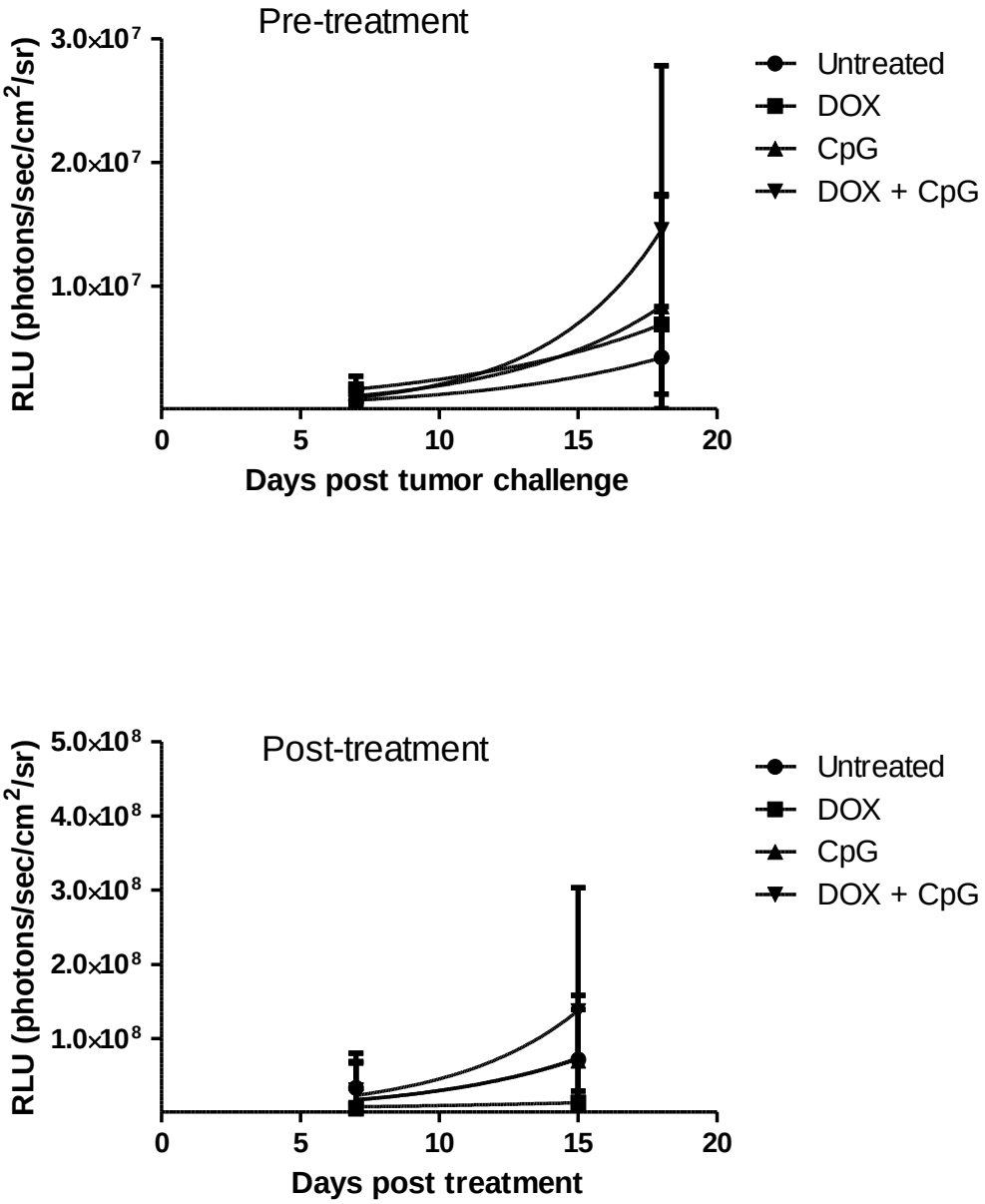

Figure V-14: Mean tumor growth comparison amongst various PLGA 75:25 (MW 30000 Da) MP treatment groups pre and post treatment in a repeat study in an A20 B-cell lymphoma tumor model. Data is represented as mean ± standard deviation (*n = 4*).

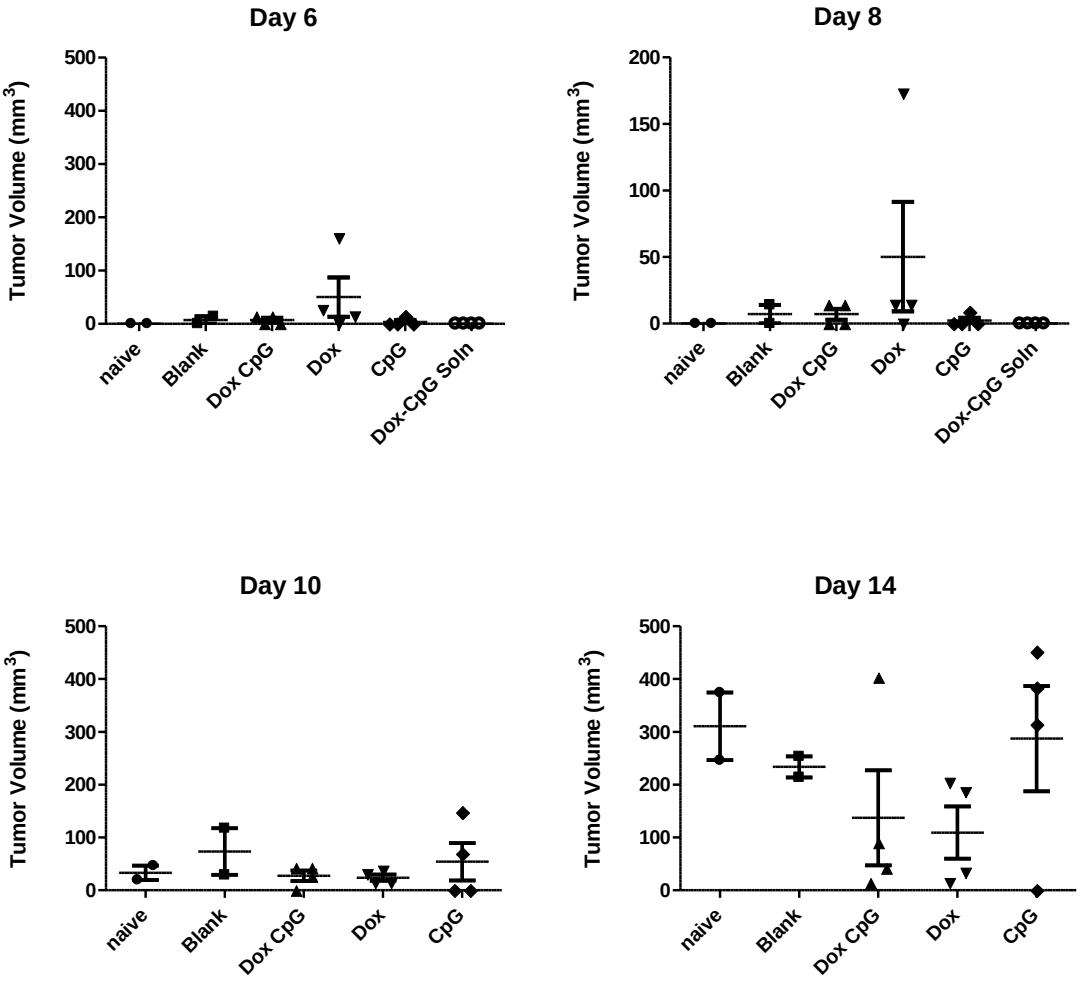

Figure V-15: Tumor growth comparison amongst groups at earlier time points following tumor challenge with EG.7 tumor cells. (Treatment was initiated 3 days after tumor challenge). Data is represented as mean ± standard deviation, *n = 4*. (No statistically significant difference was observed amongst groups until day 14 post tumor challenge, $p > 0.01$).

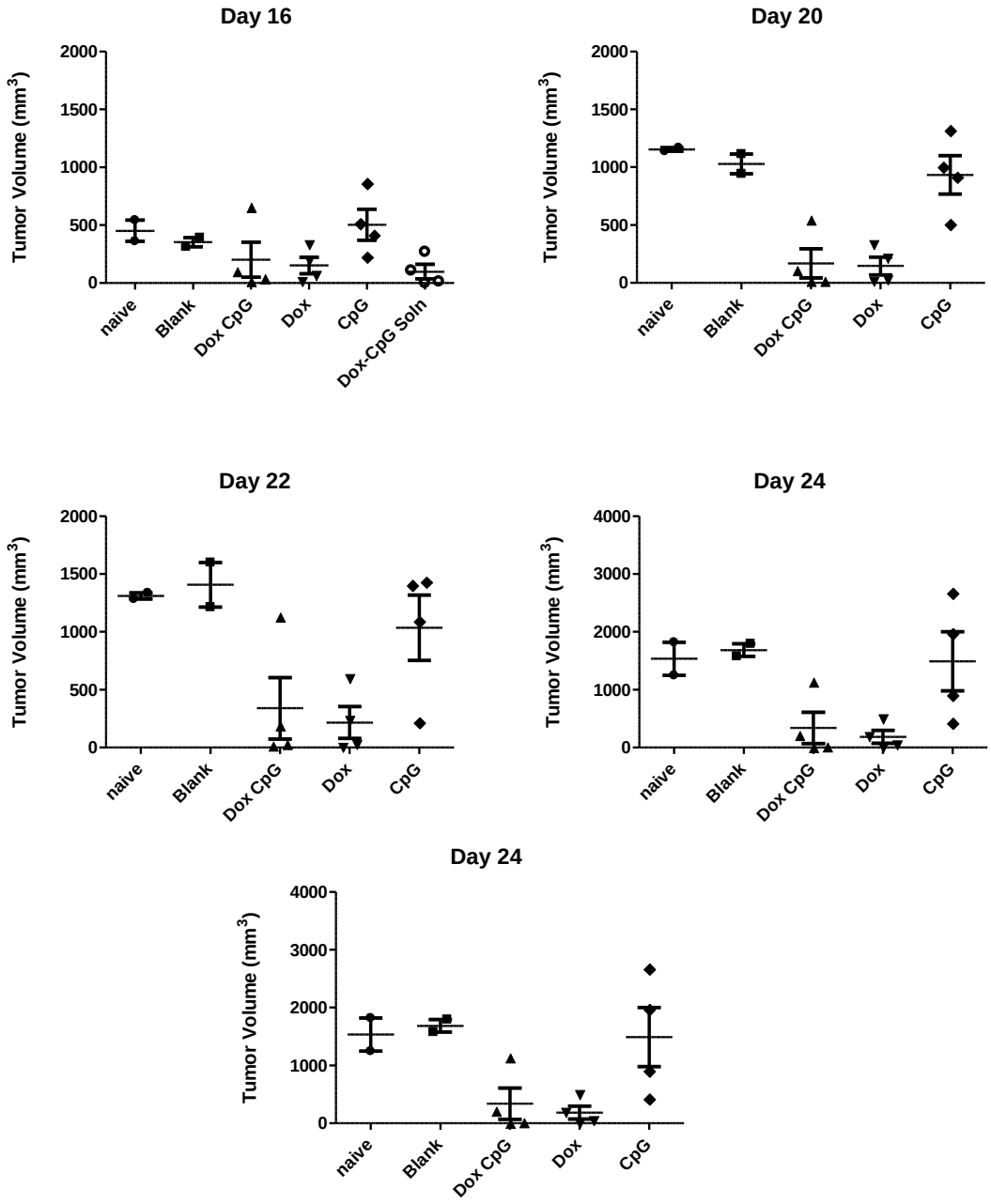

Figure V-16: Comparison of tumor challenge amongst various treatment groups at later time points post tumor challenge with EG.7 tumor cells. (Treatment was initiated 3 days post tumor challenge). Data is represented as mean ± standard deviation, *n = 4*. (Statistically significant difference was observed amongst groups post 20 onwards following tumor challenge, $p < 0.01$).

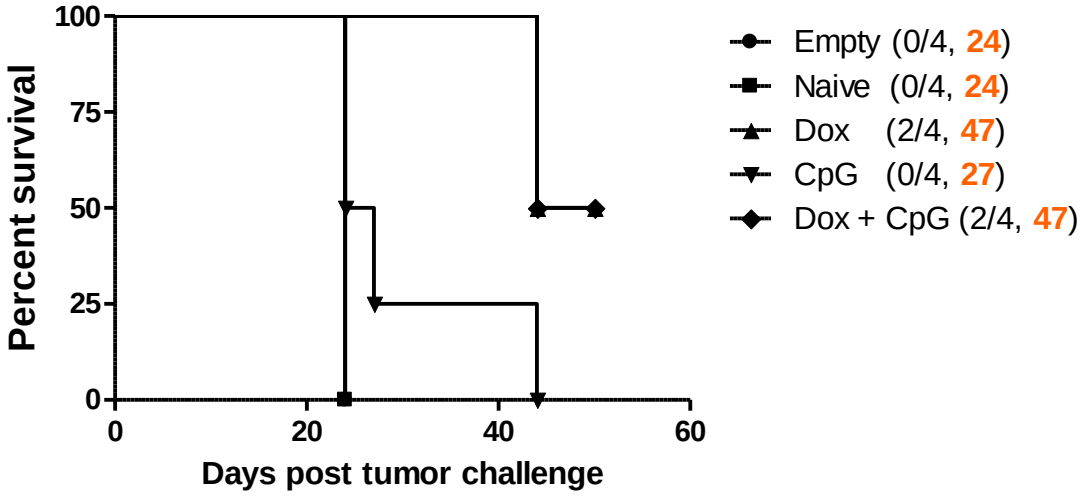

Figure V-17: Effect of various PLGA 75:25 (MW 30000 Da) MP treatment groups on the survival proportion of mice following tumor challenge with EG.7 therapeutic tumor challenge. (The numbers in the parentheses indicate median survival time of mice in each group, *n = 4*).

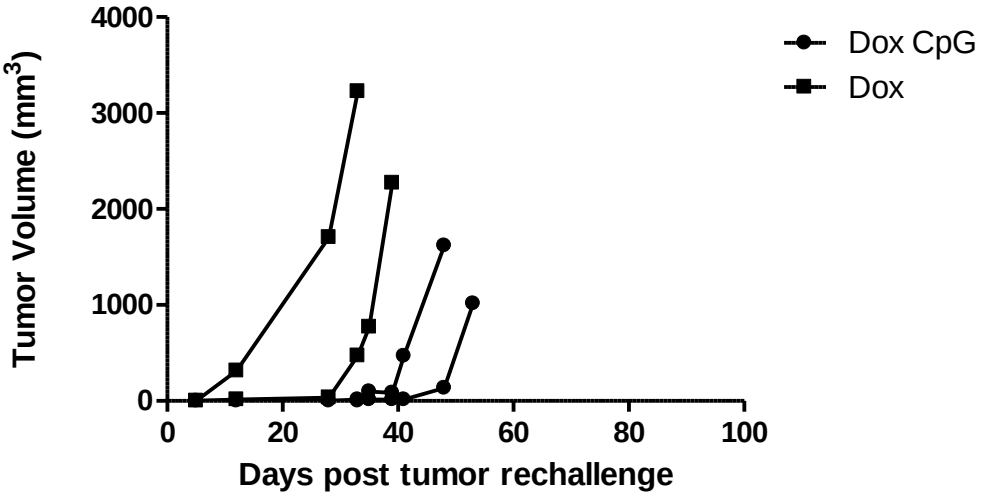

Figure V-18: Tumor growth progression upon EG.7 tumor re-challenge in the mice surviving from the DOX and DOX + CpG PLGA MP treatment groups, *n = 2*.

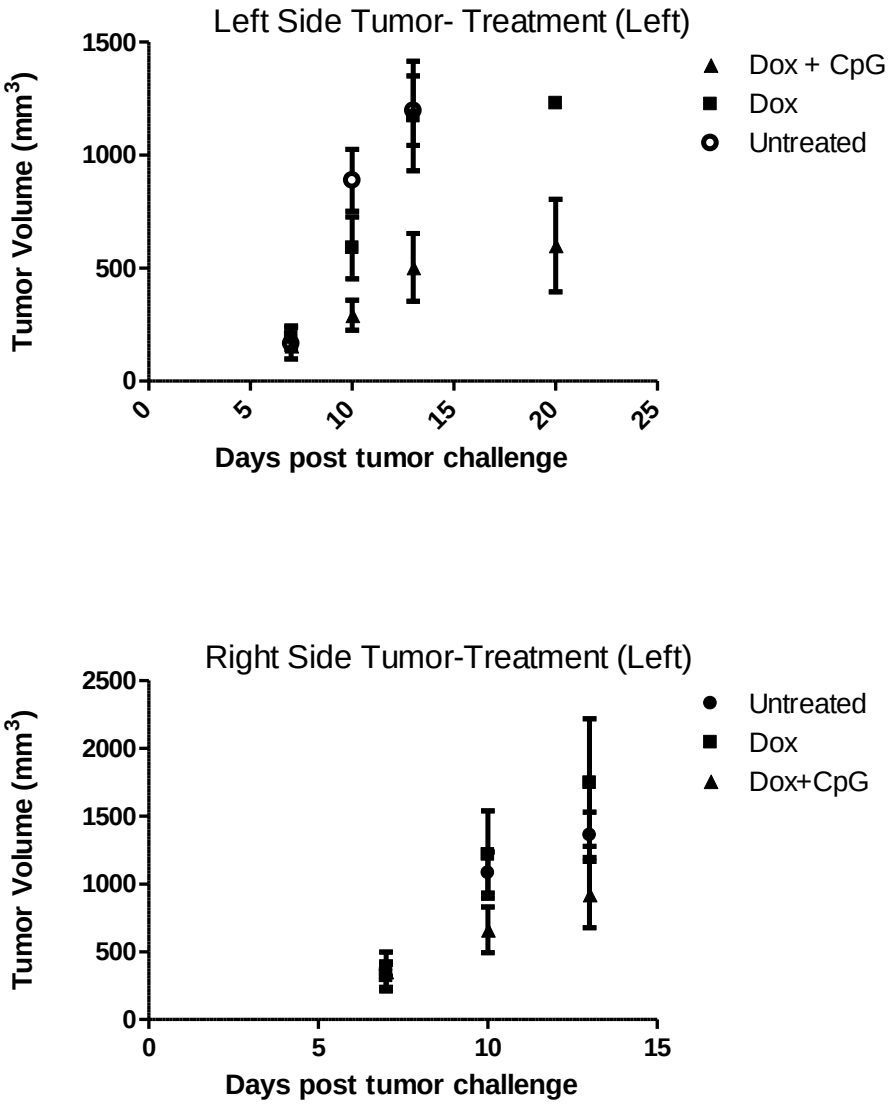

Figure V-19: Tumor growth comparison of a locally treated tumor (upper) and a distant tumor (lower) in a response to a systemic immune response tumor model using an EG.7 tumor cells using PLGA 75:25 (MW 30000 Da) MP. Data is represented as mean ± standard deviation (*n = 4*).

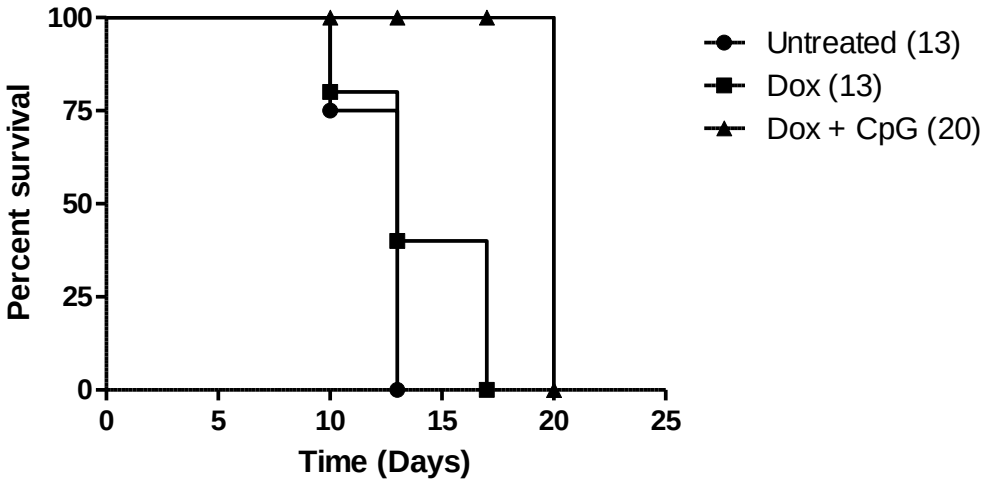

Figure V-20: Survival proportions of mice following response to a systemic immune response tumor model using an EG.7 tumor model with various PLGA 75:25 (MW 30000 Da) MP based treatment groups.

Table V-1: Entrapment Efficiency of various PLGA 75:25 (MW 30000 Da) MP based treatment groups

Formulation	**Entrapment Efficiency (%)**	**Average Loading (µg/mg PLGA**
DOX	35	9 µg/mg PLGA
CpG	41	5 µg/mg PLGA

Table V-2. Characterization of DOX-loaded PLGA85:15-carboxylic acid terminated (MW 40000 Da) MP before and after PEI conjugation

Particle Size (µm)		**Zeta Potential (mV)**	
Before PEI	After PEI	Before PEI	After PEI
1.3 ± 0.6	2.5 ± 0.6	-4.15 ± 3.4	+ 21.8 ± 4.1

Table V-3. Characteristics of DOX-loaded cationic PLGA PEI particles after CpG adsorption. PLGA used was 85:15- carboxylic acid terminated (MW 30000 Da) grade.

Particle Size (µm)	**Zeta Potential (mV)**	**Average DOX (µg/mg of PLGA)**	**Average CpG (µg/mg of PLGA)**
2.5 ± 0.6	-20.6 ± 2.8	12	30

CHAPTER VI: CONCLUSIONS AND FUTURE RECOMMENDATIONS

The goal of this research has been to improve upon existing treatment strategies for cancer therapy. The three widely used therapeutic modalities until recently has been surgery, radiotherapy and chemotherapy. While some of these modalities are more successful than others, important improvements in their research concepts for widespread applications are needed. Immunotherapy is the newest and one of the most exciting of the therapeutic modalities in the treatment of clinical oncology and therefore formed the subject of our study. Tumor associated antigens are capable of eliciting humoral and cell-mediated immune responses whose possible manipulation to achieve tumor rejection is of considerable clinical interest.

PLGA microparticles are ideal carriers for tumor antigen as PLGA MP of appropriate size are efficiently taken up by mouse and human DCs, and they are slowly hydrolyzed so that prolonged antigen presentation ensues. However, vaccines based on antigens alone lack the ability to optimally activate dendritic cells (DCs) and are notoriously poor at stimulating strong protective immune responses. We have previously shown that co-delivering a toll-like (TLR9) adjuvant like CpG elicits a significantly higher cytotoxic T cell response that is crucial for tumor eradication. With this as the basis of our vaccine delivery system, our goal is to further augment the strength of the immune response and the duration of protection. To do this, we aimed to combine the advantages of particulate delivery system and Th-1 polarizing TLR adjuvants like CpG and poly I:C. Activation of the TLRs leads not only to the induction of inflammatory responses but also to the development of antigen- specific adaptive immunity.

In chapter III, we examined the feasibility of formulation of co-delivery carriers for the simultaneous delivery of a model antigen ovalbumin (OVA) and a TLR3 adjuvant; poly I:C or a TLR9 adjuvant; CpG. Given the challenges in entrapping

hydrophilic components like these in hydrophobic PLGA carriers, we chose to employ a double emulsion solvent evaporation technique for the fabrication of these carriers. Optimizing formulation variables like polymer and surfactant concentration and minimizing the internal aqueous phase volume improved the entrapment efficiencies of each of these components while maintaining the carriers in a size range suitable for phagocytosis by the immune cells. Inclusion of additives like sodium chloride for adjustment of osmolarity improved the process efficiency further. Our study demonstrated the feasibility of fabricating a co-delivery vehicle co-entrapping an antigen and poly I:C as the adjuvant for the first time. As the next step, we sought to determine, whether different TLRs cooperate in DC activation and mount a stronger immune response. While, fabrication of co-delivery systems was relatively easier, the development of a tri-component carrier delivering OVA, poly I:C and CpG posed several challenges. Limitations included repulsive electrostatic forces between the two adjuvants and lack of enough literature studies to serve as a resource to initiate the fabrication of such a system. After several attempts, a novel tri-component carrier was fabricated that entrapped OVA and poly I:C on the inside of the particles and following surface modification had CpG adsorbed on the external surface. Our studies thus far indicated that microparticulate vaccine carriers can be manufactured with relative ease and could serve as promising delivery systems for cancer immunotherapy.

After demonstrating the fabrication of these carriers, we next studied the ability of these carriers to find applications in prophylactic and therapeutic tumor treatment models. OVA when co-entrapped with poly I:C or CpG showed several-fold stronger antibody and cytotoxic T cell responses in comparison to use of OVA alone. Although there was no significant apparent synergism between poly I:C and CpG in mounting a T cell response, the two adjuvants when administered together in the tri-component carrier induced a synergistic antigen-specific antibody response in our prophylactic lymphoma tumor model. Such a response could hold great promise for treatment of colon and

colorectal and several other cancers where the tumor antigen is expressed on the cell surface as opposed to being secreted. A strong antigen-specific antibody response induces complement activation by the antibody secreting B-cells causing tumor cell lysis. An example of such a surface associated antigen is the MUC1 peptide. Mucin 1 (MUC1) is a cell surface associated mucin, the protein part of which is encoded by the *MUC1* gene in humans. Over expression of this protein is often associated with colon and other forms of cancer. Such a prophylactic vaccine can serve as maintenance therapy following cancer treatment either by chemotherapy or by surgical route. The systemic immune response mounted is capable of inducing immunogenic memory preventing tumor relapse. The dual and the tri-component carriers also showed slower tumor progression in prophylactic and therapeutic tumor setting. The carriers also showed strong evidence for the generation of anti-tumor immunogenic memory. Our PLGA microparticle based vaccine system, in the form of antigen OVA with poly I:C and/or CpG, is a novel system aimed at exploiting the maximum benefits of each component in the carrier.

The basic assumption in cancer treatment is that cure requires the destruction or removal of all malignant cells or at least reduction to a level that can be controlled by the host's defense mechanisms. While immunotherapy continues to grow as a potential treatment strategy for cancer, cancer biologists advocate the use of combination therapy as the ultimate treatment modality to attain this objective of complete cancer cure. Studies have shown that existing drugs can capitalize on and manipulate natural anti-tumor immunity and thus be used for combinatorial tumor therapy. With this as our underlying goal, Chapter V focuses on the fabrication of such a combinatorial chemo-immunotherapeutic carrier. We chose doxorubicin HCl (DOX) as the chemotherapeutic agent owing to its proven efficacy in cancer clinics and CpG as the immunotherapeutic component owing its proven immunostimulatory ability. Given the success of PLGA particulate carriers in our study and several others, we pursued with the same delivery system for this study too. We showed that DOX and DOX + CpG co-loaded

microparticles showed promise for therapeutic cancer treatment and the latter strategy holds promise for eliciting a systemic anti-tumor immune response and immunogenic memory.

In summary, the current study has laid an interesting premise for the use of immunotherapy using a combination of antigen and TLR adjuvants alone or in conjunction with chemotherapy as a treatment strategy for tumor therapy. The further steps in this direction would be to evaluate other TLR ligands like imiquimod (TLR7) that can synergize with TLR3 and TLR9 to promote a stronger anti-tumor activity. In addition to these, it would be critical to examine the biodistribution of these particulate carriers following vaccination by various routes and investigate dose-response immune kinetics. The current study used an aggressive tumor challenge modality to study the efficacy of the various treatment groups. A future study can involve tumor challenge at varying tumor burden to delineate between treatment groups more clearly and help design treatment strategy based on tumor staging.

Rational combinations of agents will require elucidation of their mechanism of action in order to choose the agents in a precise manner. Careful preclinical evaluation in well characterized animal models will be necessary to screen combinations before translating these results in a real clinic. In conclusion, the next decade will be the time to test and optimize these combinations to maximize efficacy to find a potent cure for cancer.

REFERENCES

1. Cancer Facts & Figures 2009, American Cancer Society, Atlanta, 2009.

2. Facts & Statistics, 2009, American Brain Tumor Association, Des Plaines, IL, 2009.

3. R. Goforth, A.K. Salem, X. Zhu, S. Miles, X.Q. Zhang, J.H. Lee, and A.D. Sandler. Immune stimulatory antigen loaded particles combined with depletion of regulatory T-cells induce potent tumor specific immunity in a mouse model of melanoma. Cancer Immunology, Immunotherapy. 58:517-530 (2009).

4. Y. Krishnamachariand A.K. Salem. Innovative strategies for co-delivering antigens and CpG oligonucleotides. Advanced Drug Delivery Reviews. 61:205-217 (2009).

5. J.N. Blattmanand P.D. Greenberg. Cancer immunotherapy: A treatment for the masses. Science. 305:200-205 (2004).

6. E. Brusamolinoand A.M. Carella. Treatment of refractory and relapsed Hodgkin's lymphoma: facts and perspectives. Haematologica-the Hematology Journal. 92:6-10 (2007).

7. D. Steinbach, J. Lengemann, A. Voigt, J. Hermann, F. Zintl, and A. Sauerbrey. Response to chemotherapy and expression of the genes encoding the multidrug resistance-associated proteins MRP2, MRP3, MRP4, MRP5, and SMRP in childhood acute myeloid leukemia. Clinical Cancer Research. 9:1083-1086 (2003).

8. X.Q. Yu, C.C. Xue, G. Wang, and S.F. Zhou. Multidrug resistance associated proteins as determining factors of pharmacokinetics and pharmacodynamics of drugs. Current Drug Metabolism. 8:787-802 (2007).

9. D.M. Shepard, M.C. Ferris, G.H. Olivera, and T.R. Mackie. Optimizing the delivery of radiation therapy to cancer patients. Society for Industrial and Applied Mathematics (Siam) Review. 41:721-744 (1999).

10. S.L.P.a.S.A. Plotkin. A short history of vaccines. In S.A.P.a.W.A. Orenstein (ed.), Vaccines, WB Saunders Company, Philadelphia, 2004, pp. 1–15.

11. R.J. Prestwich, F. Errington, P. Hatfield, A.E. Merrick, E.J. Ilett, P.J. Selby, and A.A. Melcher. The immune system - is it relevant to cancer development, progression and treatment? Clinical Oncology. 20:101-112 (2008).

12. C. Janeway. Immunobiology : the immune system in health and disease, Garland Science, New York, 2005.

13. P.A. Bovier. Epaxal: a virosomal vaccine to prevent hepatitis A infection. Expert Reviews, Vaccines. 7:1141-1150 (2008).

14. F.M. Burnet. The concept of immunological surveillance. Progress in Experimental Tumor Research. 13:1-27 (1970).

15. M. Dardenne, M. Papiernik, J.F. Bach, and O. Stutman. Studies on thymus products. 3. Epithelial origin of the serum thymic factor. Immunology. 27:299-304 (1974).
16. C.R. Dassand M.A. Burton. Lipoplexes and tumours. A review. Journal of Pharmacy and Pharmacology. 51:755-770 (1999).

17. G. Dranoff. Targets of protective tumor immunity. Annals of the New York Academy of Science. 1174:74-80 (2009).

18. G.P. Dunn, L.J. Old, and R.D. Schreiber. The immunobiology of cancer immunosurveillance and immunoediting. Immunity. 21:137-148 (2004).

19. M.R. Ejtehadi, S.P. Avall, and S.S. Plotkin. Three-body interactions improve the prediction of rate and mechanism in protein folding models. Proceedings of the Natioanal Academy of Sciences U S A. 101:15088-15093 (2004).

20. K.P. Murphy, P. Travers, M. Walport, and C. Janeway. Janeway's immunobiology, Garland Science, New York, 2008.

21. A.F. Ochsenbein. Principles of tumor immunosurveillance and implications for immunotherapy. Cancer Gene Therapy. 9:1043-1055 (2002).

22. F. Sakurai, T. Terada, K. Yasuda, F. Yamashita, Y. Takakura, and M. Hashida. The role of tissue macrophages in the induction of proinflammatory cytokine production following intravenous injection of lipoplexes. Gene Therapy. 9:1120-1126 (2002).

23. P. Guermonprez, J. Valladeau, L. Zitvogel, C. Thery, and S. Amigorena. Antigen presentation and T cell stimulation by dendritic cells. Annual Review of Immunology. 20:621-667 (2002).

24. E. Turnbulland G. MacPherson. Immunobiology of dendritic cells in the rat. Immunological Reviews. 184:58-68 (2001).

25. D.M. Pardolland S.L. Topalian. The role of CD4(+) T cell responses in antitumor immunity. Current Opinion in Immunology. 10:588-594 (1998).

26. C. Janewayand P. Travers. Immunobiology : the immune system in health and disease, Current Biology Limited ;Garland Pub. Inc., London ; San Francisco New York, 1994.

27. Y. Men, R. Audran, C. Thomasin, G. Eberl, S. Demotz, H.P. Merkle, B. Gander, and G. Corradin. MHC class I- and class II-restricted processing and presentation of microencapsulated antigens. Vaccine. 17:1047-1056 (1999).

28. S. Hamdy, O. Molavi, Z. Ma, A. Haddadi, A. Alshamsan, Z. Gobti, S. Elhasi, J. Samuel, and A. Lavasanifar. Co-delivery of cancer-associated antigen and Toll-like receptor 4 ligand in PLGA nanoparticles induces potent CD8+ T cell-mediated anti-tumor immunity. Vaccine. 26:5046-5057 (2008).

29. A. Iwasakiand R. Medzhitov. Toll-like receptor control of the adaptive immune responses. Nature Immunology. 5:987-995 (2004).

30. K. Hung, R. Hayashi, A. Lafond-Walker, C. Lowenstein, D. Pardoll, and H. Levitsky. The central role of CD4(+) T cells in the antitumor immune response. Journal of Experimental Medicine. 188:2357-2368 (1998).

31. T. Nishimura, K. Iwakabe, M. Sekimoto, Y. Ohmi, T. Yahata, M. Nakui, T. Sato, S. Habu, H. Tashiro, M. Sato, and A. Ohta. Distinct role of antigen-specific T helper type 1 (Th1) and Th2 cells in tumor eradication in vivo. Journal of Experimental Medicine. 190:617-627 (1999).

32. T. Nishimura, M. Nakui, M. Sato, K. Iwakabe, H. Kitamura, M. Sekimoto, A. Ohta, T. Koda, and S. Nishimura. The critical role of Th1-dominant immunity in tumor immunology. Cancer Chemotherapy and Pharmacology. 46:S52-S61 (2000).

33. H. Ikeda, K. Chamoto, T. Tsuji, Y. Suzuki, D. Wakita, T. Takeshima, and T. Nishimura. The critical role of type-1 innate and acquired immunity in tumor immunotherapy. Cancer Science. 95:697-703 (2004).

34. S. Romagnani. Induction of th1 and th2 responses - a key role for the natural immune-response. Immunology Today. 13:379-381 (1992).

35. R.K. Gupta, B.E. Rost, E. Relyveld, and G.R. Siber. Adjuvant properties of aluminum and calcium compounds. Pharmaceutical Biotechnology. 6:229-248 (1995).

36. K. Inaba, J.W. Young, and R.M. Steinman. Direct activation of CD8+ cytotoxic T lymphocytes by dendritic cells. Journal of Experimental Medicine. 166:182-194 (1987).

37. J.E. Talmadge, J. Adams, H. Phillips, M. Collins, B. Lenz, M. Schneider, and M. Chirigos. Immunotherapeutic potential in murine tumor-models of polyinosinic-polycytidylic acid and poly-l-lysine solubilized by carboxymethylcellulose. Cancer Research. 45:1066-1072 (1985).

38. C. Trumpfheller, M. Caskey, G. Nchinda, M.P. Longhi, O. Mizenina, Y.X. Huang, S.J. Schlesinger, M. Colonna, and R.M. Steinman. The microbial mimic poly IC induces durable and protective CD4(+) T cell immunity together with a dendritic cell targeted vaccine. Proceedings of the National Academy of Sciences, USA. 105:2574-2579 (2008).

39. D.M. Lubaroffand D. Karan. CpG oligonucleotide as an adjuvant for the treatment of prostate cancer. Advanced Drug Delivery Reviews. 61:268-274 (2009).

40. M. Schnare, G.M. Barton, A.C. Holt, K. Takeda, S. Akira, and R. Medzhitov. Toll-like receptors control activation of adaptive immune responses. Nature Immunology. 2:947-950 (2001).

41. T. Akagi, T. Kaneko, T. Kida, and M. Akashi. Preparation and characterization of biodegradable nanoparticles based on poly(gamma-glutamic acid) with l-phenylalanine as a protein carrier. Journal of Controlled Release. 108:226-236 (2005).

42. J.L. Arias, V. Gallardo, F. Linares-Molinero, and A. Delgado. Preparation and characterization of carbonyl iron/poly(butylcyanoacrylate) core/shell nanoparticles. Journal of Colloid and Interface Science. 299:599-607 (2006).

43. C.E. Asteteand C.M. Sabliov. Synthesis and characterization of PLGA nanoparticles. Journal of Biomaterial Science Polymer Ed. 17:247-289 (2006).

44. L. Brannon-Peppas, B. Ghosn, K. Roy, and K. Cornetta. Encapsulation of nucleic acids and opportunities for cancer treatment. Pharmaceutical Research. 24:618-627 (2007).

45. C. Coester, P. Nayyar, and J. Samuel. In vitro uptake of gelatin nanoparticles by murine dendritic cells and their intracellular localisation. European Journal of Pharmaceutics and Biopharmaceutics. 62:306-314 (2006).

46. J.A. Cohen, T.T. Beaudette, W.W. Tseng, E.M. Bachelder, I. Mende, E.G. Engleman, and J.M.J. Frechet. T-Cell Activation by Antigen-Loaded pH-Sensitive Hydrogel Particles in Vivo: The Effect of Particle Size. Bioconjugate Chemistry. 20:111-119 (2009).

47. M. Gaumet, A. Vargas, R. Gurny, and F. Delie. Nanoparticles for drug delivery: the need for precision in reporting particle size parameters. European Journal of Pharmaceutics and Biopharmaceutics. 69:1-9 (2008).

48. A. Ito, Y. Kuga, H. Honda, H. Kikkawa, A. Horiuchi, Y. Watanabe, and T. Kobayashi. Magnetite nanoparticle-loaded anti-HER2 immunoliposomes for combination of antibody therapy with hyperthermia. Cancer Letters. 212:167-175 (2004).

49. G. Kauland M. Amiji. Long-circulating poly(ethylene glycol)-modified gelatin nanoparticles for intracellular delivery. Pharmaceutical Research. 19:1061-1067 (2002).

50. S.H. Nezhadi, P.F.M. Choong, F. Lotfipour, and C.R. Dass. Gelatin-based delivery systems for cancer gene therapy. Journal of Drug Targeting. 17:731-738 (2009).

51. T. Niiand F. Ishii. Encapsulation efficiency of water-soluble and insoluble drugs in liposomes prepared by the microencapsulation vesicle method. International Journal of Pharmaceutics. 298:198-205 (2005).

52. Y. Krishnamachari, S.M. Geary, C.D. Lemke, and A.K. Salem. Nanoparticle Delivery Systems in Cancer Vaccines. Pharmaceutical Research (2010).

53. Y. Krishnamachariand A.K. Salem. Innovative strategies for co-delivering antigens and CpG oligonucleotides. Advanced Drug Delivery Reviews. 61:205-217 (2009).

54. A.U. Bielinska, K.W. Janczak, J.J. Landers, D.M. Markovitz, D.C. Montefiori, and J.R. Baker, Jr. Nasal immunization with a recombinant HIV gp120 and nanoemulsion adjuvant produces Th1 polarized responses and neutralizing antibodies to primary HIV type 1 isolates. AIDS Research and Hum Retroviruses. 24:271-281 (2008).

55. G. Chikhand M.P. Schutze-Redelmeier. Liposomal delivery of CTL epitopes to dendritic cells. Bioscience Reports. 22:339-353 (2002).

56. S. de Jong, G. Chikh, L. Sekirov, S. Raney, S. Semple, S. Klimuk, N. Yuan, M. Hope, P. Cullis, and Y. Tam. Encapsulation in liposomal nanoparticles enhances the immunostimulatory, adjuvant and anti-tumor activity of subcutaneously administered CpG ODN. Cancer Immunology Immunotherapy. 56:1251-1264 (2007).

57. S.W. Dow, L.G. Fradkin, D.H. Liggitt, A.P. Willson, T.D. Heath, and T.A. Potter. Lipid-DNA complexes induce potent activation of innate immune responses and antitumor activity when administered intravenously. Journal of Immunology. 163:1552-1561 (1999).

58. A. Heit, F. Schmitz, T. Haas, D.H. Busch, and H. Wagner. Antigen co-encapsulated with adjuvants efficiently drive protective T cell immunity. European Journal of Immunology. 37:2063-2074 (2007).

59. W. Jiang, R.K. Gupta, M.C. Deshpande, and S.P. Schwendeman. Biodegradable poly(lactic-co-glycolic acid) microparticles for injectable delivery of vaccine antigens. Advanced Drug Delivery Reviews. 57:391-410 (2005).

60. L. Krishnanand G.D. Sprott. Archaeosome adjuvants: immunological capabilities and mechanism(s) of action. Vaccine. 26:2043-2055 (2008).

61. M. Lanuti, S. Rudginsky, S.D. Force, E.S. Lambright, W.M. Siders, M.Y. Chang, K.M. Amin, L.R. Kaiser, R.K. Scheule, and S.M. Albelda. Cationic lipid : bacterial DNA complexes elicit adaptive cellular immunity in murine intraperitoneal tumor models. Cancer Research. 60:2955-2963 (2000).

62. S.J. Draperand J.L. Heeney. Viruses as vaccine vectors for infectious diseases and cancer. Nature Reviews of Microbiology. 8:62-73 (2010).

63. D.C. Drummond, O. Meyer, K. Hong, D.B. Kirpotin, and D. Papahadjopoulos. Optimizing liposomes for delivery of chemotherapeutic agents to solid tumors. Pharmacological Reviews. 51:691-743 (1999).

64. C.M. Solbrig, J.K. Saucier-Sawyer, V. Cody, W.M. Saltzman, and D.J. Hanlon. Polymer nanoparticles for immunotherapy from encapsulated tumor-associated antigens and whole tumor cells. Molecular Pharmaceutics. 4:47-57 (2007).

65. A.M. Krieg. Development of TLR9 agonists for cancer therapy. Journal of Clinical Investigation. 117:1184-1194 (2007).

66. X.Q. Zhang, C.E. Dahle, N.K. Baman, N. Rich, G.J. Weiner, and A.K. Salem. Potent antigen-specific immune responses stimulated by codelivery of CpG ODN and antigens in degradable microparticles. Journal of Immunotherapy. 30:469-478 (2007).

67. C.L. Cooper, J.B. Angel, I. Seguin, H.L. Davis, and D.W. Cameron. CPG 7909 adjuvant plus hepatitis B virus vaccination in HIV-infected adults achieves long-term seroprotection for up to 5 years. Clinical and Infectious Diseases. 46:1310-1314 (2008).

68. C.L. Cooper, N.K. Ahluwalia, S.M. Efler, J. Vollmer, A.M. Krieg, and H.L. Davis. Immunostimulatory effects of three classes of CpG oligodeoxynucleotides on PBMC from HCV chronic carriers. Journal of Immune Based Therapies and Vaccines. 6:3 (2008).

69. C.L. Cooper, H.L. Davis, M.L. Morris, S.M. Efler, A.M. Krieg, Y. Li, C. Laframboise, M.J. Al Adhami, Y. Khaliq, I. Seguin, and D.W. Cameron. Safety and immunogenicity of CPG 7909 injection as an adjuvant to Fluarix influenza vaccine. Vaccine. 22:3136-3143 (2004).

70. C.R. Steinman, U. Deesomchok, and H. Spiera. Detection of anti-DNA antibody using synthetic antigens. Characterization and clinical significance of binding of poly (deoxyadenylate-deoxythymidylate) by serum. Journal of Clinical Investigation. 57:1330-1341 (1976).

71. K. Tewari, B.J. Flynn, S.B. Boscardin, K. Kastenmueller, A.M. Salazar, C.A. Anderson, V. Soundarapandian, A. Ahumada, T. Keler, S.L. Hoffman, M.C. Nussenzweig, R.M. Steinman, and R.A. Seder. Poly(I:C) is an effective adjuvant for antibody and multi-functional CD4+ T cell responses to Plasmodium falciparum circumsporozoite protein (CSP) and alphaDEC-CSP in non human primates. Vaccine. 28:7256-7266 (2010).

72. M.P. Longhi, C. Trumpfheller, J. Idoyaga, M. Caskey, I. Matos, C. Kluger, A.M. Salazar, M. Colonna, and R.M. Steinman. Dendritic cells require a systemic type I interferon response to mature and induce CD4+ Th1 immunity with poly IC as adjuvant. Journal of Experimental Medicine. 206:1589-1602 (2009).

73. X.Q. Zhang, C.E. Dahle, G.J. Weiner, and A.K. Salem. A comparative study of the antigen-specific immune response induced by co-delivery of CpG ODN and antigen using fusion molecules or biodegradable microparticles. Journal of Pharmaceutical Sciences. 96:3283-3292 (2007).

74. D.T. Ohagan, H. Jeffery, and S.S. Davis. Long-term antibody-responses in mice following subcutaneous immunization with ovalbumin entrapped in biodegradable microparticles. Vaccine. 11:965-969 (1993).

75. T. Uchida, S. Martin, T.P. Foster, R.C. Wardley, and S. Grimm. Dose and load studies for subcutaneous and oral delivery of poly(lactide-co-glycolide) microspheres containing ovalbumin. Pharmaceutical Research. 11:1009-1015 (1994).

76. M. Igartua, R.M. Hernandez, A. Esquisabel, A.R. Gascon, M.B. Calvo, and J.L. Pedraz. Enhanced immune response after subcutaneous and oral immunization with biodegradable PLGA microspheres. Journal of Controlled Release. 56:63-73 (1998).

77. Y. Waeckerle-Menand M. Groettrup. PLGA microspheres for improved antigen delivery to dendritic cells as cellular vaccines. Advanced Drug Delivery Reviews. 57:475-482 (2005).

78. S.A. Miles, R. Goforth, A.K. Salem, X.Y. Zhu, X.Q. Zhang, J. Lee, and A.D. Sandler. Immune stimulatory antigen loaded particles combined with depletion of regulatory T-cells induce potent tumor specific immunity. Journal of Leukocyte Biology:103 (2007).

79. J.R. Bertrand, M. Pottier, A. Vekris, P. Opolon, A. Maksimenko, and C. Malvy. Comparison of antisense oligonucleotides and siRNAs in cell culture and in vivo. Biochemical and Biophysical Research Communications. 296:1000-1004 (2002).

80. C. Brus, H. Petersen, A. Aigner, F. Czubayko, and T. Kissel. Efficiency of polyethylenimines and polyethylenimine-graft-poly (ethylene glycol) block copolymers to protect oligonucleotides against enzymatic degradation. European Journal of Pharmaceutics and Biopharmaceutics. 57:427-430 (2004).

81. M.M. Whitmore, M.J. DeVeer, A. Edling, R.K. Oates, B. Simons, D. Lindner, and B.R.G. Williams. Synergistic activation of innate immunity by double-stranded RNA and CpG DNA promotes enhanced antitumor activity. Cancer Research. 64:5850-5860 (2004).

82. T. Warger, P. Osterloh, G. Rechtsteiner, M. Fassbender, V. Heib, B. Schmid, E. Schmitt, H. Schild, and M.P. Radsak. Synergistic activation of dendritic cells by combined Toll-like receptor ligation induces superior CTL responses in vivo. Blood. 108:544-550 (2006).

83. M.L. Salem, S.A. El-Naggar, A. Kadima, W.E. Gillanders, and D.J. Cole. The adjuvant effects of the toll-like receptor 3 ligand polyinosinic-cytidylic acid poly (I:C) on antigen-specific CD8+ T cell responses are partially dependent on NK cells with the induction of a beneficial cytokine milieu. Vaccine. 24:5119-5132 (2006).

84. M.L. Salem, A.N. Kadima, D.J. Cole, and W.E. Gillanders. Defining the antigen-specific T-cell response to vaccination and poly(I:C)/TLR3 signaling: evidence of enhanced primary and memory CD8 T-cell responses and antitumor immunity. Journal of Immunotherapy. 28:220-228 (2005).

85. A.M. Lundberg, S.K. Drexler, C. Monaco, L.M. Williams, S.M. Sacre, M. Feldmann, and B.M. Foxwell. Key differences in TLR3/poly I : C signaling and cytokine induction by human primary cells: a phenomenon absent from murine cell systems. Blood. 110:3245-3252 (2007).

86. R.C. Mehta, B.C. Thanoo, and P.P. DeLuca. Peptide containing microspheres from low molecular weight and hydrophilic poly(d,l-lactide-co-glycolide). Journal of Controlled Release. 41:249-257 (1996).

87. U. Bilati, E. Allemann, and E. Doelker. Poly(D,L-lactide-co-glycolide) protein-loaded nanoparticles prepared by the double emulsion method-processing and formulation issues for enhanced entrapment efficiency. Journal of Microencapsulation. 22:205-214 (2005).

88. X.M. Deng, S.B. Zhou, X.H. Li, J. Zhao, and M.L. Yuan. In vitro degradation and release profiles for poly-dl-lactide-poly(ethylene glycol) microspheres containing human serum albumin. Journal of Controlled Release. 71:165-173 (2001).

89. V. Kanchanand A.K. Panda. Interactions of antigen-loaded polylactide particles with macrophages and their correlation with the immune response. Biomaterials. 28:5344-5357 (2007).

90. C. Foged, B. Brodin, S. Frokjaer, and A. Sundblad. Particle size and surface charge affect particle uptake by human dendritic cells in an in vitro model. International Journal of Pharmaceutics. 298:315-322 (2005).

91. S.T. Reddy, M.A. Swartz, and J.A. Hubbell. Targeting dendritic cells with biomaterials: developing the next generation of vaccines. Trends in Immunology. 27:573-579 (2006).

92. J.C. Reece, N.J. Vardaxis, J.A. Marshall, S.M. Crowe, and P.U. Cameron. Uptake of HIV and latex particles by fresh and cultured dendritic cells and monocytes. Immunology and Cell Biology. 79:255-263 (2001).

93. P. Johansen, Y. Men, H.P. Merkle, and B. Gander. Revisiting PLA/PLGA microspheres: an analysis of their potential in parenteral vaccination. European Journal of Pharmaceutics and Biopharmaceutics. 50:129-146 (2000).

94. P. Malyala, D.T. O'Hagan, and M. Singh. Enhancing the therapeutic efficacy of CpG oligonucleotides using biodegradable microparticles. Advanced Drug Delivery Reviews. 61:218-225 (2009).

95. R. Alexand R. Bodmeier. Encapsulation of water-soluble drugs by a modified solvent evaporation method .1. Effect of process and formulation variables on drug entrapment. Journal of Microencapsulation. 7:347-355 (1990).

96. Y. Ogawa, M. Yamamoto, H. Okada, T. Yashiki, and T. Shimamoto. A new technique to efficiently entrap leuprolide acetate into microcapsules of polylactic acid or copoly(lactic glycolic) acid. Chemical & Pharmaceutical Bulletin. 36:1095-1103 (1988).

97. S. Prior, B. Gander, N. Blarer, H.P. Merkle, M.L. Subira, J.M. Irache, and C. Gamazo. In vitro phagocytosis and monocyte-macrophage activation with poly(lactide) and poly(lactide-co-glycolide) microspheres. European Journal of Pharmaceutical Sciences. 15:197-207 (2002).

98. J. Banchereau, F. Briere, C. Caux, J. Davoust, S. Lebecque, Y.T. Liu, B. Pulendran, and K. Palucka. Immunobiology of dendritic cells. Annual Review of Immunology. 18:767-+ (2000).

99. A.M. Butler, H. Blatt, and H. Southgate. The solubility of the plasma proteins II. Dependence on pH, temperature, and lipid content in concentrated solutions of potassium phosphate and application to their separate precipitation. Journal of Biological Chemistry. 109:755-767 (1935).

100. C.Q. Liand G.X. Zhang. Nanosize delivery as an emerging platform for cancer therapy Commentary. Cancer Biology & Therapy. 7:1860-1862 (2008).

101. P.R. Lockman, R.J. Mumper, M.A. Khan, and D.D. Allen. Nanoparticle technology for drug delivery across the blood-brain barrier. Drug Development and Industrial Pharmacy. 28:1-13 (2002).

102. V. Manolova, A. Flace, M. Bauer, K. Schwarz, P. Saudan, and M.F. Bachmann. Nanoparticles target distinct dendritic cell populations according to their size. European Journal of Immunology. 38:1404-1413 (2008).

103. O. Molavi, A. Mahmud, S. Hamdy, R. Hung, J. Samuel, R. Lai, and A. Lavasanifar. Development of a poly(D,L-lactic-co-glycolic acid) (PLGA) nanoparticle formulation of STAT3 inhibitor JSI-124: Implication for cancer immunotherapy. Molecular Pharmaceutics (2009).

104. S. Munier, I. Messai, T. Delair, B. Verrier, and Y. Ataman-Onal. Cationic PLA nanoparticles for DNA delivery: Comparison of three surface polycations for DNA binding, protection and transfection properties. Colloids and Surfaces B-Biointerfaces. 43:163-173 (2005).

105. D.T. O'Hagan, M. Singh, and J.B. Ulmer. Microparticle-based technologies for vaccines. Methods. 40:10-19 (2006).

106. Y. Waeckerle-Men, E.U. Allmen, B. Gander, E. Scandella, E. Schlosser, G. Schmidtke, H.P. Merkle, and M. Groettrup. Encapsulation of proteins and peptides into biodegradable poly(D,L-lactide-co-glycolide) microspheres prolongs and enhances antigen presentation by human dendritic cells. Vaccine. 24:1847-1857 (2006).

107. A. Eratalay, F.F. Coskun-Ari, F. Oner, and E. Ozcengiz. In vitro and in vivo evaluations of PLGA microsphere vaccine formulations containing pDNA coexpressing Hepatitis B surface antigen and Interleukin-2. Journal of Microencapsulation. 27:48-56 (2010).

108. T. Uchida, S. Martin, T.P. Foster, R.C. Wardley, and S. Grimm. Dose and load studies for subcutaneous and oral delivery of poly(lactide-co-glycolide) microspheres containing ovalbumin. Pharmaceutical Research. 11:1009-1015 (1994).

109. R. Jeyanthi, R.C. Mehta, B.C. Thanoo, and P.P. DeLuca. Effect of processing parameters on the properties of peptide-containing PLGA microspheres. Journal of Microencapsulation. 14:163-174 (1997).

110. M.L. Ye, S. Kim, and K. Park. Issues in long-term protein delivery using biodegradable microparticles. Journal of Controlled Release. 146:241-260 (2010).

111. P. Malyala, J. Chesko, M. Ugozzoli, A. Goodsell, F. Zhou, M. Vajdy, D.T. O'Hagan, and M. Singh. The potency of the adjuvant, CpG oligos, is enhanced by encapsulation in PLG microparticles. Journal of Pharmaceutical Sciences. 97:1155-1164 (2008).

112. B.S. Roman, J.M. Irache, S. Gomez, N. Tsapis, C. Gamazo, and M.S. Espuelas. Co-encapsulation of an antigen and CpG oligonucleotides into PLGA microparticles by TROMS technology. European Journal of Pharmaceutics and Biopharmaceutics. 70:98-108 (2008).

113. J.L. Chen, M.K. Yeh, and C.H. Chiang. The mechanism of surface-indented protein-loaded PLGA microparticle formation: the effects of salt (NaCl) on the solidification process. Journal of Microencapsulation. 21:877-888 (2004).

114. K.F. Pisteland T. Kissel. Effects of salt addition on the microencapsulation of proteins using W/O/W double emulsion technique. Journal of Microencapsulation. 17:467-483 (2000).

115. G. Napolitani, A. Rinaldi, F. Bertoni, F. Sallusto, and A. Lanzavecchia. Selected Toll-like receptor agonist combinations synergistically trigger a T helper type 1-polarizing program in dendritic cells. Nature Immunology. 6:769-776 (2005).

116. A. Bagchi, E.A. Herrup, H.S. Warren, J. Trigilio, H.S. Shin, C. Valentine, and J. Hellman. MyD88-dependent and MyD88-independent pathways in synergy, priming, and tolerance between TLR agonists. Journal of Immunology. 178:1164-1171 (2007).

117. H. Xie, I. Gursel, B.E. Ivins, M. Singh, D.T. O'Hagan, J.B. Ulmer, and D.M. Klinman. CpG oligodeoxynucleotides adsorbed onto polylactide-co-glycolide microparticles improve the immunogenicity and protective activity of the licensed anthrax vaccine. Infection and Immunity. 73:828-833 (2005).

118. R.G. Fenton, C.J. Keller, N. Hanna, and D.D. Taub. Induction of t-cell immunity against ras oncoproteins by soluble-protein or ras-expressing escherichia-coli. Journal of the National Cancer Institute. 87:1853-1861 (1995).

119. S. Hamdy, P. Elamanchili, A. Alshamsan, O. Molavi, T. Satou, and J. Samuel. Enhanced antigen-specific primary CD4(+) and CD8(+) responses by codelivery of ovalbumin and toll-like receptor ligand monophosphoryl lipid A in poly(D,L-lactic-co-glycolic acid) nanoparticles. Journal of Biomedical Materials Research Part A. 81A:652-662 (2007).

120. S. Hamdy, O. Molavi, Z.S. Ma, A. Haddadi, A. Alshamsan, Z. Gobti, S. Elhasi, J. Samuel, and A. Lavasanifar. Co-delivery of cancer-associated antigen and Toll-like receptor 4 ligand in PLGA nanoparticles induces potent CD8(+) T cell-mediated anti-tumor immunity. Vaccine. 26:5046-5057 (2008).

121. A.S. Giermasz, J.A. Urban, Y. Nakamura, P. Watchmaker, R.L. Cumberland, W. Gooding, and P. Kalinski. Type-1 polarized dendritic cells primed for high IL-12 production show enhanced activity as cancer vaccines. Cancer Immunology Immunotherapy. 58:1329-1336 (2009).

122. S.F. Shariat, S. Desai, W.T. Song, T. Khan, J. Zhao, C. Nguyen, B.A. Foster, N. Greenberg, D.M. Spencer, and K.M. Slawin. Adenovirus-mediated transfer of inducible caspases: A novel "death switch" gene therapeutic approach to prostate cancer. Cancer Research. 61:2562-2571 (2001).

123. S.L. Demento, N. Bonafe, W.G. Cui, S.M. Kaech, M.J. Caplan, E. Fikrig, M. Ledizet, and T.M. Fahmy. TLR9-Targeted Biodegradable Nanoparticles as Immunization Vectors Protect against West Nile Encephalitis. Journal of Immunology. 185:2989-2997 (2010).

124. M. Yoshida, J. Mata, and J.E. Babensee. Effect of poly(lactic-co-glycolic acid) contact on maturation of murine bone marrow-derived dendritic cells. Journal of Biomedical Materials Research Part A. 80A:7-12 (2007).

125. M.S. Ernstoff, T.S. Crocenzi, J.D. Seigne, N.A. Crosby, B.F. Cole, J.L. Fisher, J.C. Uhlenhake, D. Mellinger, C. Foster, C.J. Farnham, K. Mackay, Z.M. Szczepiorkowski, S.M. Webber, A.R. Schned, R.D. Harris, R.J. Barth, J.A. Heaney, and R.J. Noelle. Developing a rational tumor vaccine therapy for renal cell carcinoma: Immune Yin and Yang. Clinical Cancer Research. 13:733S-740S (2007).

126. S.K. Leeand R.T.D. Oliver. Autologous leukemia-specific t-cell-mediated lymphocytotoxicity in patients with acute myelogenous leukemia. Journal of Experimental Medicine. 147:912-922 (1978).

127. K. Hariharan, G. Braslawsky, A. Black, S. Raychaudhuri, and N. Hanna. The induction of cytotoxic t-cells and tumor-regression by soluble-antigen formulation. Cancer Research. 55:3486-3489 (1995).

128. R.M. Verdijk, T. Mutis, B. Esendam, J. Kamp, C.J.M. Melief, A. Brand, and E. Goulmy. Polyriboinosinic polyribocytidylic acid (poly(I : C)) induces stable maturation of functionally active human dendritic cells. Journal of Immunology. 163:57-61 (1999).

129. G. Napolitani, A. Rinaldi, F. Bertoni, F. Sallusto, and A. Lanzavecchia. Selected Toll-like receptor agonist combinations synergistically trigger a T helper type 1-polarizing program in dendritic cells. Nature Immunology. 6:769-776 (2005).

130. A.S. Lonsdorf, H. Kuekrek, B.V. Stern, B.O. Boehm, P.V. Lehmann, and M. Tary-Lehmann. Intratumor CpG-oligodeoxynucleotide injection induces protective antitumor T cell immunity. Journal of Immunology. 171:3941-3946 (2003).

131. B. Maletto, A. Ropolo, V. Moron, and M.C. Pistoresi-Palencia. CpG-DNA stimulates cellular and humoral immunity and promotes Th1 differentiation in aged BALB/c mice. Journal of Leukocyte Biology. 72:447-454 (2002).

132. S.M. Kangand R.W. Compans. Host Responses from Innate to Adaptive Immunity after Vaccination: Molecular and Cellular Events. Molecules and Cells. 27:5-14 (2009).

133. C. Esserand A. Radbruch. Immunoglobulin class switching - molecular and cellular analysis. Annual Review of Immunology. 8:717-735 (1990).

134. S.A. North, K. Graham, D. Bodnar, and P. Venner. A pilot study of the liposomal MUC1 vaccine BLP25 in prostate specific antigen failures after radical prostatectomy. Journal of Urology. 176:91-95 (2006).

135. F. Tewes, E. Munnier, B. Antoon, L.N. Okassa, S. Cohen-Jonathan, H. Marchais, L. Douziech-Eyrolles, M. Souce, P. Dubois, and I. Chourpa. Comparative study of doxorubicin-loaded poly(lactide-co-glycolide) nanoparticles prepared by single and double emulsion methods. European Journal of Pharmaceutics and Biopharmaceutics. 66:488-492 (2007).

136. T.L. Jackson. Intracellular accumulation and mechanism of action of doxorubicin in a spatio-temporal tumor model. Journal of Theoretical Biology. 220:201-213 (2003).

137. D.A. Gewirtz. A critical evaluation of the mechanisms of action proposed for the antitumor effects of the anthracycline antibiotics Adriamycin and daunorubicin. Biochemical Pharmacology. 57:727-741 (1999).

138. L. Apetoh, A. Tesniere, F. Ghiringhelli, G. Kroemer, and L. Zitvogel. Molecular interactions between dying tumor cells and the innate immune system determine the efficacy of conventional anticancer therapies. Cancer Research. 68:4026-4030 (2008).

139. L.E. Kandalaft, N. Singh, J.B. Liao, A. Facciabene, J.S. Berek, D.J. Powell, and G. Coukos. The emergence of immunomodulation: Combinatorial immunochemotherapy opportunities for the next decade. Gynecologic Oncology. 116:222-233 (2010).

140. C.N. Baxevanis, S.A. Perez, and M. Papamichail. Combinatorial treatments including vaccines, chemotherapy and monoclonal antibodies for cancer therapy. Cancer Immunology Immunotherapy. 58:317-324 (2009).

141. N. Casares, M.O. Pequignot, A. Tesniere, F. Ghiringhelli, S. Roux, N. Chaput, E. Schmitt, A. Hamai, S. Hervas-Stubbs, M. Obeid, F. Coutant, D. Metivier, E. Pichard, P. Aucouturier, G. Pierron, C. Garrido, L. Zitvogel, and G. Kroemer. Caspase-dependent immunogenicity of doxorubicin-induced tumor cell death. Journal of Experimental Medicine. 202:1691-1701 (2005).

142. R. Houotand R. Levy. T-cell modulation combined with intratumoral CpG cures lymphoma in a mouse model without the need for chemotherapy. Blood. 113:3546-3552 (2009).

143. W.L. Chen, Y.Z. Yu, C. Shao, M.H. Zhang, W. Wang, L.H. Zhang, and X.T. Cao. Enhancement of antigen-presenting ability of B lymphoma cells by immunostimulatory CpG-oligonucleotides and anti-CD40 antibody. Immunology Letters. 77:17-23 (2001).

144. J.L. Li, W.R. Song, D.K. Czerwinski, B. Varghese, S. Uematsu, S. Akira, A.M. Krieg, and R. Levy. Lymphoma immunotherapy with CpG oligodeoxynucleotides requires TLR9 either in the host or in the tumor itself. Journal of Immunology. 179:2493-2500 (2007).

145. H.S. Yoo, K.H. Lee, J.E. Oh, and T.G. Park. In vitro and in vivo anti-tumor activities of nanoparticles based on doxorubicin-PLGA conjugates. Journal of Controlled Release. 68:419-431 (2000).

146. A.A. van Apeldoorn, H.J. van Manen, J.M. Bezemer, J.D. de Bruijn, C.A. van Blitterswijk, and C. Otto. Raman imaging of PLGA microsphere degradation inside macrophages. Journal of the American Chemical Society. 126:13226-13227 (2004).

147. G. Pratesi, G. Petrangolini, M. Tortoreto, A. Addis, S. Belluco, A. Rossini, S. Selleri, C. Rumio, S. Menard, and A. Balsari. Therapeutic synergism of gemcitabine and CpG-oligodeoxynucleotides in an orthotopic human pancreatic carcinoma xenograft. Cancer Research. 65:6388-6393 (2005).